

PERFORMANCE EVALUATION OF SILT
FENCES FOR CONTROLLING
SEDIMENT RELEASE

By

SHERRY LYNN BRITTON

Bachelor of Science

Oklahoma State University


Stillwater, Oklahoma

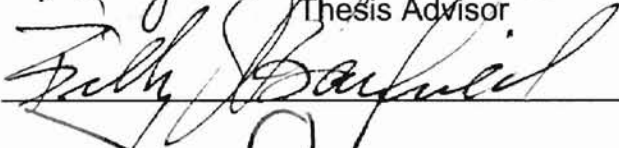
1999


Submitted to the Faculty of the
Graduate College of the
Oklahoma State University
in partial fulfillment of
the requirements for
the Degree of
MASTER OF SCIENCE
December, 2000


PERFORMANCE EVALUATION OF SILT
FENCES FOR CONTROLLING
SEDIMENT RELEASE

Thesis Approved:


Thesis Advisor






Dean of the Graduate College

ACKNOWLEDGMENTS

The work upon which this report is based was supported by funds provided by the U. S. Department of Agriculture (USDA), Agricultural Research Service (ARS), as well as the Oklahoma State University Biosystems and Agricultural Engineering Department. I would like to extend my gratitude to Darrel Temple, Acting Laboratory Director of the USDA-ARS Hydraulics Engineering Research Laboratory, and the Biosystems Engineering Department, headed by Dr. Bill Barfield, for providing the research assistantship and facilities that made this research possible.

I would like to express my sincere appreciation to Dr. Kerry M. Robinson, my research advisor, for his advice, encouragement, and direction. He has been a true mentor, and I cannot thank him enough for his endless support throughout my graduate studies at Oklahoma State University. My gratitude is also extended to Dr. Bill Barfield, my academic advisor, for his continued support, guidance, and insight in this project. I would also like to thank Dr. Dan Storm for serving on my graduate committee and for his time and support throughout this research effort.

I would especially like to thank Kem Kadavy for his assistance during the construction phase of this project as well as his continuous support and guidance. The computer and equipment assistance provided by Kevin Cook is

truly appreciated. My gratitude also goes to Dr. Greg Hanson for his helpful advice and to Ray Cox for his contributions during the construction phase of this project. The assistance of Nathan Priest during testing and data processing is also greatly appreciated.

My sincere appreciation also goes to the faculty, staff, and students in the Biosystems and Agricultural Engineering Department for their continued support during my stay at Oklahoma State University.

Finally, I would like to thank my family, especially my parents, Buddy and Janet Britton, for their unconditional love and support throughout my life. They have taught me the true meaning of hard work, and their belief in me has given me the courage to face any challenge. To my brothers, thank you for setting the bar high and constantly challenging me to aim higher. You're the best brothers a sister could ever ask for. To my family, I sincerely dedicate this thesis.

TABLE OF CONTENTS

Chapter	Page
I. INTRODUCTION.....	1
<i>Problem Statement</i>	1
<i>Objective</i>	2
II. LITERATURE REVIEW.....	3
<i>Silt Fence</i>	3
Function.....	3
Design, Installation, and Maintenance.....	4
<i>Types of Geotextiles</i>	11
Woven Geotextiles.....	11
Nonwoven Geotextiles.....	12
<i>Physical Properties of Geotextiles</i>	13
Apparent Opening Size (AOS).....	13
Percent Open Area (POA).....	15
Permittivity.....	16
Filtration.....	16
<i>Summary</i>	18
III. EXPERIMENTAL EQUIPMENT.....	20
<i>Test Flume</i>	20
<i>Geotextile Fabrics</i>	21
<i>Measuring Devices</i>	22
IV. METHODS AND PROCEDURES.....	24
<i>Flow Conditions</i>	24
<i>Sediment Preparation</i>	28
<i>Total Suspended Solids Concentrations</i>	30
<i>Particle Size Analysis</i>	30
<i>Trapping Efficiencies</i>	32
V. RESULTS AND DISCUSSION.....	34
<i>Soil Deposition</i>	34
<i>Flow through the Geotextile Fabrics</i>	36
<i>Total Suspended Solids Concentrations</i>	51
<i>Particle Size Distributions</i>	53
<i>Trapping Efficiencies</i>	55

Chapter	Page
VI. SUMMARY AND CONCLUSIONS.....	57
<i>Summary.....</i>	<i>57</i>
<i>Conclusions.....</i>	<i>59</i>
<i>Recommendations for Future Studies.....</i>	<i>60</i>
VII. BIBLIOGRAPHY.....	63
VIII. APPENDICES.....	66
<i>Appendix A - - Operating Procedure for Microscan II.....</i>	<i>67</i>
<i>Appendix B - - Hydrometer and Sieve Analysis Procedure.....</i>	<i>71</i>
<i>Appendix C - - Plots of Impounded Head versus Time.....</i>	<i>74</i>
<i>Appendix D - - Head-discharge Plots.....</i>	<i>86</i>
<i>Appendix E - - Particle Size Distribution Plots.....</i>	<i>95</i>

LIST OF TABLES

Table	Page
1. Maximum slope and slope length for silt fence	6
2. Vender fabric specifications.....	21
3. Summary of test flow conditions.....	24
4. Vender particle size specifications.....	28
5. Total suspended solids concentrations.....	52
6. Summary of trapping efficiencies.....	55

LIST OF FIGURES

Figure	Page
1. Schematic of a silt fence.....	4
2. Test configuration.....	20
3. Photograph of a test flow through the fabric.....	25
4. View of the silt fence field site.....	26
5. Grab sample collection at the field site.....	27
6. Photograph of the tumbler.....	29
7. Particle size distribution of calibration beads using the PSA.....	32
8. Sediment trapped within fabric B.....	34
9. Soil deposition behind fabric A.....	35
10. Impounded volume versus inflow rate.....	36
11. An example of the recession curves for the impounded head data.....	37
12. Long-term impounded head plot for fabric A.....	38
13. Long-term impounded head plot for fabric B.....	39
14. Long-term impounded head plot for fabric C.....	39
15. Linear relationship between the orifice area and AOA.....	42
16. Clear-water flow prediction versus the experimental data for fabric A.....	43
17. Clear-water flow prediction versus the experimental data for fabric B.....	43
18. Clear-water flow prediction versus the experimental data for fabric C.....	44
19. Observed versus predicted clear-water flow for fabric A.....	44

Figure	Page
20. Observed versus predicted clear-water flow for fabric B.....	45
21. Observed versus predicted clear-water flow for fabric C.....	45
22. Linear relationship of the plugging coefficient and AOS.....	47
23. Sediment-laden flow prediction versus experimental data for fabric A.....	47
24. Sediment-laden flow prediction versus experimental data for fabric B.....	48
25. Sediment-laden flow prediction versus experimental data for fabric C.....	48
26. Observed versus predicted sediment-laden flow for fabric A.....	49
27. Observed versus predicted sediment-laden flow for fabric B.....	49
28. Observed versus predicted sediment-laden flow for fabric C.....	50
C1. Test 1: Impounded head versus time plot.....	75
C2. Test 2: Impounded head versus time plot.....	75
C3. Test 3: Impounded head versus time plot.....	76
C4. Test 4: Impounded head versus time plot.....	76
C5. Test 5: Impounded head versus time plot.....	77
C6. Test 6: Impounded head versus time plot.....	77
C7. Test 7: Impounded head versus time plot.....	78
C8. Test 8: Impounded head versus time plot.....	78
C9. Test 9: Impounded head versus time plot.....	79
C10. Test 10: Impounded head versus time plot.....	79
C11. Test 11: Impounded head versus time plot.....	80
C12. Test 12: Impounded head versus time plot.....	80
C13. Test 13: Impounded head versus time plot.....	81

Figure	Page
C14. Test 14: Impounded head versus time plot.....	81
C15. Test 15: Impounded head versus time plot.....	82
C16. Test 16: Impounded head versus time plot.....	82
C17. Test 17: Impounded head versus time plot.....	83
C18. Test 18: Impounded head versus time plot.....	83
C19. Test 19: Impounded head versus time plot.....	84
C20. Test 20: Impounded head versus time plot.....	84
C21. Test 21: Impounded head versus time plot.....	85
D1. Test 5: Head-discharge plot.....	87
D2. Test 6: Head-discharge plot.....	87
D3. Test 7: Head-discharge plot.....	88
D4. Test 9: Head-discharge plot.....	88
D5. Test 10: Head-discharge plot.....	89
D6. Test 11: Head-discharge plot.....	89
D7. Test 12: Head-discharge plot.....	90
D8. Test 14: Head-discharge plot.....	90
D9. Test 15: Head-discharge plot.....	91
D10. Test 16: Head-discharge plot.....	91
D11. Test 17: Head-discharge plot.....	92
D12. Test 18: Head-discharge plot.....	92
D13. Test 19: Head-discharge plot.....	93
D14. Test 20: Head-discharge plot.....	93

Figure	Page
D15. Test 21: Head-discharge plot.....	94
E1. Test 1: Particle size distribution plot.....	96
E2. Test 2: Particle size distribution plot.....	96
E3. Test 3: Particle size distribution plot.....	97
E4. Test 4: Particle size distribution plot.....	97
E5. Test 5: Particle size distribution plot.....	98
E6. Test 6: Particle size distribution plot.....	98
E7. Test 7: Particle size distribution plot.....	99
E8. Test 8: Particle size distribution plot.....	99
E9. Test 9: Particle size distribution plot.....	100
E10. Test 10: Particle size distribution plot.....	100
E11. Test 11: Particle size distribution plot.....	101
E12. Test 14: Particle size distribution plot.....	101
E13. Test 15: Particle size distribution plot.....	102
E14. Test 16: Particle size distribution plot.....	102
E15. Test 17: Particle size distribution plot.....	103
E16. Test 18: Particle size distribution plot.....	103
E17. Test 19: Particle size distribution plot.....	104
E18. Test 20: Particle size distribution plot.....	104
E19. Test 21: Particle size distribution plot.....	105

NOMENCLATURE

A	opening area
AOA	apparent opening area
AOS	apparent opening size
C'	orifice coefficient
C _p	plugging coefficient
Fabric A	Nilex 2127
Fabric B	Nilex 915
Fabric C	Nilex 2130
g	gravitational constant
h	number of filaments in the weft direction per meter
H	hydraulic head
m	number of fabric openings
POA	percent open area
PSA	particle size analyzer
PSD	particle size distribution
Q	flow rate
TSS	total suspended solids
v	number of filaments in the warp direction per meter
W	fabric width

DISCLAIMER

Mention of trade names or commercial products in this publication is solely for the purpose of providing specific information and does not imply recommendation or endorsement by the U.S. Department of Agriculture or Oklahoma State University. This contribution is from Oklahoma State University and the Agricultural Research Service, U. S. Department of Agriculture, in cooperation with the Oklahoma Agricultural Experiment Station.

CHAPTER I

INTRODUCTION

Problem Statement

In recent reports, the Environmental Protection Agency (EPA) named urban and agricultural runoff as the leading pollutant in U. S. waters (EPA, 1998). Sediment is a major contaminant transported and deposited in lakes, rivers, storm drainage systems, and other waterways. Over 4 billion tons of sediment are lost each year as a result of erosion (Brady and Weil, 1999). Erosion is simply the detachment, transport, and deposition of soil materials. A single raindrop is the greatest force detaching and transporting sediment, and human activities make the soil more vulnerable to the elements of nature (Brady and Weil, 1999). For example, plowing, livestock grazing, vehicular movement, and surface grading for construction alter the erosion of soil. Increased activity ultimately leads to an increase in soil loss.

Sediment, in addition to being a pollutant in its own right, also absorbs other contaminants such as oil, fertilizers, metals, and other toxins (Herzog et al., 2000). Waters that receive these contaminants have increased susceptibility to long-term ecological and economic effects. Ecologically, the deposition of sediment in rivers, lakes, and other waterways inhibits light for photosynthesizing plants and depletes oxygen for aquatic life (Waters, 1995). From an economist's viewpoint, the damages associated with soil erosion by water exceed over \$11 billion per year (Herzog et al., 2000). These damages include a decrease in the recreational use and commercial fishing of waterways and an increase in the

flood potential and use of water treatment operations (Herzog et al., 2000).

Obviously, sediment controls are needed to protect our waterways from contamination of harmful pollutants.

A device commonly used for sediment control is a silt fence. Silt fence is typically constructed of a woven geotextile fabric fastened to wooden or steel posts, with a wire mesh fence occasionally attached for structural support (Sherwood and Wyant, 1976). Although woven geotextile fabrics have been around since the 1950's for erosion control applications, little is known about the hydraulic performance of these fabrics used in silt fence designs. Wyant (1980), Kouwen, (1990), Barrett et al. (1995), and Wishowski et al. (1998) are among the few who have conducted comprehensive studies on silt fence. These studies suggest that the high trapping efficiencies of the tested silt fences are directly related to the types of fabric used in the experiments. Sediment is capable of blocking fabric openings; consequently, increasing the impounded volume behind the fence and trapping more sediment. However, research conducted thus far has failed to investigate the problems associated with sediment clogging the fabric openings.

Objective

This research is part of an overall program aimed at modeling the effectiveness of silt fences at trapping sediment. Specifically, the objective of this study was to examine the hydraulic performance of silt fences exposed to a range of sediment-laden flows. This research can potentially lead to improved design criteria and installation procedures for silt fence.

CHAPTER II

LITERATURE REVIEW

Silt Fence

Function

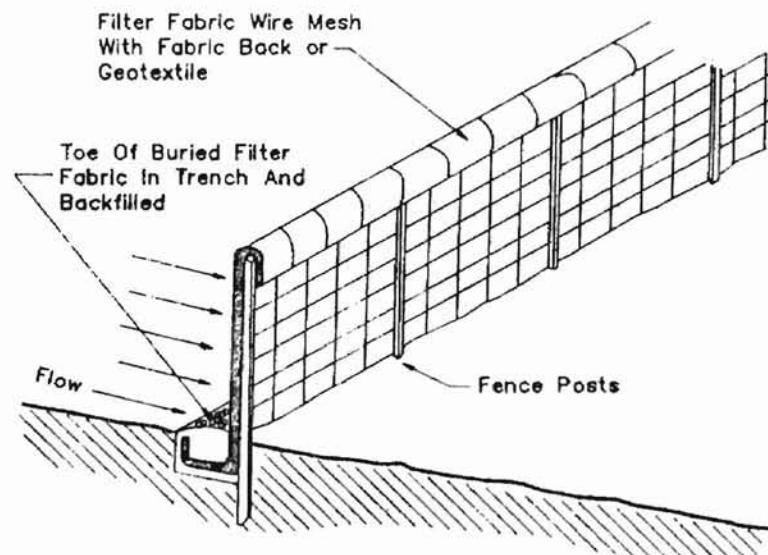
Silt fence is a common method for trapping sediment and slowing the erosion process on drastically disturbed lands. The primary function of silt fence is to screen soil particles from runoff water (Theisen, 1992), which is accomplished by serving as a temporary porous dam for impounding surface water (FHWA, 1998). As the impounded water level rises, eroded soil particles begin to deposit; however, some particles are small enough to pass through the fence while others become trapped in the fabric. Because the sediment trapped in the fence clogs some of the openings, the flow velocity is reduced, allowing more impoundment and increased detention time for the suspended particle fines to settle (FHWA, 1998).

Silt fence placement is primarily targeted in locations where water sources are threatened by the release of sediment. Common locations for silt fence are along highways, sidewalks, the perimeter of construction sites, and other places where the soil has been disturbed significantly. Silt fences are more successful at trapping sediment from sheet erosion rather than from concentrated flow (FHWA, 1998). Consequently, placement becomes an important factor in controlling sediment release.

Design, Installation, and Maintenance

As illustrated in figure 1, silt fence is made simply by fastening geotextile fabric to wood or steel posts, with a wire mesh fence occasionally attached for structural support (Sherwood and Wyant, 1976). Historically, silt fence has often proven to be an ineffective sediment control because of improper design, installation, and inadequate maintenance.

Figure 1: Schematic of a silt fence (Haan et al., 1994).



Currently, guidelines governing the design and installation procedures of silt fence vary significantly between regulatory authorities. For example, North Carolina requires the fabric height of silt fence to be 0.46 m (1.5 ft) tall, while Tennessee recommends a 0.91 m (3 ft) tall fabric (NCSCC, 1993; Smoot and Smith, 1998). These variations can lead to performance differences and problems. Additionally, the carelessness of the designer, installer, and inspector often lead to silt fence failures like undercutting, overtopping, and flanking.

Undercutting occurs by water movement underneath the fabric and is caused by failure to properly bury the toe of the fabric. Overtopping is often blamed on improper design and/or inadequate maintenance. When a fence cannot handle the volume of flow from intense rainfall events or when sediment deposition behind the fence has not been removed, overtopping can occur (Britton et al., 2000). Flanking is caused by improper fence placement, that allows water to divert around the end of the fence (Britton et al., 2000). For a silt fence to work properly; design criteria, installation procedures, and maintenance practices must be addressed.

According to Richardson and Middlebrooks (1991), silt fence design should be based on three criteria: estimated runoff volume, estimated sediment volume, and geotextile selection. Most silt fences are designed to handle 10-year, 24-hour storm events and have life expectancies of 6 months (FHWA, 1998). Furthermore, the drainage area for overland flow to the silt fence should not exceed 1012 m² (0.25 acres) per 30 m (100 ft) of silt fence (Richardson and Middlebrooks, 1991). The North Carolina Sedimentation Control Commission (NCSCC, 1993) along with Richardson and Middlebrooks (1991) also provide criteria for silt fence applications in relation to slope length. Table 1 provides a recommended maximum slope and slope length for silt fence installations (NCSCC, 1993; Richardson and Middlebrooks, 1991). Richardson and Middlebrooks (1991) recommend using the Rational Method (Linsley et al., 1958) to calculate the peak discharge delivered to a silt fence and the Universal Soil

Loss Equation (NRCS, formerly SCS, 1977) to estimate sediment volume behind the fence.

Table 1: Maximum slope and slope length for silt fence.

Slope (%)	Slope Length (m)
<2	31
2 to 5	23
5 to 10	15
10 to 20	7.6
>20	4.6

Selecting geotextile for silt fence applications is difficult because of the variety and number of geotextiles available in the market. Currently, geotextile selection is based upon past performance. That is, selections are made based on what has worked well in the past. Using this practical approach, Richardson and Middlebrooks (1991) suggest selecting geotextiles with the following properties:

1. Silt fence composed of woven slit film fabrics should have an apparent opening size (AOS) between 0.15 mm and 0.60 mm.
2. Silt fences constructed of other types of geotextiles should have an AOS between 0.15 mm and 0.30 mm.
3. The permittivity of the fabrics should be greater than 0.2 s^{-1} .

Although Wyant (1980) states that AOS and permittivity are not indicators of silt fence performance, Theisen (1992) agrees with Richardson and Middlebrooks (1991) that the required storage capacity and soil deposition behind the fence are directly related to the fabric AOS.

AOS indicates the opening sizes of the fabric, that in turn affects the amount of flow passed by the fabric. Smaller openings restrict the flow, allowing more water impoundment and increased detention time for particles to settle. Larger openings allow water to pass more freely; therefore, the impounded volume of water is less than fabrics with smaller opening sizes. Consequently, the AOS could be used as an indicator of the fabric storage capacity and the amount of sediment that settles behind the fence.

Although most installation and maintenance practices are conducted as rules of thumb, a silt fence can only perform as well as it is installed and maintained. Depending on the impounded heights, stakes are normally placed between 2 and 3 m (6 and 10 ft) apart. Wyant (1980) suggests using a wire mesh fence for structural support when the strength of the geotextile fabric is lower than 8.8 kN/m (50 lbs/linear inch) and posts are spaced more than 3 m (10 ft) apart. To avoid undercutting the fence, burial of the fabric toe is recommended between 0.15 to 0.20 m (6 to 8 inches) deep (Sherwood and Wyant, 1976; NCSCC, 1993). Colored filaments are often woven in the fabric to provide contractors guidance in how deep to bury the fabric toe. Regular inspections of silt fences are recommended, with soil deposition behind the fence never exceeding 1/3 of the fabric height (FHWA, 1998). These rules are merely suggestions based upon observed performance of silt fence in the field.

In addition to the installation and maintenance practices, the quality of the product should be addressed. After visiting several silt fence vendors, the quality assurance of the product was observed in many cases to be poor. Silt fence

products are typically sold in 100 ft rolls and often stored outdoors or in warehouses. Because of the environmental conditions (rain, sunlight, etc.), deterioration of the silt fence products stored outdoors was observed. Wooden stakes were also observed to vary in quality. During field installation, several wooden stakes were broken while hammering them into the ground. Additionally, fabric filaments can exhibit variability, resulting in fabric holes and/or larger than normal openings. Poor quality products would be expected to trap less sediment.

To date, limited research has been conducted on silt fence to aid in its design, yet Wyant (1980), Kouwen (1990), Barrett et al. (1995), and Wishowski et al. (1998) are among the few who have performed comprehensive laboratory studies on silt fence. Wyant (1980), whose work developed ASTM D 5141, initiated the research on silt fence by examining geotextile filter efficiency, strength, resistance to damage by ultraviolet rays, and the effects of pH on the fabric. These tests included both laboratory and field studies on the fabrics, with Wyant (1980) making the following conclusions from his research:

1. Fabrics that remove at least 75% of the soil particles from runoff water are recommended for silt fence design.
2. Structural support provided by a wire mesh fence can be eliminated from a silt fence design only if the fabric has tensile strength of 8.8 kN/m (50 lbs/linear in) or more and stakes less than 3 m (10 ft) apart.
3. Extreme values of pH showed no adverse effects on the fabrics tested. Therefore, pH is not considered an indicator for geotextile selection.

According to Wyant (1980), an optimal silt fence design would include fabrics with high filter efficiencies, faster flow rates without compromising filter efficiencies, and adequate tensile strength.

Wyant (1980) reported high trapping efficiencies in his studies. Sand particles were almost entirely trapped by the fabrics and clay size particles passed the fabrics. Although Wyant reported most trapping efficiencies higher than 90%, most of the tests were conducted on nonwoven fabrics under low flow conditions. Nonwoven fabrics are not traditionally used in silt fence applications because they impound more flow and overtop more easily than woven fabrics. It is recognized, however, that nonwoven fabrics can potentially trap more sediment as a result of increased impounded volume and increased detention time.

Kouwen (1990), Barrett et al. (1995), and Wishowski et al. (1998) conducted similar studies to Wyant's (1980) examination on the trapping efficiencies of silt fence. Deviations between studies included fabric types, soil distributions, approach slopes, and method of flow introduction (batch mixes versus continuous feed). Kouwen (1990) reported trapping efficiencies of 90% and higher, while Barrett, et al. (1995) observed trapping efficiencies between 68 and 90%. Wishowski et al. (1998) reported trapping efficiencies ranging from 69 to 81%. Kouwen (1990), Barrett et al. (1995), and Wishowski et al. (1998) concluded the high trapping efficiencies were a result of flow restriction through the fabrics and increased impounded volume behind the fence caused by soil particles lodged in the fabrics. Additionally, Kouwen (1990) reported using a #56

Barnes silica sand with an average particle size of 0.2 mm. Because sand with larger particle diameters was the test sediment in this study, higher trapping efficiencies were expected.

Tests conducted by Barrett et al. (1995) varied slightly from those conducted by Kouwen (1990) and Wyant (1980). Barrett et al. (1995) tested both nonwoven and woven fabrics, using a silty clay soil as the test sediment. Higher trapping efficiencies were observed from the nonwoven fabrics because more flow was impounded, increasing the detention time. In addition to laboratory tests, Barrett et al. (1995) also investigated a number of silt fence field installations. While lower trapping efficiencies were observed in these field studies, the sampling technique was cited as major reason for this difference. Barrett et al. (1995) also observed that detention times for woven fabrics decreased after major rainfall events. Barrett et al. (1995) suggests that accumulated sediment in the woven fabric was initially washed from the fence; thereby, increasing the flow rate through the fence and decreasing the impounded volume and detention time.

Wishowski et al. (1998) tested both high-density and low-density fabrics, that showed significant differences in performance. The high-density fabric trapped approximately 50% of the particles less than 2 microns, and the low-density fabric trapped an estimated 30%; while both primarily trapped sand. Wishowski et al. (1998) concluded that the type of fabric used for silt fences makes a dramatic impact on trapping efficiency.

Each of these studies suggests that the type of fabric used in silt fence applications governs the amount of sediment trapped. For instance, nonwoven fabrics trapped more sediment. This occurrence is due to increased flow impoundment and increased detention time. Essentially all fabrics were able to trap sand particles. This was expected since settling velocities are primarily dependent on the particle diameter. That is, larger diameter particles have faster settling velocities. While these studies present valuable information about the sediment trapped behind silt fence, research has yet to focus on the blockage of fabric openings caused by sediment.

Types of Geotextiles

Woven Geotextiles

In 1958, Carthage Mills produced the first woven geotextile fabric used for erosion control in the United States (Mlynarek and Lombard, 1997). Woven geotextiles are polymer-based fabrics mechanically made by textile-weaving machines (Koerner, 1998). These machines interlace weft (horizontal-direction) yarns with warp (vertical-direction) yarns in one of four weave patterns: plain, basket, twill, or satin (Koerner, 1998). The plain weave fabric has the simplest pattern in which each weft yarn is alternated over and under each warp yarn (Mlynarek and Lombard, 1997; Koerner, 1998). The basket weave fabric refers to a pattern where two or more threads are recognized as an individualized unit (Koerner, 1998). The manufacturing of twill weave fabrics is similar to the fabrication of the plain weave fabrics. The twill fabric alternates each weft yarn over and under two warp yarns. Satin fabrics vary in design, meaning each weft

yarn may alternate over three or more yarns and under one yarn (Mlynarek and Lombard, 1997; Koerner, 1998). Each of these weave patterns adds to the complexity of predicting the flow through a fabric.

Another influential component of the fabric is the individual yarn. Three types of fibers are currently used in woven fabric designs: monofilament, multifilament, and slit-film. A monofilament fiber is typically made by forcing melted polymer through a spinneret, allowing it to take the form of an uniform round or oval shaped thread (Mlynarek and Lombard, 1997; Koerner, 1998). A multifilament yarn is a grouping of monofilament yarns that are twisted together to form a single filament (Koerner, 1998). Slit-film fibers are described as tapes of thread made by cutting continuous sheets of polymer into single fibers and are often referred to as slit-film monofilament fibers. However, they may be twisted to form slit-film multifilament fibers (Koerner, 1998).

Each woven fabric is unique, with varying filaments and weave patterns. The filaments and weave patterns determine the opening sizes and fabric thickness. The passage of water and particulates through the fabric is dependent on these physical features, and these features add an element of difficulty in modeling flow through a geotextile fabric.

Nonwoven Geotextiles

Unlike woven geotextiles, nonwoven fabrics have no set pattern but instead have a randomness associated with them (Mlynarek and Lombard, 1997). Nonwoven fabrics are either made mechanically, thermally, or chemically. A mechanical method for manufacturing nonwoven geotextiles is needle-

punching. Needle-punching describes the action of the needles through the fabric in which the fibers of the fabric are reoriented to create the randomness of its pattern (Koerner, 1998). A thermal process for fabricating nonwoven fabrics is heat bonding. Heat bonding creates a stiff, low-weight fabric by melting filaments together at their points of intersection (Koerner, 1998). Chemically, nonwoven fabrics are made by resin bonding. To fabricate a resin-bonded fabric, an acrylic resin is sprayed upon the filaments to create an adhesive connection between them (Koerner, 1998). Each of these manufacturing processes influences the ultimate flow rate through the fabric and the particle size that will be trapped.

As stated previously, nonwoven fabrics are more random, resulting in an undefined opening pattern. Fabrics of this nature are rarely used in silt fence applications because the filament randomness decreases the percent open area of the fabric and increase the likelihood of overtopping. Although laboratory silt fence studies have shown an increase in sediment trapped by nonwoven fabrics when compared to woven fabrics, the increased risk of overtopping limits the use of these fabrics in field installations. Additionally, the flow through nonwoven fabrics is difficult to model because no standard exists to evaluate the percent open area of these geotextiles

Physical Properties of Geotextiles

Apparent Opening Size (AOS)

Developed by the U. S. Army Corps of Engineers, ASTM D 4751 is the standard test method for determining the apparent opening size (AOS) of a geotextile (Koerner, 1998). The AOS of a geotextile fabric is an indirect

measurement of the fabric pore size, which is essentially equivalent to the largest particle a fabric can pass (ASTM, 1995). To evaluate the opening size of a fabric, a test specimen is attached to a sieve frame with known-diameter glass beads placed on top of the fabric surface (ASTM, 1995; Koerner, 1998). By shaking the framed fabric back and forth, the beads are set into motion, allowing the beads to potentially pass the openings of the fabric (ASTM, 1995). This process is repeated with increasingly larger diameter beads until no more than 5% of the beads pass through the fabric (Koerner, 1998). When less than 5% of the beads have passed the fabric, the geotextile is defined by its O_{95} -size. O_{95} is a term based on the diameter of the beads, which describes the opening size of the fabric in millimeters. The AOS is typically reported as a standard U. S. sieve size number, which is easily converted from the O_{95} -size reported (Koerner, 1998).

Although ASTM D 4751 is a quick and simple method for determining the opening size of geotextiles, Koerner (1998) identifies the following problems associated with this method:

1. Glass beads become lodged in the fibers of the geotextile.
2. Fibers within a fabric shift easily, allowing beads to pass through larger, non-typical pore sizes.
3. Repeatability of the method is poor because of the variations in bead sizes and fabrics.

Additionally, the determination of the opening size using the ASTM D 4751 method is not representative of a real-world application of geotextiles used in silt

fences. Fabrics used in silt fences are vertically placed, and impounded water can alter fabric openings. Consequently, ASTM D 4751 for AOS determination may not accurately represent geotextile used in silt fence applications.

Percent Open Area (POA)

The percent open area (POA) of a geotextile is a term used to describe the ratio of void spaces between adjacent yarns in a fabric to the total area of the test fabric (Mlynarek and Lombard, 1997; Koerner, 1998). POA is a measurable property; however, no standard has been established to estimate this value. Koerner (1998) suggests projecting a light through the fabric onto a surface where the openings can be measured and counted. Mlynarek and Lombard (1997) suggest a more sophisticated means for measuring the POA of a fabric based on an image analysis approach. This method requires specialized equipment like an image analyzer microscope, which registers light projection through openings in a test specimen and analyzes them based on a minimum, maximum, and average opening size. POA is traditionally measured at a 90° angle of light projection; however, the image analyzer allows rotation of the sample so other light projection angles can be measured as well. An image analyzer can determine the maximum POA of a fabric (Mlynarek and Lombard, 1997).

POA could be a useful property for indicating the flow through a geotextile. Unfortunately, light projection through the fabric is often difficult to observe because of how the fibers are oriented. As a result, this property is usually

eliminated from the reported fabric specifications because the results are deemed unreliable.

Permittivity

ASTM D 4491 is the standard test method for water permeability of geotextiles by permittivity, and this test is also used to report flow through a geotextile. Permittivity is defined as the volumetric flow rate of water per unit cross sectional area per unit head under laminar flow conditions, in the normal direction through a geotextile (ASTM, 1992). Permittivity indicates the amount of flow a geotextile can pass under isolated head conditions (ASTM, 1992). A geotextile is placed horizontally in a permeability device with a head of 50 mm of water maintained on its surface (ASTM, 1992; Koerner, 1998). The flow rate through the fabric is measured under these conditions and used to calculate the permittivity of the fabric (ASTM, 1992; Koerner 1998). Although this test method indicates the flow through a geotextile fabric, it is important to note that this method tests the geotextile under zero normal stress, which is uncommon in real-world applications of geotextiles (ASTM, 1992). Therefore, the information from these tests may not be representative of geotextiles used in silt fence design.

Filtration

Geotextiles in silt fences are used to filter sediment from runoff water. Over time sediment can alter the performance of geotextile by clogging, blocking, or blinding the fabric (Mlynarek and Lombard, 1997). Clogging is defined when particles are retained within the fabric, causing flow restriction (Mlynarek and Lombard, 1997). Blocking and blinding occur when particles settle in front of the

fabric, forming a deposition pattern known as a filter cake (Mlynarek and Lombard, 1997). This layer of sediment blocks fabric openings; therefore, altering the filtration and drainage functions of the fabric (Mlynarek and Lombard, 1997; Smith et al., 1999).

Most studies conducted to evaluate the influence of sediment accumulation on geotextiles have examined fabrics oriented in a horizontal plane. Fisher and Jarrett (1984) and Smith et al. (1999) tested the filtration capabilities of several woven and nonwoven fabrics oriented in this fashion. Fisher and Jarrett (1984) observed that the fabrics retained most of the sand and coarse silt particles, while very little of the fine silt and clay particles were trapped by the fabrics. Fisher and Jarrett (1984) also observed a decrease in flow through the fabrics and concluded that soil accumulation on the fabrics restricted the transmission of water. Testing fabrics in a similar fashion, Smith et al. (1999) drew the following conclusions from their research:

1. More sediment was retained by the nonwoven fabrics than by woven fabrics having similar opening sizes. This occurrence is thought to be due to the distribution of pore sizes within the fabric.
2. Blinding and clogging were considered unrelated to the porosity of the fabrics.
3. The porosity and AOS of the fabric are believed to be unimportant in the clogging behaviors of geotextiles.

Although this information is valuable, further studies on geotextile clogging should be examined to evaluate the vertical fabric orientation like that typical of silt fence applications.

Summary

Silt fence is a common method for trapping sediment on-site and slowing the erosion process. For a silt fence to function properly and successfully trap sediment, attention must be given to the fence design, installation, and maintenance practices. To avoid failures such as undercutting, overtopping, and flanking, regulations should be followed. For instance, proper burial of the fabric toe may prevent undercutting, while adequate tensile strength and post spacing may reduce fence overtopping. While silt fence design, installation, and maintenance practices are based primarily on past performance evaluations; successful use of silt fences must begin by following regulatory guidelines.

To date, silt fence research has concentrated on the trapped sediment behind the fabrics, proving primarily that nonwoven fabrics trap higher percentages of sediment than woven fabrics. However, nonwoven fabrics are rarely used in silt fence applications because of their reduced flow through capacity. This reduced flow causes the impounded volume behind the fabric to increase, thereby increasing the risk of overtopping. Increasing the impounded volume was also observed to trap more sediment because of a corresponding increase in detention time. Additionally, studies have shown high percentages of trapped sand particles, which is not surprising since larger diameter particles settle more rapidly than smaller particles. Although the information on the fabric

trapping efficiencies is valuable, research has failed to examine the influence of impounded volume on sediment trapping efficiency.

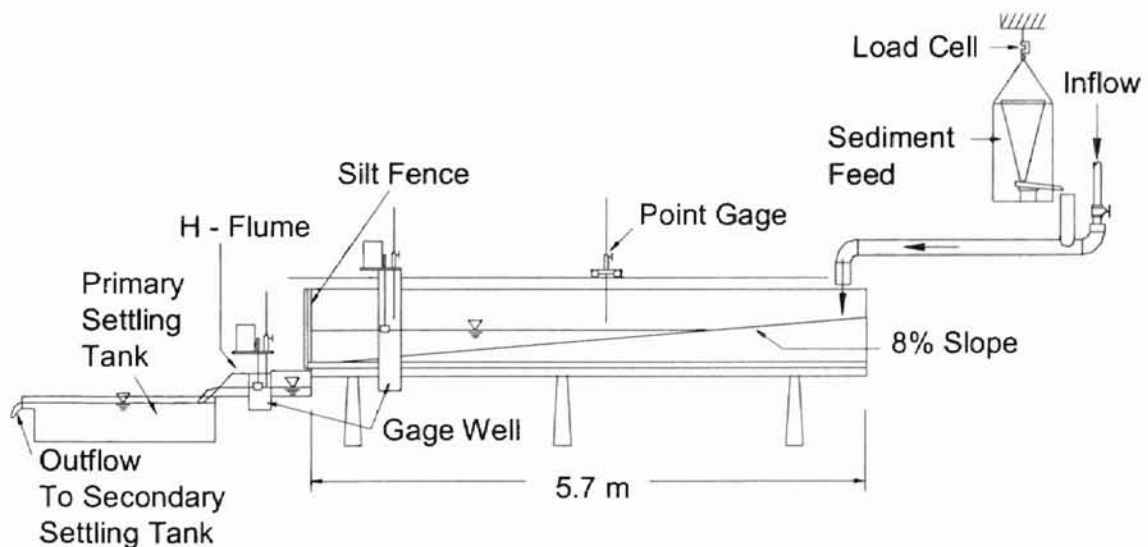
Silt fence designers need additional guidance in selecting woven geotextile fabrics for silt fence applications. This research attempts to fill that void by modeling the effectiveness of silt fences at trapping sediment. This research can potentially lead to improved design criteria for selecting woven geotextile fabrics.

CHAPTER III
EXPERIMENTAL EQUIPMENT

Test Flume

Tests were conducted indoors in a 5.7 m (18.7 ft) long by 0.9 m (3 ft) wide flume (Fig.2) located at the USDA-ARS Hydraulics Engineering Research Laboratory in Stillwater, Oklahoma. The flume floor was constructed with a 0.3 m (1 ft) horizontal section upstream of the fabric with the remainder of the floor sloping upstream at an 8% incline. A 2.4 m (8 ft) long section of the flume wall was constructed out of a clear acrylic material for observation of sediment deposition near the fabric barrier. The fabrics were 0.9-m (3 ft) tall and cut in approximately 1.2 m (4 ft) wide sections for attachment to the flume. The fabric was securely fastened to the end of the flume such that the maximum height of the fabric exposed to the flow conditions was 0.8 m (2.5 ft).

Figure 2: Test configuration.



Geotextile Fabrics

Research on three woven silt fence products (fabrics A, B, and C) was conducted to evaluate their effectiveness at separating sediment from runoff water (Table 2). Fabric A is described as an open, plain weave fabric made of slit-film monofilament fibers. Fabric B is also a plain weave fabric that is more tightly woven. It appears to be fabricated from a combination of slit-film monofilament fibers in the warp (vertical) direction and fibrous monofilament fibers in the weft (horizontal) direction. Fabric C is similar to fabric A, having a plain weave pattern made of slit-film monofilament fibers.

Table 2: Vender fabric specifications (Nilex Corporation, 2000).

Property	Test Method	Fabric A Nilex 2127	Fabric B Nilex 915	Fabric C Nilex 2130
Grab Tensile (N)	ASTM D 4632	350	665 x 555	550
Grab Elongation (%)	ASTM D 4632	15	15	15
Mullen Burst (kPa)	ASTM D 3786	1720	2410	2060
Puncture (N)	ASTM D 4833	130	290	290
Trapezoidal Tear (N)	ASTM D 4533	220	290 x 290	290
AOS (Sieve No.)	ASTM D 4751	10	40	30
Flow Rate (l/min/m ²)	ASTM D 4491	1220	1020	410
Permittivity (sec ⁻¹)	ASTM D 4491	0.3	0.4	0.05
UV Resistance (%)	ASTM D 4355	80	90	80

The primary difference between the three fabrics lies in the number of yarns in the warp and weft direction per unit area of fabric. For instance, fabric A has an average of 48 yarns per 100 mm in the warp direction and 32 yarns per 100 mm in the weft direction. Fabrics B and C were observed to have an average of 90 and 47 yarns in the warp direction and 31 and 44 yarns in the weft direction, respectively. Subsequently, the number of yarns is an indicator of how many openings are in a given fabric area.

Measuring Devices

Test flows were delivered to the flume in a continuous flow from a recirculation system. Flow entered a constant head tank and was then delivered through a 0.30-m (12-inch) diameter pipeline where the flow rate was measured with an orifice meter and differential manometer. The differential manometer was routinely checked to insure a constant flow rate.

To obtain sediment-laden conditions, a sediment shaker released a glass bead mixture directly into the flow over feed rates ranging from 5.9 g/sec (0.78 lb/min) to 26 g/sec (3.44 lb/min). A load cell and computer monitored the sediment feed rate from the shaker.

To determine the fabric flow rate, the impounded water level behind the fabric was measured in two fashions: manually with a carriage mounted point gage and electronically using a digital encoder. The impounded water level, or head, is the water level elevation above the lowest point on the flume floor. A 0.04-m (1.5-inch) diameter port was placed in the floor 0.15 meters (6 inches) upstream of the fabric, and a 0.05-m (2-inch) diameter sidewall port was placed 0.51 meters (20 inches) upstream of the fabric just above floor elevation. Both of these ports directed flow to a wet well where the water level was recorded by the digital encoder. The encoder recorded changes in head behind the fabric in five-second intervals.

The changes in impounded head were used to calculate the volumetric changes in storage for the flow recession period of each test. The recession period of the test starts when the inflow to the flume is terminated and continues

until the flume has completely drained. To accurately calculate the flow rate exiting the fabric, a head versus flume volume relationship was developed. The flume volume was determined by measuring the flume width from top to bottom with a micrometer in vertical increments of 0.15 m (0.5 ft) and horizontal increments of 0.61 m (2 ft). The flow rate exiting the flume was also monitored with a strip chart recorder on a 0.23-m (0.75-ft) H-flume downstream of the fabric. Point gage readings were taken at 5-minute intervals at the H-flume.

CHAPTER IV
METHODS AND PROCEDURES

Flow Conditions

Twenty-one tests were conducted on three woven silt fence products with the fabrics exposed to both clear-water and sediment-laden flow conditions. Based on a 10-year, 24-hour storm event, Sedimont II (Wilson et al. 1984), a computer program for estimating runoff from rainfall events through sediment control structures, was used to approximate the maximum flow a silt fence could handle without overtopping. Table 3 summarizes the flow conditions selected.

Table 3: Summary of test flow conditions.

Test #	Fabric	Inflow (m ³ /s)	Feed Rate (g/s)
1	B	1.6E-03	7.1
2	B	6.3E-04	26.0
3	A	1.6E-03	11.0
4	A	6.3E-04	22.7
5	B	3.2E-03	6.4
6	A	3.2E-03	8.2
7	B	1.6E-03	21.4
8	A	1.6E-03	23.7
9	A	1.6E-03	6.8
10	A	6.3E-04	5.9
11	B	6.3E-04	7.9
12	B	1.6E-03	11.6
13	A	6.3E-04	11.2
14	B	6.3E-04	10.1
15	C	1.6E-03	11.0
16	C	6.3E-04	12.3
17	C	1.6E-03	7.6
18	C	6.3E-04	7.6
19	C	3.2E-03	7.7
20	C	1.6E-03	24.1
21	C	6.3E-04	21.3

Each fabric was exposed to two clear-water tests typically lasting 20 minutes and one sediment-laden test typically lasting 60 minutes. A typical flow through a fabric is illustrated in figure 3. The first clear water flow was usually twice the flow rate of the second clear-water flow and the sediment-laden flow. This method verified that the clear-water flows behave similarly for each test and allowed direct comparison of clear-water and sediment-laden flows at higher impounded heads.

Figure 3: Photograph of a test flow through the fabric.



To achieve sediment-laden conditions, glass beads were directly fed into the flow at rates ranging from 5.9 g/sec (0.78 lb/min) to 26 g/sec (3.44 lb/min) (Table 3). Sediment feed rates were selected based on a combination of previous research experience as well as samples collected from a silt fence field site located on the USDA-ARS Hydraulic Engineering Research Laboratory grounds. Wyant (1980) observed maximum suspended solids concentrations of 3000 mg/L in the field, while Barrett et al. (1995) observed much lower concentrations.

Because of the variations in observed concentrations in the literature, a field plot was constructed on the grounds of the USDA-ARS Hydraulic Engineering Research Laboratory to evaluate the total suspended solids concentrations from collected runoff samples. The site was 15.2 m (50 ft) by 15.2 m (50 ft) with an 11.5% slope. A red sandy clay soil was used for the field plot because it was readily available. Based on the Unified Soil Classification System, this CL soil exhibited a particle size distribution of 25% clay, 40% silt, and 35% sand. Approximately 15.2 m (50 ft) of silt fence was placed on the downstream end of the plot to capture sediment in runoff water. The Oklahoma Department of Transportation pre-fabricated silt fence (Nilex 2130) was used at the site, and it was installed according to documented silt fence installation practices. For instance, the toe of the fabric was buried in a trench approximately 15.2 cm (6 in) deep, and the ends of the silt fence were angled upstream to prevent the fence from being flanked. The silt fence as installed in the field is illustrated in Figure 4.

Figure 4: View of the silt fence field site.



The field plot was evaluated based on runoff grab samples collected at the site during intense rainfall events and field surveys collected after storm events. Figure 5 shows the impounded runoff behind the fence and sample collection downstream of the fence during a rainfall event. Collected grab samples exhibited suspended solids concentrations between 18000 and 43000 mg/L, 10 times greater than that observed by Wyant (1980). Based on these results, feed rates for the laboratory experiments were selected.

Figure 5: Grab sample collection at the field site.



Additional data collected at the site indicated that the silt fence performed as intended. For instance, field surveys indicated an average of 13 cm (5 inches) of soil deposited behind the fence over a 6-month period. The Federal Highway Administration (1998) estimates a 6-month life expectancy for silt fence. In this field study, the silt fence failed approximately six months after installation because of the increased load placed on one of the stakes by impounded water and sediment. If properly maintained, this fence would have continued to trap sediment.

Sediment Preparation

Four spherically shaped bead sizes were mixed and introduced into the flow to simulate sediment. Although clay particles are typically plate-like in shape, selecting beads as a representative soil allowed repeatability and uniformity in testing. It is also recognized that sand and silt particles are typically round in shape, so glass beads were thought to be a suitable substitute. A disadvantage of using glass beads as the test sediment is that they are inert. Soils can be more influenced by physical and chemical bonds that can bind particles together. Additionally, organic matter and other materials are often present in sediment, causing soil particles to aggregate. These materials were absent in the glass bead mixture.

Using the beads, the same particle size distribution could be examined for each test. A Microscan II particle size analyzer (PSA) was chosen as the primary method for determining particle size distribution. Because the PSA limits the maximum diameter used in the machine to 300 microns, the beads selected for the experiments ranged from a clay to fine sand size (Table 4). The manufacturer of the beads describes them as a soda lime material with a specific gravity of 2.5 for the three larger sized beads and 2.65 for the smallest beads.

Table 4: Vender particle size specifications (Plonsker, 1999).

Bead Product I.D.	Particle Size (microns)			
	Mean	10%	50%	90%
A-2024	180	116	160	285
A-2429	93	60	89	138
A-3000	35	13	32	61
Bead Product I.D.	100%	50%	21%	2%
L-207A	10	5	3	1

The bead mixture consisted of 9.1 kg (20 lbs) each of glass A-2024 and A-2429, 11.3 kg (25 lbs) of glass A-3000, and 15.9 kg (35 lbs) of glass L-207A. To ensure the beads were thoroughly mixed, 45-kg (100 lb) batches were placed in a tumbler and mixed for 10 minutes (Fig. 6). The tumbler was constructed out of a stainless steel tank with interior ribbing and rotated approximately 5 revolutions per minute. The tank was constructed with a frame that allowed rapid adjustment in tank position. The bead mixture usually ranged in size from 1.5 to 177 μm . Using the Unified Soil Classification System, the original bead mixture was classified typically as a loam or silt loam soil.

Figure 6: Photograph of the tumbler.



Total Suspended Solids Concentrations

Total suspended solids concentrations were evaluated for each of the fabrics tested. At ten-minute intervals during the tests, 1-L grab samples were collected upstream and downstream of the fabric. Upstream samples were collected at mid-depth of the impounded flow. Plastic sheeting was attached to the bottom downstream edge of the flume to direct the entire flow passing the fabric into the downstream sample bottles. Samples were processed 24-hours later, so the suspended particles had time to settle. Excess water was decanted from the samples, and the remainder of the sample was transferred to 250-mL beakers. The samples were then oven-dried at a temperature of 105 °C for a minimum of 24 hours. Samples were then weighed, so concentrations could be determined.

Particle Size Analysis

Particle size analyses were obtained on both the original beads introduced into the flow and the particles passing the fabric. Particles passing the fabric were collected approximately 24 hours after testing from the primary settling tank located downstream of the H-flume. After allowing time for particles to settle, excess water was then decanted from the settling tank through an exit port. The remaining water and beads were washed from the primary settling tank into a stainless steel bucket and placed in a convection oven for drying. The drying process typically lasted at a minimum of 48 hours. After drying, the beads were weighed and stored until particle size analysis was performed.

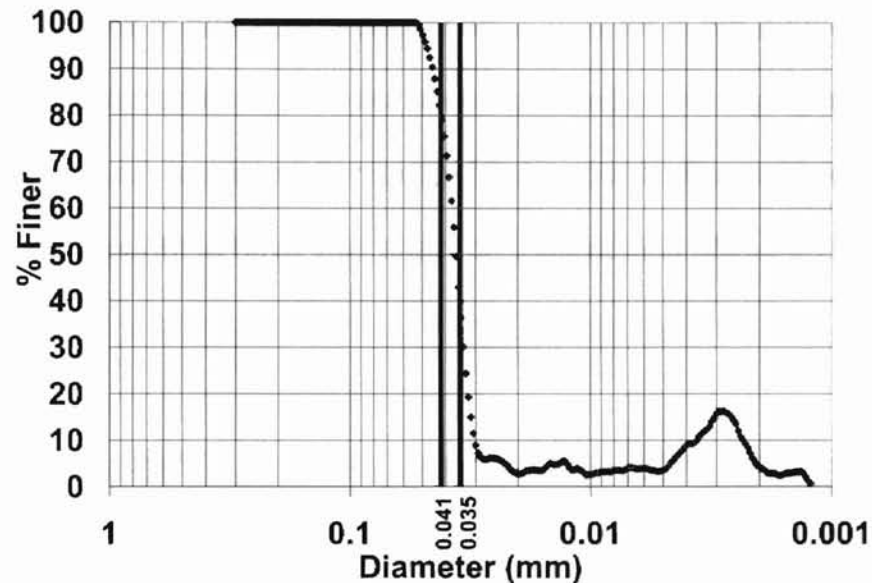
Microscan II as well as a hydrometer and sieve stack combination were used to determine the particle size distribution of the original bead mixture and the beads passing the fabric. The Microscan II eliminates much of the time needed for processing samples. A hydrometer or pipette method requires 24 hours for determining the particle sizes; however, the PSA can provide the results in a matter of minutes. The only limitation associated with the PSA was the size of the particles that it could analyze, which was 0.1 to 300 microns in diameter.

Microscan II uses Stoke's Law to determine particle sizes (Quantachrome, 1998). This technique yields particle diameters, assuming they are settling at the same rate as spherical particles. The PSA engages a narrow, low energy X-ray beam to scan particles as they settle in a sample cell (Quantachrome, 1998). Optimal results were observed to occur with sample sizes of approximately 7.5 grams dry weight. Larger sample sizes caused clogging in the analyzer hardware, and smaller samples resulted in inaccurate readings.

Since the PSA is not the standard test method for determining particle size, calibration beads were purchased to evaluate its performance. Commercially available beads with a guaranteed particle size range of 38 microns \pm 7% were tested in the PSA. Figure 7 depicts the particle size distribution of the calibration beads as determined by the PSA. The PSA distribution fits the guaranteed particle size range of 35 to 41 microns reasonably well, with more than 50% of the particles falling in the targeted ranged guaranteed by the vendor. Complete instructions for operating the PSA are

found in Appendix A; however, the operator of the PSA should be aware that radiation safety training must be received prior to operating the machine.

Figure 7: Particle size distribution of calibration beads using the PSA.



A hydrometer and sieve combination was also used to determine particle sizes. ASTM D 422 and D 1140 were followed for the particle size analysis. Appendix B describes the test equipment and the procedure used to determine particle size.

Trapping Efficiencies

The trapping efficiency for each experiment was determined. A load cell monitored the amount of sediment introduced into the system. After each test, the glass beads trapped in the flume were collected and placed in a tumbler for drying. An electric heater attached to the frame of the tumbler provided the necessary hot air for bead drying. Drying time took 24 to 72 hours depending on the volume of beads trapped in the flume and the bead moisture content. After the beads were dried, they were weighed to evaluate the trapping efficiency of the fabrics. The trapping efficiency of the fabrics was estimated by taking the

ratio of the dry bead weight trapped in the flume to the dry bead weight fed into the flume.

Some error is expected in this determination because the beads trapped within the filaments of the fabric were not accounted for in the trapped weight. Other beads were lost during transfer operations and in the drying process. Yet, the amount of beads lost in relation to the total amount collected from the flume was small and thought to have little effect on the trapping efficiency calculation.

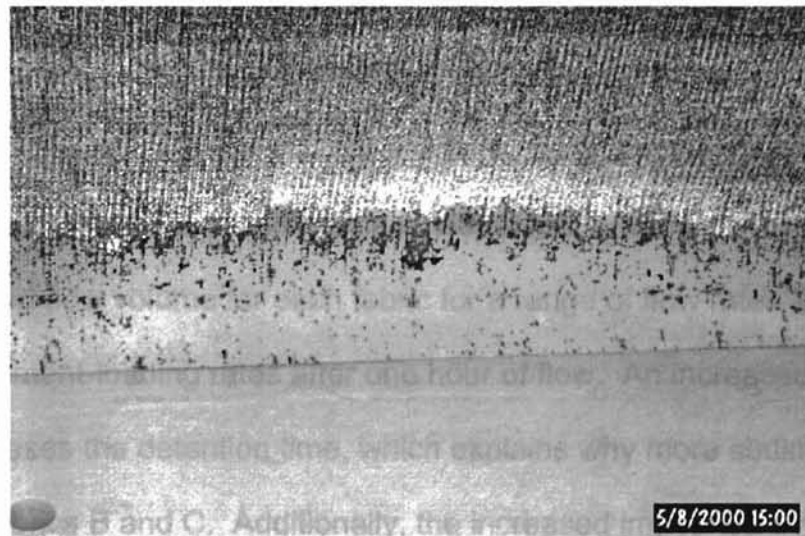
CHAPTER V

RESULTS AND DISCUSSION

Soil Deposition

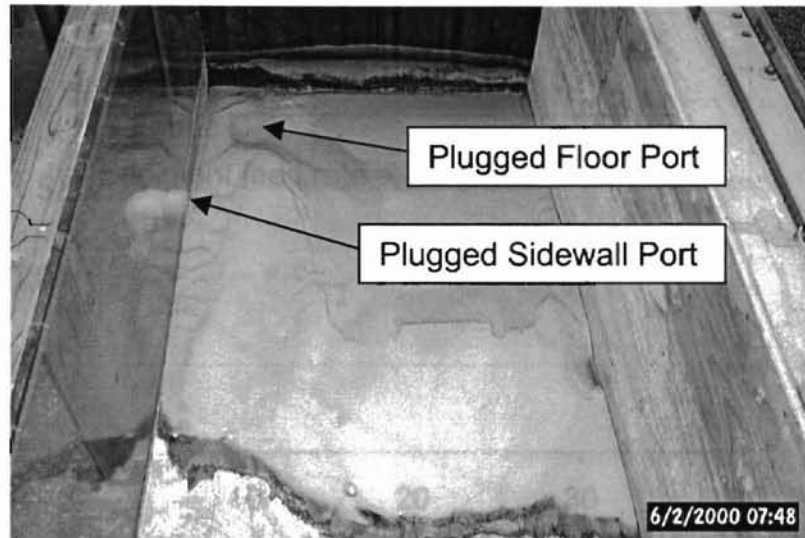
The fabric acted as a flow retarding structure to trap sediment. As flow moved through the barrier, sediment blocked some of the fabric openings. The blockage caused by filtration was more evident after the flow completely drained from the flume. It is apparent, as illustrated in figure 8, that sediment can block some of the fabric openings and impede the flow through the fabric.

Figure 8: Sediment trapped within fabric B.



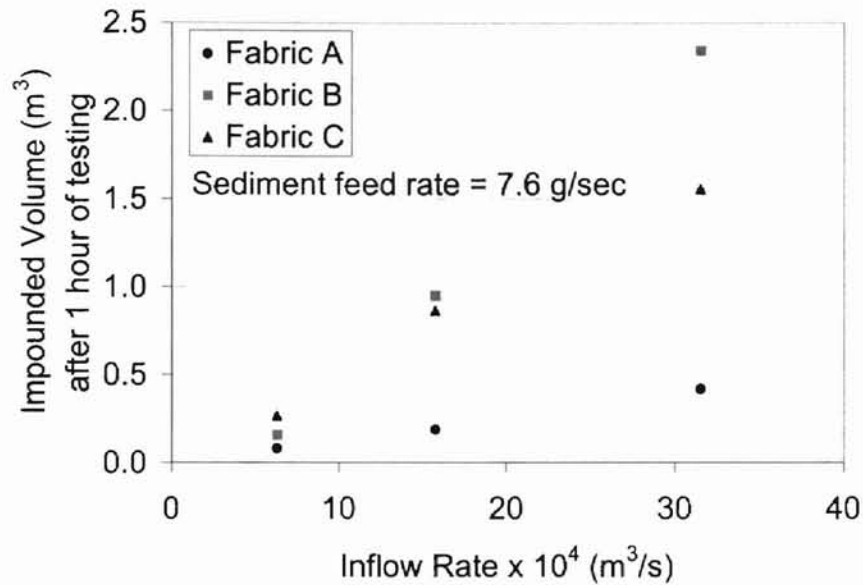
As flow impounded against the fabric, sediment began to settle behind the fabric. Visually, more sediment was observed near the fabric for tests conducted on fabric A than on fabrics B and C. On two occasions when testing fabric A, deposited sediment severely blocked the floor port to the wet well and partially plugged the sidewall port, restricting flow to the wet well and causing inaccurate impounded head readings. Figure 9 illustrates the soil deposition behind fabric A when both ports to the wet well were blocked with glass beads.

Figure 9: Soil deposition behind fabric A.



Fabric A has larger openings, allowing more flow and sediment to pass, so the water impoundment behind the fabric is less than that of fabrics B and C. Because fabrics B and C have smaller openings, sediment is more likely to block the openings and increase the impounded water volume. Figure 10 illustrates the impounded flow volume for each fabric for a range of flow rates and relatively constant sediment-loading rates after one hour of flow. An increased impounded volume increases the detention time, which explains why more sediment was trapped by fabrics B and C. Additionally, the increased impounded volume for fabrics B and C explains the location of deposited sediment. Deposited sediment was observed closer to fabric A than fabrics B and C, because fabrics B and C impounded more flow allowing particles to settle further upstream.

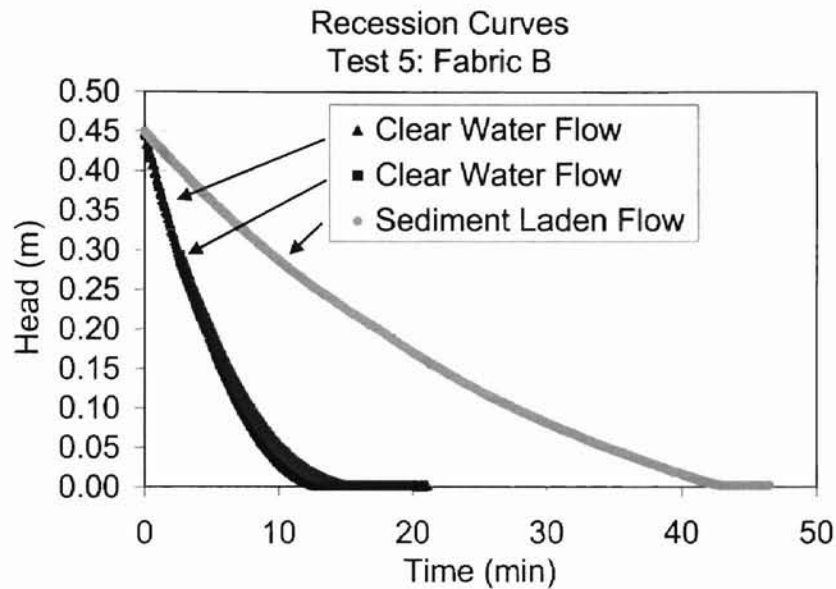
Figure 10: Impounded volume versus inflow rate.



Flow through the Geotextile Fabrics

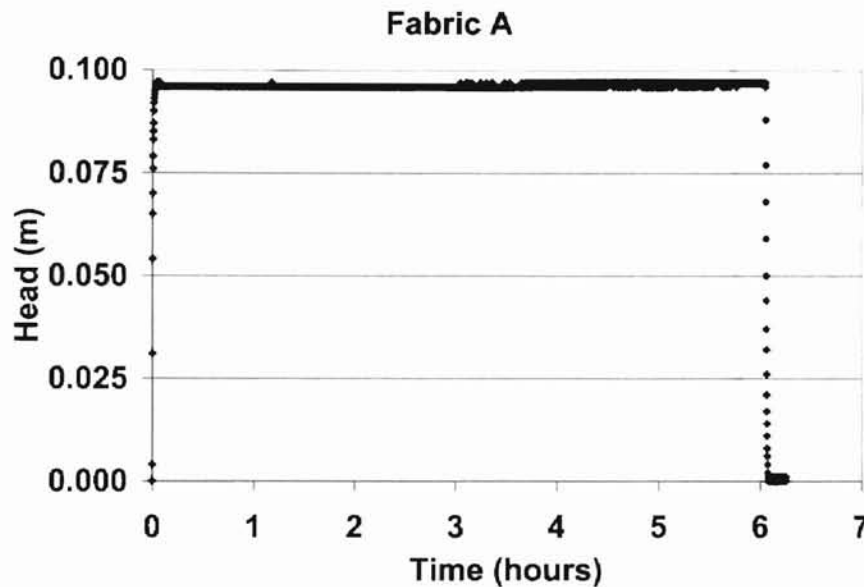
The changes in head over time for each test provided valuable information about the fabric performance. The original impounded head data for both clear-water and sediment-laden tests are plotted in Appendix C. The recession curves of the impounded head data (Fig. 11) were used to calculate the volumetric changes in flow exiting the flume. The recession curves were used for this purpose to avoid corrections for flow rate and feed rate. As illustrated in figure 11, the influence of sediment on the fabric flow rate is clearly shown. The two clear-water flows produced similar results, suggesting no flow correction is needed as a result of contamination or changes in fabric properties.

Figure 11: An example of the recession curves for the impounded head data.



As observed in Appendix C, the impounded clear-water flows continue to rise with time, indicating either that enough time did not lapse for the flow to stabilize, that contamination in the clear-water flow caused micro-plugging in the fabric and an increase the impounded volume, or that the properties of the fabric changed. To evaluate whether enough time had lapsed during testing, the three fabrics were exposed to long-term clear-water tests that lasted from 6 to 24 hours. Figure 12 illustrates the impounded head data from the long-term test of fabric A.

Figure 12: Long-term impounded head plot for fabric A.



From figure 12, the impounded head rises very little behind fabric A as a function of time. Fabric A has larger openings; therefore, micro-plugging of the openings would be expected to have less of an influence on the flow through the fabric than with fabrics B and C. After approximately 23 hours of testing, it was more evident that micro-plugging existed in fabric B (Fig. 13). Upon examining fabric B after testing, it was obvious that small sediment or rust particles from the pipes blocked some of the fabric openings. This micro-plugging impeded the flow through the fabric and caused the water elevation behind the fabric to rise. Likewise, the clear-water flow through fabric C, as shown in figure 14, was influenced by contamination, causing the impounded water volume to increase. Visual examination of fabric C provided evidence that rust and sediment particles clogged some of the fabric openings.

Figure 13: Long-term impounded head plot for Fabric B.

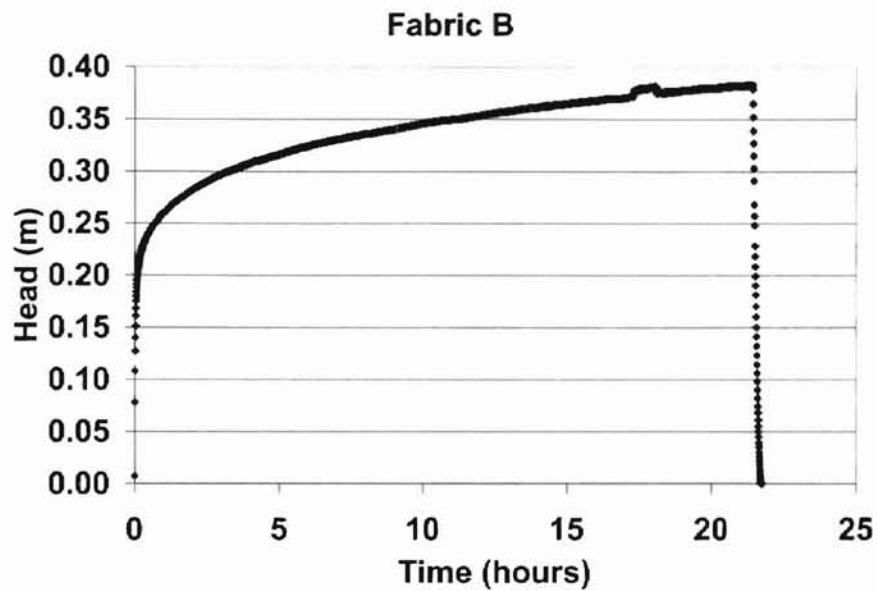
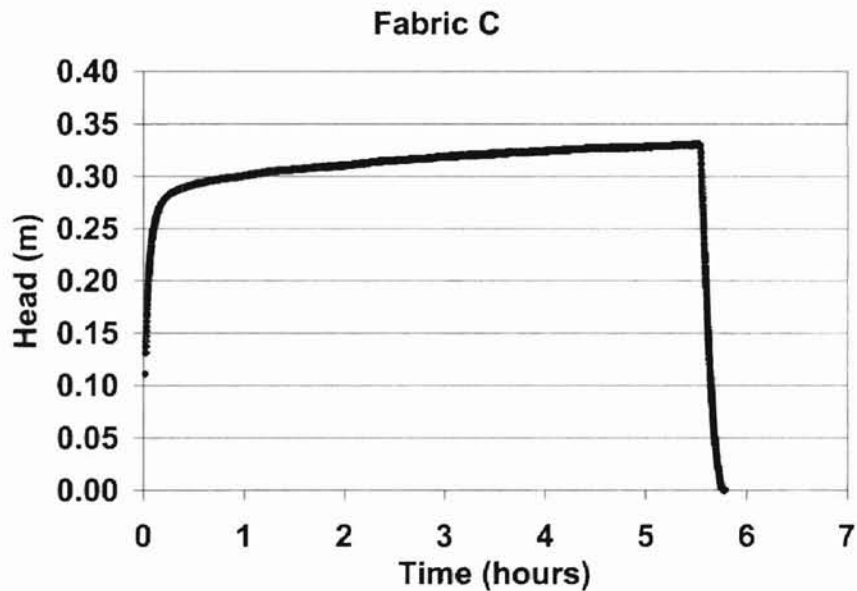


Figure 14: Long-term impounded head plot for fabric C.



Based on visual observations of the fabrics, micro-plugging was concluded as the reason for the increased impounded head over time. Although filaments in the fabrics may have shifted during testing and the force of water against the fabrics may have changed their properties, no evidence was

collected to suggest the increasing impounded flow volume was a result of fabric property changes.

Since clear-water flows typically lasted 20 minutes, micro-plugging was assumed to have little effect on the clear water fabric flow. No correction was applied when calculating the sediment-laden fabric flow. This assumption is supported by the repeatability of the two clear-water recession curves, as illustrated in figure 11.

Because of modifications in the test flume, tests 1, 2, 3, and 4 were omitted from flow evaluation. Additionally, tests 8 and 13 were not evaluated on flow behavior because sediment primarily deposited in front of the fabric, causing both the floor and sidewall ports to plug with beads and thus restricting flow to the wet well. Head-discharge plots were developed for the remaining tests. Appendix D includes the head-discharge graphs generated from the data. Each of these plots demonstrates unique clear-water and sediment-laden flow patterns. This observation provided insight in developing a prediction equation for the flow each fabric can pass for a range of impounded heads.

Because each fabric is unique, with variations in opening size and weave patterns, certain physical features of the fabric were considered. Each fabric is composed of a matrix of openings. Consequently, the flow through the fabric becomes dependent upon the number and size of the fabric openings. To develop a fabric clear-water flow equation, the following assumptions were made.

1. The number of filaments in the weft and warp directions are an indication of the number of openings in the fabric.

2. The geometry of the fabric openings is a rectangular orifice opening.

Equation 1 calculates the number of openings experiencing a hydraulic head:

$$m = (hW)(vH) \quad (1)$$

where m is the number of openings, h equals the number of weft filaments per meter, W is the width of the fabric in meters, v is the number of warp filaments per meter, and H is the hydraulic head in meters. In this study, a 0.1 m (0.33 ft) by 0.1 m (0.33 ft) sample area was selected arbitrarily to represent the entire fabric, and the number of filaments in both the horizontal and vertical directions were counted.

Since the assumption was also made that the openings were orifices, the clear-water flow through the fabric was written as a modified form of the orifice equation (Eq. 2), which takes into account the number of orifice openings from equation 1.

$$Q = C' mA(2gH)^{0.5} \quad (2)$$

where Q is the flow in m^3/s , C' is an orifice coefficient (assumed to be a sharp-edged orifice with coefficient of 0.61), m is the number of openings, A is the orifice area (m^2), g is the gravitational constant, and H is the hydraulic head impounded by the fabric (m).

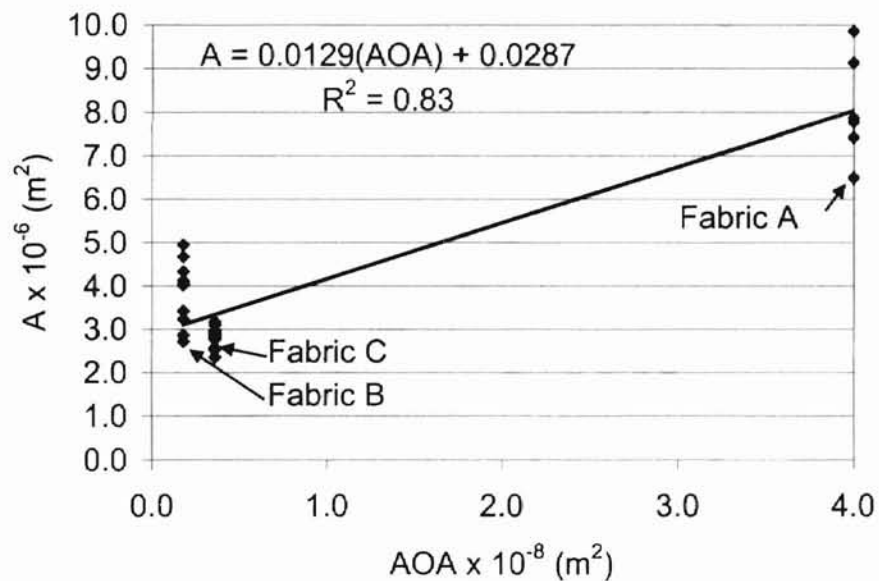
Clear-water flow rate through the fabric is dependent on the area of the fabric openings. Because the openings are small and would be difficult to measure, a simple relationship was developed between the collected data and the fabric specifications given by the company. Each impounded head measurement has a corresponding flow associated with it. These data were

used to back calculate the area of the opening by using equation 2. As illustrated in figure 15, the calculated area was plotted against the square AOS (m^2) of the fabrics. For example, a fabric denoted as an AOS No. 10 in the fabric specifications has a corresponding AOS of 2 mm, and by assuming the AOS is perfectly square, the apparent opening area (AOA) becomes 4 mm^2 . Because of insufficient data, a linear relationship, as shown in figure 15, was chosen to relate AOA and calculated orifice area. From this linear interpretation, the following linear equation was used to estimate the area of the orifice:

$$A = 0.0129(AOA) + 0.0287 \quad (3)$$

where the A is the orifice (opening) area in m^2 and AOA is the AOS squared (m^2).

Figure 15: Linear relationship between the orifice area and AOA.



With all parameters known, the clear-water flow rate through the fabric is predicted by substituting equation 3 into equation 2. Figures 16, 17, and 18 compare the predicted clear-water flow rate for fabrics A, B, and C, respectively, to the experimental data collected during the tests.

Figure 16: Clear-water flow prediction versus the experimental data for fabric A.

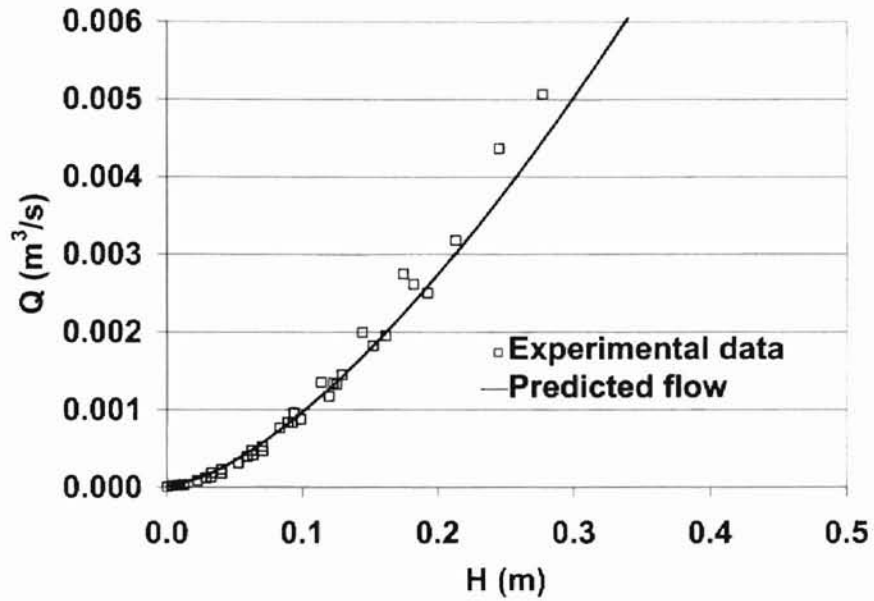


Figure 17: Clear-water flow prediction versus the experimental data for fabric B.

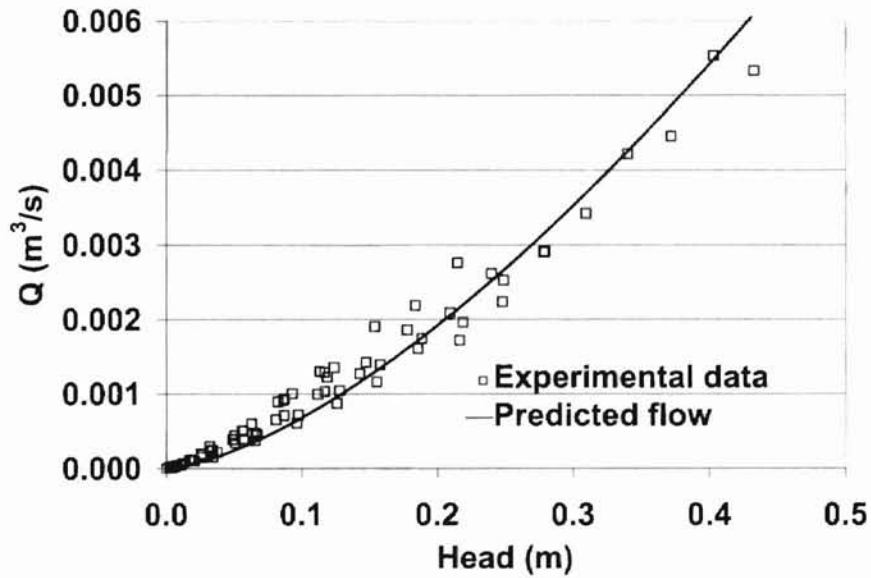
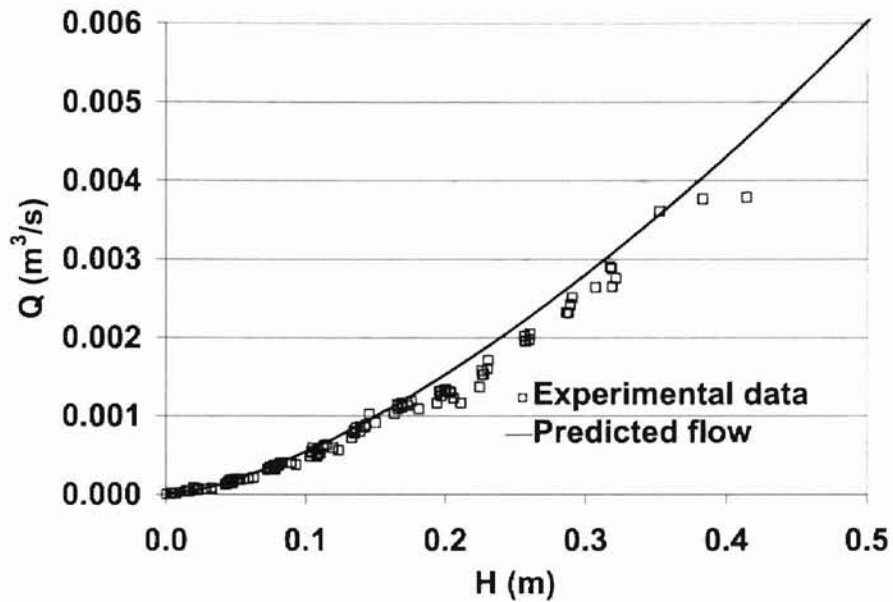


Figure 18: Clear-water flow prediction versus the experimental data for fabric C.



From visual observation of figures 16 thru 18, the clear-water flow equation does a reasonable job predicting flow through the fabrics. To evaluate the prediction equation further, the observed and predicted flow data for fabrics A, B, and C were plotted with figures 19, 20, and 21 illustrating them respectively.

Figure 19: Observed versus predicted clear-water flow for fabric A.

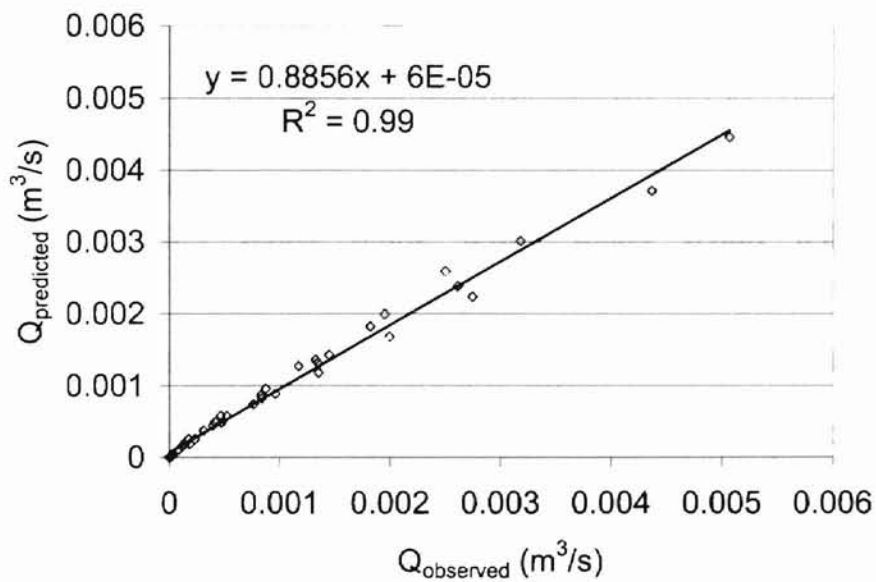


Figure 20: Observed versus predicted clear-water flow for fabric B.

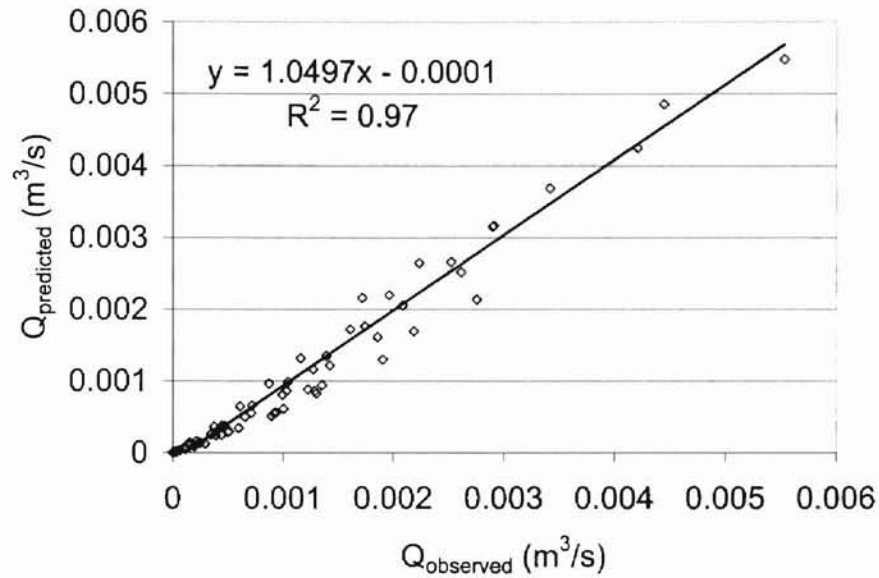
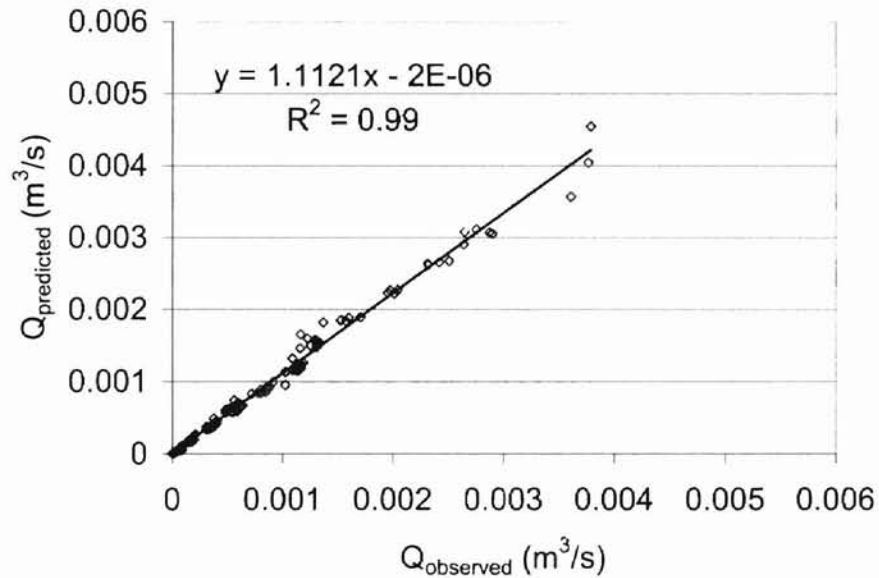


Figure 21: Observed versus predicted clear-water flow for fabric C.



A linear regression was performed on the observed versus predicted flow data, yielding correlation coefficients of 0.99, 0.97, and 0.99 for fabrics A, B, and C, respectively. Minor deviation from the line of best fit is observed, but is likely accounted for by the fabric variability. For example, the assumption was made

that the openings were uniform throughout the fabric. From visual examination of the fabric, the openings are not uniform because the fibers in the fabric shift easily, making some openings larger than others. Yet, the simplicity of the prediction equation allows the silt fence designer to evaluate the performance of the fabric based on the manufacturer's specifications rather than going through the difficult task of measuring each individual fabric opening. Although this procedure is not without error, it is simple and easy to apply.

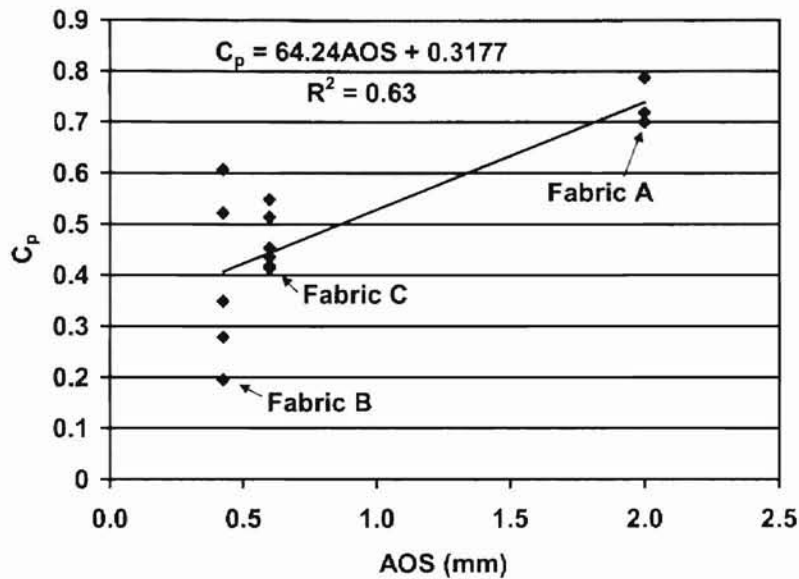
As observed in Appendix D, sediment clearly had an effect on the flow through the fabric. Sediment plugged some of the openings in the fabric causing flow restriction. To account for the influence of sediment, the clear-water flow equation was modified to include a plugging coefficient, C_p :

$$Q = C_p C' mA(2gH)^{0.5} \quad (4)$$

Like the area of the opening, C_p was back calculated for each test and plotted against the AOS of the fabrics. Figure 22 illustrates the linear regression performed on the parameters, which produced the following fit equation:

$$C_p = 64.24 AOS + 0.3177 \quad (5)$$

Figure 22: Linear relationship of the plugging coefficient and AOS.



Substituting equation 5 into equation 4, the sediment-laden flow through the each fabric was calculated. Figures 23, 24, and 25 depict the sediment-laden flow prediction and the experimental data for fabrics A, B, and C, respectively. From visual observation, the performance of fabrics A and C (Figs. 23 and 25) are reasonably predicted with this technique. The performance of fabric B (Fig. 24) was not predicted as well as the other two fabrics.

Figure 23: Sediment-laden flow prediction versus experimental data for fabric A.

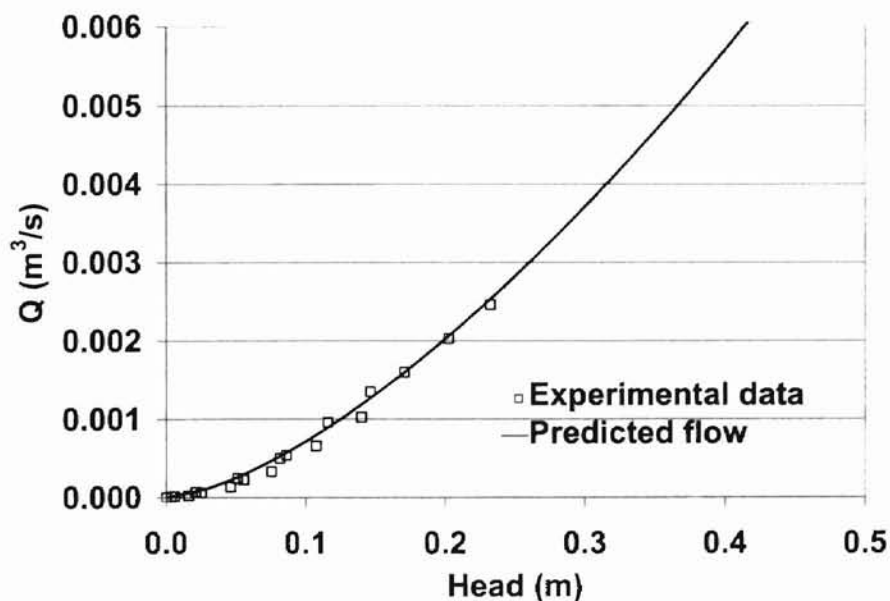


Figure 24: Sediment-laden flow prediction versus experimental data for fabric B.

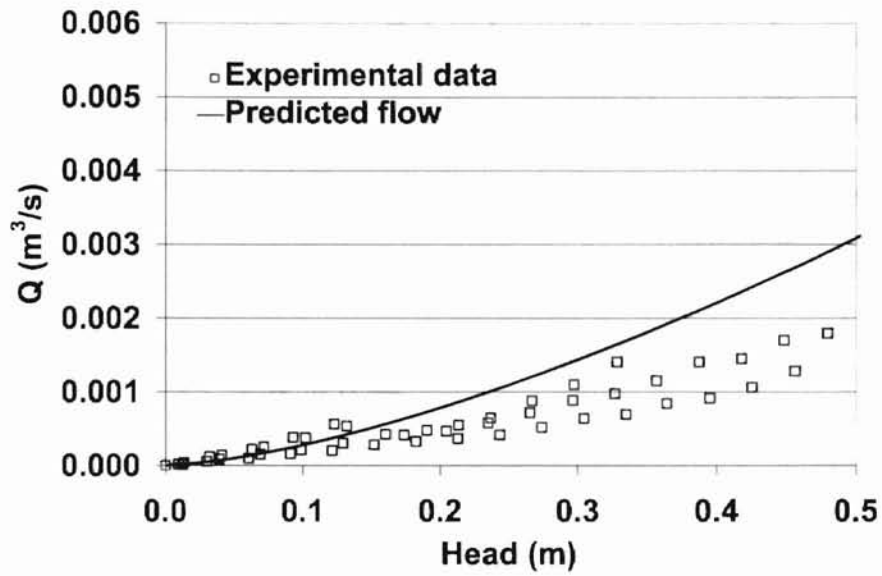
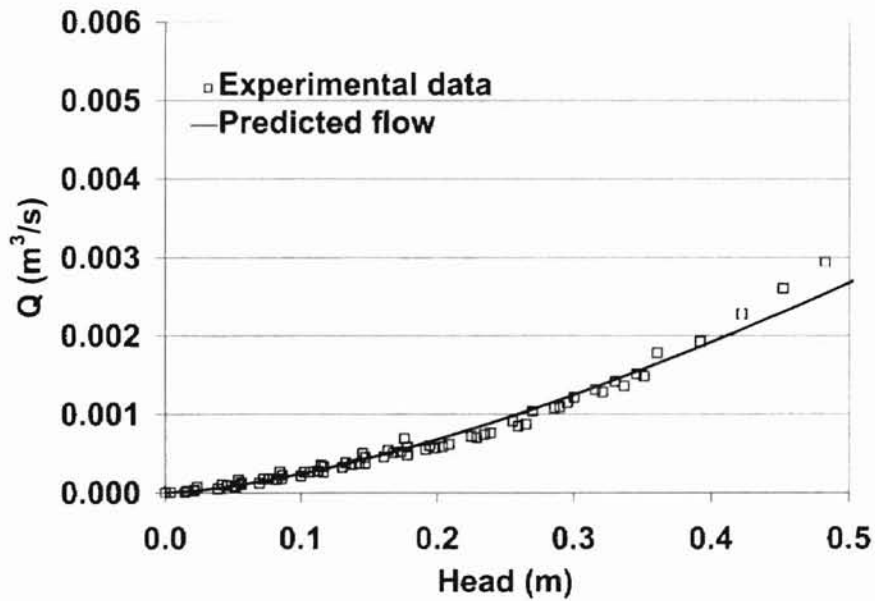


Figure 25: Sediment-laden flow prediction versus experimental data for fabric C.



To evaluate the observed and predicted sediment-laden flow more closely, plots of observed and predicted sediment-laden flow were developed, and a

linear regression was performed. Figures 26, 27, and 28 illustrate the observed and predicted sediment-laden flow for fabrics A, B, and C, respectively. With respect to fabric A, the correlation coefficient for sediment-laden flow is 0.99, while fabrics B and C have correlation coefficients of 0.93 and 0.98, accordingly.

Figure 26: Observed versus predicted sediment-laden flow for fabric A.

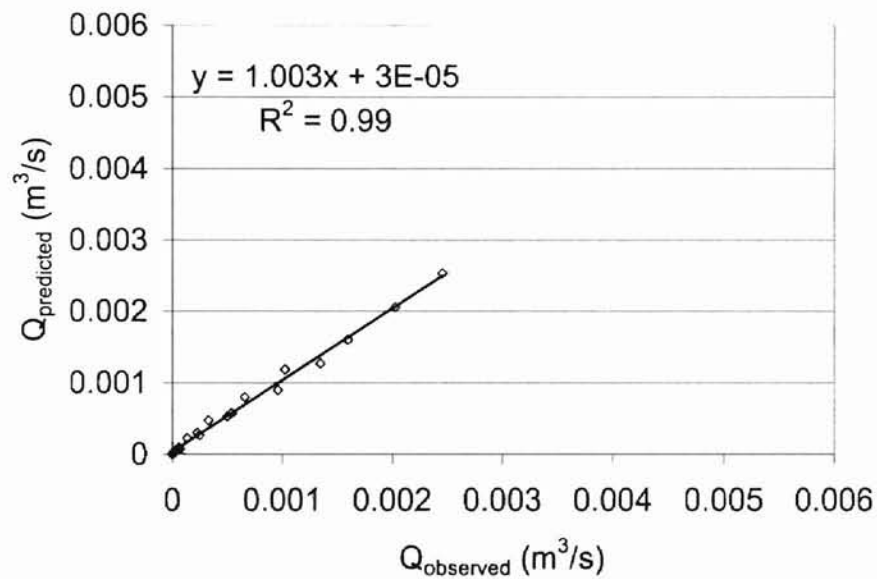


Figure 27: Observed versus predicted sediment-laden flow for fabric B.

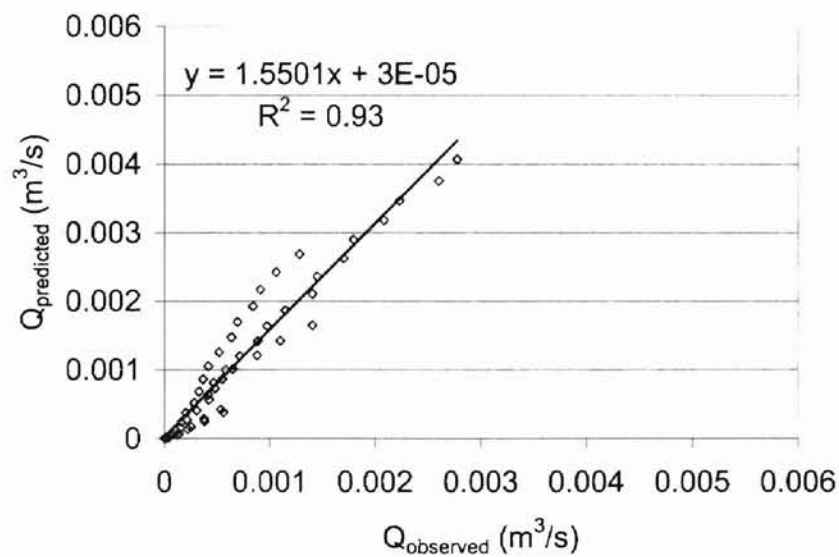
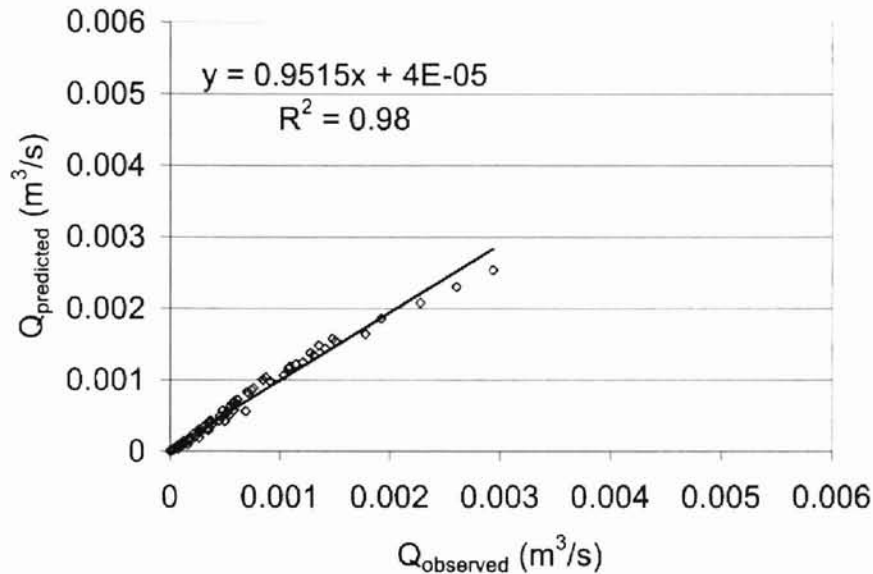


Figure 28: Observed versus predicted sediment-laden flow for fabric C.

Figure 28: Observed versus predicted sediment-laden flow for fabric C.



Many observations can be made from the simple fit of the sediment-laden flow equation to the experimental data. Upon closer examination, the prediction for fabric B (Fig. 24) does a reasonable job fitting the experimental data for the first 0.15 m (0.5 ft) of head, indicating that other factors influenced the flow through the fabric at higher impounded volumes. This influence is more apparent upon further inspection of figure 22, which shows more variation in the C_p for fabric B. Based on these results, it must be noted that the simple fit relationship does not account for the influence of sediment feed rate, inflow rate, particle size distribution, and fabric property changes. The observation was also made that fabrics A and C were not greatly influenced by sediment feed rate and/or inflow rate, resulting in less scatter of C_p , as shown in figure 22. Although further study may allow refinement of this relationship, it is important to note that fabric B has smaller openings than fabrics routinely installed in the field.

This simple silt fence flow model provides the designer and installer the tools necessary to evaluate the performance of the fabric prior to installing them in the field. By developing a relationship using fabric specifications provided by industry, the designer can make a more informed decision on which fabric to use. Let it be noted, however, that this research was limited to only three fabrics and one particle size distribution. More testing is recommended to evaluate the influence of particle sizes blocking the fabric openings, so future geotextile selection can also be based upon the eroded soil distribution found at a particular site.

Total Suspended Solids Concentrations

Grab samples collected during testing were evaluated for total suspended solids (TSS) concentrations, with table 5 summarizing the average of six upstream and six downstream samples collected during the tests. Initial entrance concentrations are also provided in table 5. Entrance concentrations were calculated based on the known sediment feed rate introduced into the known flow rate of water entering the flume.

As the sediment-laden flow moved towards the fabric, particles settled in the flume and TSS concentrations decreased. Grab samples in front of the fabric indicated average total suspended solids concentrations ranging from 519 to 11100 mg/L, while the average TSS concentrations exiting the fabric were slightly higher (Table 5). Lower concentrations observed in front of the fabric are believed to be a result of the sampling technique. The grab samples upstream of

the fabric were taken at approximately one-half of the impounded depth, and they do not represent a vertically integrated composite sample.

Table 5: Total suspended solids concentrations.

Test #	Fabric	Entrance Concentration (mg/L)	Ave. Concentration in Front of the Fabric (mg/L)	Ave. Concentration Exiting the Fabric (mg/L)
1	B	4510	1370	1500
2	B	41200	11100	11600
3	A	7000	2840	3000
4	A	35900	10700	12800
5	B	2010	519	563
6	A	2610	802	863
7	B	13600	3240	3310
8	A	15100	7360	7480
9	A	4310	1550	1670
10	A	9350	2950	3790
11	B	12500	3260	4070
12	B	7380	2200	2320
13	A	17700	6430	7390
14	B	16100	3810	5340
15	C	7000	1810	2150
16	C	19500	4830	5600
17	C	4840	1240	1490
18	C	12100	2870	3620
19	C	2440	757	900
20	C	15300	4110	4880
21	C	33800	6930	9570

For the same inflow rate and similar sediment loading rates, fabric B typically passed the lowest suspended solids concentration. Fabric A passed the highest concentrated flow, with fabric C passing concentrations close to that of fabric B. Since each test essentially had the same particle size distribution introduced in the flow, the following conclusions can be made about the TSS concentrations passing the fabrics.

Alphama State University, Ikenne

1. Since fabrics B and C have relatively small opening sizes, the detention time for the particles to settle increased, allowing a reduction in TSS concentrations.
2. Fabric A has more open area than the other two fabrics; therefore, the detention time for particles to settle is shorter. Higher concentrations and larger particle sizes were expected to pass through the fabric.

Particle Size Distributions

Each test was evaluated on the particle sizes passing the fabric. As indicated earlier, the bead mixture introduced in the flow had a make-up typical of a loam or silt loam soil. The particle size distribution of the bead mixture introduced in each test and the particle size distribution of the beads passing the fabric are depicted in Appendix E. Tests 12 and 13 are omitted from the analysis because samples were mistakenly discarded.

The particle size distributions describe the characteristics of the particles trapped by the fabrics and those passing the fabrics. From the plots in Appendix E, the conclusion was drawn that all of the fabrics trapped 90% of the sand-sized beads, those particles greater than 0.075 mm in diameter. For fabric A (Nilex 2127), coarse silt particles passed with ease through the fabric. Settling velocity and overflow rate explain this behavior. As flow depth increases, the surface area increases thus overflow rate decreases. Trapping efficiency is proportional to settling velocity per overflow rate.

The plots in Appendix E also illustrate that the majority of the clay component of the original mix escaped through fabric A. The concept of settling

Mohammed Othman Al-Muradhi / 1/1/2011

velocity and overflow rate explains the loss of clay as well. Because clay has small particle diameters, the settling velocity is slow. Additionally, fabric A has larger openings, resulting in a decrease of flow depth and surface area. A decrease in both settling velocity and surface area lead to a decrease in trapping efficiencies for clay particles.

Upon examining the particle size distributions for fabric B (Nilex 915), the results were dramatically different from fabric A. All plots show that 95% or more of the sand particles were trapped by the fabric. For the sediment passing fabric B, 80% of the particles were 0.035 mm in diameter or less. It is recognized that a high percentage of the clay component passed through the fabric, while coarser silt particles became trapped. This tight weave fabric dramatically altered the initial particle size distribution because flow impoundment increased, resulting in a decrease in overflow rate.

The particles passing fabric C were similar to those passing fabric B. Fabric C trapped nearly all of the sand material. Eighty percent of the particles passing the fabric were smaller than 0.03 mm in diameter, with the majority of the clay particles escaping through the fabric. Like fabric B, fabric C was selective in which glass beads were passed.

Regardless of which fabric is selected for silt fence design, the sand component of the soil can be successfully trapped. Silt and clay size particles in their eroded form create more of a challenge for silt fence, yet they too can be trapped in an aggregated form. Since fabrics B and C had less open area, more particles had the potential to plug the openings and increase the hydraulic head

Mohammed Othman / M. Othman / M. Othman

on the fabrics, whereas fabric A did not have this problem. Further study could determine the influence particle size has on fabric plugging and could further assist the designer on selecting geotextiles to trap particular soil types.

Trapping Efficiencies

Final analysis of the fabric performance was based on their trapping efficiencies (Table 6). The average trapping efficiency for fabrics A, B, and C were 55, 66, and 65%, respectively. For seven tests on each fabric the standard deviation for fabrics A, B, and C was 7.08%, 5.93%, and 4.89%, respectively. More sediment was trapped as the impounded volume increased.

Table 6: Summary of trapping efficiencies.

Test #	Fabric	Trapping Efficiency (%)
1	B	68
2	B	76
3	A	56
4	A	68
5	B	64
6	A	56
7	B	75
8	A	46
9	A	50
10	A	58
11	B	63
12	B	63
13	A	49
14	B	62
15	C	65
16	C	68
17	C	63
18	C	64
19	C	59
20	C	68
21	C	74

Misham Data / Infrared / Thermo

Although the flow passing through each fabric was dramatically different, the fabrics on average still trapped approximately the same amount of sediment. Similar results in fabrics B and C were expected because the openings in fabrics B and C were smaller than fabric A, restricting more flow and allowing more detention time for the particles to settle. Fabric A passed higher flows at smaller impounded heads because it had larger openings for the flow to move through. Therefore, it is not surprising that fabric A also passed more material.

Compared to previous research results, the trapping efficiencies reported from this study are considerably lower. Higher trapping efficiencies indicated in other research are linked to the fabric types and sediment sizes used in the studies. In many instances, nonwoven geotextiles were tested with the sand component of a soil as the test sediment. Silt fences are more typically constructed of a woven geotextile and exposed to natural particle size distributions ranging from clay to sand size particles. Therefore, it is believed that the results reported in this study represent a broader range of soil found at typical construction sites.

7/1/2014 10:44 AM Nathan J. Thompson

CHAPTER VI

SUMMARY AND CONCLUSIONS

Summary

Sediment in agriculture and urban runoff is the leading pollutant contaminating our water sources today. Because of the ecological and economic effects sediment deposition has on streams, rivers, lakes and other waterways, it is necessary to recognize the importance of sediment controls such as silt fences. In this study, a first generation model was developed to predict the effectiveness of silt fences at separating sediment from runoff water. Although this model could effectively help the designer select geotextiles for silt fence applications, it needs to be tested and validated for additional fabrics and particle size distributions.

A review of literature indicated several research studies conducted on silt fence products. Most studies report high trapping efficiencies, which is rarely seen in real-world silt fence applications. These high trapping efficiencies are attributed to many experiments evaluating nonwoven fabrics, which are non-typical of current silt fence designs. Additionally, researchers limited fabric evaluation to one component of a test soil such as sand. As observed in this study, nearly all sand would be trapped regardless of the fabric used. While these studies provide valuable information, little research has examined the influence of soil particles on flow through the fabrics.

The performance of three woven silt fence products was examined for a range of flow rates and sediment feed rates. Flow through the fabric along with

Michigan State University

total suspended solids concentrations, particle sizes passing the fabric, and trapping efficiencies were measured to determine the effectiveness of the fabrics in removing sediment from runoff water.

The fabrics were exposed to both clear-water and sediment-laden flow conditions. A modified orifice equation was developed to predict the clear-water flow through the fabric for a given hydraulic head.

Since sediment has a dramatic influence on the flow behavior through woven geotextiles, modification to the clear-water equation is needed to account for the influence of sediment. Sediment has a greater influence on fabrics with smaller openings than fabrics with larger openings. The clear-water flow equation developed herein was altered to evaluate the performance of the fabrics exposed to sediment-laden flow by incorporating a plugging coefficient in the equation. This simple fit relationship was developed for only one particle size distribution and may not be applicable to others. However, this model is a first attempt to assist designers in evaluating silt fence fabrics.

Dramatic differences were observed in how these fabrics pass flow. The fabrics also exhibited the ability to selectively trap different sediment sizes. For instance, fabric A continually passed higher concentrations and larger particle sizes than the other two fabrics. This was expected since fabric A had larger openings and impounded smaller volumes. If a designer selected fabrics based solely on the trapping efficiency and the fabric flow rate, fabric A would be selected because more flow can pass through the fabric at lower heads, while trapping only 10% less sediment than the other two fabrics. While it is

Michigan State University

recognized that the other two fabrics trapped more material and reduced the sediment concentrations in the runoff, the overtopping potential of the structure would influence the final silt fence selection.

Conclusions

The clear-water and sediment-laden flow equations did reasonable jobs of predicting the flow through three woven geotextile fabrics. More variation was observed in fabric B, which was more tightly woven and had the smallest AOS. The inflow rate, sediment-loading rate, and/or particle size distribution may be responsible for the observed variation of flow behavior through this particular fabric. Inflow, sediment-loading, and particle size distribution did not greatly influence the flow through fabrics A and C. Although additional research may improve this method, it is recognized that fabric B is less frequently used in silt fence design.

The introduction of sediment dramatically reduced flow through fabrics B and C, while sediment did not dramatically reduce flow through fabric A. Fabric A had larger openings, allowing more flow at higher concentrations. Additionally, larger particles passed through Fabric A. Fabrics B and C trapped more sediment because sediment plugging the fabric openings caused the impounded volume and detention time to increase allowing more particles to settle.

This research provides information necessary to select a geotextile based on the flow behavior of the fabric. The designer can determine which fabric is likely to overtop by evaluating the fabric opening size. If the designer plans on long-term use of the silt fence, fabric A in this report would be recommended

Michigan State University

because it would be less likely to overtop and would trap almost as much material as fabrics B and C. However, the flow through fabric A would have higher sediment concentrations and would likely discharge larger particle sizes. If the silt fence is used for short-term projects, fabrics B and C would be possible solutions, since nearly all of the sand and coarse silt materials were trapped. Less concentrated flow was passed through these fabrics, yet the observation was made that the particles plugged more fabric openings, impounding more runoff volume behind the fence. Therefore, the potential for overtopping and flanking would need to be carefully considered.

Recommendations for Future Studies

The clear-water and sediment-laden flow equations can be valuable tools for selecting geotextile fabrics for silt fence design. Testing additional fabrics would be important to refine this approach. Since fabric B is less frequently used in silt fence designs, further examination of the influence of inflow rates, sediment loading rates, particle size distributions, and flow through this fabric may not be necessary. However, to achieve a better understanding of how silt fence selectively separates sediment from the runoff water, variations in particle sizes, inflow rates, and sediment loading rates are recommended.

Additionally, this study limited the tested sediment to glass beads, which did not have the chemical composition nor the particle shape of natural soil like that of angular silt particles and platy-like clay. Real soil may add an element of complexity in the flow prediction because of organic material and other

Michigan State University

compounds present in the soil. Yet, it would be helpful to evaluate the fabrics using natural soil materials.

According to the Federal Highway Administration (1998), silt fence has a life expectancy of 6 months in the field. Testing silt fence under cycling events could indicate whether the dried sediment trapped within the fabric has a continued influence on the flow through the fabric. This testing could determine if the sediment is washed from the fabric by rainfall or when the flow initially impounds against the fabric. Additionally, the impact of flow duration should be evaluated to examine how silt fence responds to cyclic loading.

By coincidence, the fabric weave patterns in this study were the same and were classified as plain weaves. More testing should be conducted on other fabrics of different weave patterns to evaluate if and how weave patterns influence fabric performance.

Field tests conducted on silt fence would be helpful to the designer because it could develop better guidelines for burying the toe of the fabric, spacing the stakes, and selecting the types of stakes. Currently, standards vary among regulatory agencies on silt fence installation techniques. Evaluating the depth of rills close to a silt fence could determine the depth for burying the fabric toe. Likewise, measuring the loading on the stakes could determine what type of stakes to use or how to space them. Field evaluation of silt fences could address issues about proper silt fence installation practices.

In the early stages of this research, the probability of an opening plugged by sediment was discussed. Although this research study does not address this

statistical approach, a probability based examination of fabric plugging could provide valuable information on how different particle size distributions affect flow through the fabrics. An image analyzer could be used to evaluate the fabric before and after testing. For instance, individual openings could be measured using an image analyzer prior to testing, and again after testing to determine whether the opening was plugged.

As suggested, many directions may be taken to continue silt fence research. The first generation model developed by this research is only a start. Additional, field and laboratory research are recommended to provide supplemental assistance on fabric selection and installation protocol.

Final Report
Silt Fence Research
Final Report

BIBLIOGRAPHY

- Annual Book of ASTM Standards*. 1992. D 4491. Standard test methods for water permeability of geotextiles by permittivity. West Conshohocken, PA: ASTM.
- Annual Book of ASTM Standards*. 1995. D 4751. Standard test method for determining apparent opening size of a geotextile. West Conshohocken, PA: ASTM.
- Annual Book of ASTM Standards*. 1998. D 422. Standard test method for particle-size analysis of soils. West Conshohocken, PA: ASTM.
- Annual Book of ASTM Standards*. 1998. D 1140. Standard test method for amount of material in soils finer than the No. 200 sieve. West Conshohocken, PA: ASTM.
- Barrett, M. E., J. E. Kearney, T. G. McCoy, J. F. Malina, R. J. Charbeneau, and G. H. Ward. 1995. An evaluation of the performance of geotextiles for temporary sediment control. Austin, TX: Center for Research in Water Resources, College of Engineering, The University of Texas at Austin.
- Brady, N. C. and R. R. Weil. 1999. *The Nature and Properties of Soils*. New Jersey: Prentice Hall, Inc.
- Britton, S. L., K. M. Robinson, B. J. Barfield, and K. C. Kadavy. 2000. Silt fence performance testing. ASAE Paper No. 002162. St. Joseph, Mich.: ASAE.
- Environmental Protection Agency (EPA). 1998. The quality of our nation's waters, a summary of the national water quality inventory: 1998 report to congress. Environmental Protection Agency, EPA841-S-00-001.
- Federal Highway Administration (FHWA). 1998. *Geosynthetic Design and Construction Guidelines Participant Handbook*. McLean, Virginia: National Highway Institute.
- Fisher, L. S. and A. R. Jarrett. 1984. Sediment retention efficiency of synthetic filter fabrics. *Transactions of ASAE* 27(2): 429-436.
- Haan, C. T., B. J. Barfield, and J. C. Hayes. 1994. *Design Hydrology and Sedimentology for Small Catchments*. San Diego, CA: Academic Press, Inc.

- Herzog, M., J. Harbor, K. McClintock, J. Law, and K. Bennett. 2000. Are green lots worth more than brown lots? An economic incentive for erosion control on residential developments. *J. of Soil and Water Conservation* 55: 43-48.
- Koerner, R. M. 1998. *Designing with Geosynthetics*. New Jersey: Prentice Hall, Inc.
- Kouwen, N. 1990. Silt fences to control sediment movement on construction sites. Downsview, Ontario: The Research and Development Branch Ontario Ministry of Transportation.
- Linsley, R. K. Jr., M. A. Kohler, and J. L. H. Paulhus. 1958. *Hydrology for Engineers*. New York: McGraw-Hill Book Company, Inc.
- Mlynarek, J. and G. Lombard. 1997. Significance of percent open area (POA) in the design of woven geotextile filters. In *Proc. of the Geosynthetics Conf.*, 1093-1107. Long Beach, Ca., 11-13 March.
- Natural Resources Conservation Service (NRCS), formerly Soil Conservation Service (SCS). 1977. *National Engineering Handbook*. Washington, D. C.: U. S. Department of Agriculture.
- Nilex Corporation. 2000. Nilex silt fence technical specifications. <http://www.nilex.com>. Englewood, CO: Nilex Corporation.
- North Carolina Sedimentation Control Commission (NCSCC). 1993. Practice standards and specifications: sediment traps and barriers. In *Erosion and Sediment Control Planning and Design Manual*, ch. 6.60.1-6.63.3. North Carolina Sedimentation Control Commission.
- Plonsker, H., personal communication from AGSCO Corporation, Wheeling, Illinois, 3 November 1999.
- Quantachrome Corporation. 1998. *Microscan II Particle Size Analyzer Operator Manual*. Boynton Beach, Florida: Quantachrome Corporation.
- Richardson, G. N. and P. Middlebrooks. 1991. A simplified design method for silt fences. In *Proc. of the Geosynthetics Conf.*, 879-888. Atlanta, Ga., 26-28 February.
- Sherwood, W. C., and D. C. Wyant. 1976. Installation of straw barriers and silt fences. Charlottesville, Virginia: Virginia Highway and Transportation Research Council.

- Smith, J. L., S. K. Bhatia, J. Ridgeway, and W. Hawkings. 1999. Are porosity and O_{95} important in the retention and particulate clogging behavior of geotextiles? In *Pro. Of the Geosynthetics Conf.*, 813-832. Boston, Mass., 28-30 April.
- Smoot, J. L. and R. D. Smith. 1998. Soil erosion prevention and sediment control: reducing nonpoint source water pollution on construction sites. <http://www.engr.utk.edu/research/water/erosion/titlepage.html>. Knoxville, Tennessee: University of Tennessee Department of Civil and Environmental Engineering.
- Theisen, M. S. 1992. The role of geosynthetics in erosion and sediment control: an overview. *J. Geotextiles and Geomembranes* 11: 535-549.
- Waters, T. F. 1995. *Sediment in Streams: Sources, Biological Effects, and Control*. Bethesda, Maryland: American fisheries Society.
- Wilson, B. W., B. J. Barfield, I. D. Moore, and R. C. Warner. 1984. A hydrology and sedimentology watershed model: Part II. sedimentology component. *Transactions of ASAE* 27(5): 1378-1384.
- Wishowski, J. M., M. Mamo, and G. D. Bubenzer. 1998. Trap efficiencies of filter fabric fence. ASAE Paper No. 982158. St. Joseph, Mich.: ASAE.
- Wyant, D. C. 1980. Evaluation of filter fabrics for use as silt fences. Charlottesville, Virginia: Virginia Highway and Transportation Research Council.

APPENDICES

APPENDICES

APPENDIX A

Operating Procedure for Microscan II

1. Prior to operating the PSA, radiation safety training should be taken; otherwise, use of the PSA is unauthorized.
2. Sign the login sheet located in the operator's manual located on top of the PSA prior to turning on the PSA.
3. Allow the PSA to warm up for 20 minutes before using by turning on the main switch located on the back left side of the analyzer and then by pressing the electronics button on front. Wait approximately 10 seconds then press the X-ray button located on the front of the machine.
4. The computer software utilized by the PSA is Microscan PSA2PC Version 3.0. To open the software package, go to windows explorer, C:\ drive, and the Msc2 file folder. Click on the Msc2pc.exe to execute the program (do not use the icon on the desktop).
5. As the analyzer warms up, sample parameters may be set by going to the parameters menu. Since the sample being analyzed is beads (representative sediment), set the parameters to soil.par.
6. After selecting soil.par, the computer will automatically go to the next window. By selecting A (data acquisition parameters), the user has the option to set the operation parameters. For instance, the maximum diameter, minimum diameter, and the specific gravity of the sample may be set under this menu. Remember never to use samples with particles larger than 300 microns because particles larger than that size have been known to clog the PSA's tubing. Other parameters such as viscosity, temperature, fluid density may be left at their default setting. After entering the necessary parameters, press escape to go back to the previous window and save the soil.par file (choice C). Press Y to overwrite the soil.par file.
7. After the soil.par file has been saved, the computer will automatically go back to the main menu. From the main menu, go to the data acquisition menu. From this menu, the following information may be entered: operator, sample preparation notes, sample description, and other comments.
8. A file name will be entered as default, or it may be changed to keep better track of the information. The default name incorporates the month, day, and sample number ran. For instance, the file name SA092002.MRD means the sample was ran on September 20, with 02 labeling the second sample ran for that day. The .MRD extension stands for Microscan raw data. This file type may be opened in another program such as Excel or Notepad as a text file.
9. On the data acquisition menu, verify that the load operation parameter file is soil.par. Then verify that the operation parameters are the same settings predetermined in step 3.

10. Once the analyzer has warmed up, pour approximately 50 mL of deionized water in the sample cell located in front of the analyzer. The pump speed dial should be set to 5 in the 12 o'clock position. Then press the pump circulation button (middle black button above the pump speed dial).
11. After circulating deionized water through the system, press the stop button located to the left of the circulation button on the front of the analyzer. Then flush the system by flipping the fill level switch located on the left side of the machine. Refill the sample cell with 50 mL of deionized water.
12. After refilling the sample cell, start the analysis from the data acquisition menu on the computer by pressing S. The analyzer will automatically go through a series of steps to initialize its settings. For instance, it will measure a "no flux" value and "max flux" value, locate the top of the cell, and go through a bubble removal routine.
13. After these steps, the computer will begin reading a delta flux. If the bubble removal was successful, the delta flux values read $0 \pm 1\%$. If the PSA is unable to remove bubbles, the delta flux will read high values and will automatically abort the analysis. At this point, the computer will automatically go back to the data acquisition menu. Press R to repeat analysis, which essentially restarts the analysis under the same fill name as used before.
14. Once the bubble removal is a success and the delta flux reads values around 0%, the system will eventually stabilize and automatically go to the next set of readings. The next readings are the flux which should read $100 \pm 1\%$. At this point, the sample may be added to the sample cell. For optimal results, samples should be approximately 7.5 g.
15. The addition of the sample will drop the flux to usually 86%. According to the operational manual located on top of the PSA, the analysis cannot start until the flux is below 95%. When the flux stabilizes within 0.5% of the dropped flux value, activate the computer to take readings by pressing R.
16. The analysis of the sample takes approximately 6.5 minutes. As the sample is being analyzed, the computer screen will show a plot of the particle size distribution.

17. After the analysis, the computer will display the choice of Y for cleaning or N for the menu. By pressing Y, the system will automatically go through a cleaning cycle where the contaminated water is drained from the system into a drain container (place in the floor so the contaminated water can easily flow into it). Fresh deionized water will then enter the system automatically from the supply container. If the water appears cloudy after the cleaning cycle, the water may be flushed from the system by flipping the fill level switch on the left side of the machine. If this process is needed, another 50-mL of deionized water must be added to the sample. By pressing N and returning to the menu, the analysis may be repeated on the same sample.
18. The data is stored on the C:\ drive in the Msc2 file folder under the data folder. The files may be copied from this location onto a disk. Files are typically 7KB; therefore, they can be easily stored on 3.5" floppies.
19. The files report the ratio of the mass passing corresponding to a given particle diameter in microns. These files may be opened in Excel; however, the data structure will have to be manipulated. For instance, Excel opens the file with all of the information in column A. To divide the data into columns, go to the data menu and then to "text to columns." A Wizard to Columns dialog box should appear. Check the box fixed width, and press next. Then click on finish. The data will then be divided into workable columns.
20. Since the mass passing is reported as a ratio, multiply the column by 100% to report the mass passing as a percentage. Then graph the percent passing versus the diameter of the particle.
21. After the tests, flush the system with deionized water by flipping the fill level switch on the left side of the machine. Close the fill level switch and fill the sample cell with deionized water again. Repeat this flushing process until the beads are completely drained from the system. Beads are flushed from the system when no visual traces are shown in the drain line.
22. Clean the sample cell thoroughly, draining all water from the cell by flipping the fill level switch to open. Once the machine is clean, turn off the X-ray and electronics by pressing the appropriate buttons located on front of the analyzer. Then turn off the main switch located in the back of the PSA.
23. Log out on the log sheet located in the operator's manual on top of the PSA.

APPENDIX B

Hydrometer and Sieve Analysis Procedure

ASTM 422 was followed for the hydrometer portion of the test, while ASTM 1140 Method A was followed for the wet sieve analysis of the samples.

Equipment

1. ASTM Hydrometer (152H model)
2. Balance sensitive to 0.01 g
3. Beakers (250-mL)
4. Dispersing agent (NaPO_3 , otherwise known as Calgon)
5. Distilled water
6. Sedimentation cylinder (1000-mL graduated cylinder)
7. Stirring apparatus (malt mixer)
8. Thermometer sensitive to 0.5 °C
9. Stopwatch
10. Set of sieves, ranging in size from 2 mm (AOS No. 10) to 0.075 mm (AOS No. 200)
11. Soil drying oven

Procedure

1. Prepare a blank by pouring 125 mL of NaPO_3 (40 g of Calgon per 1000 mL of distilled water) into 875 mL of distilled water into a 1000 mL graduated cylinder. Insert the hydrometer into the blank and take a zero reading and a meniscus reading. A temperature reading should also be taken.
2. Prepare the soil sample by weighing approximately 50-g of sample and soaking it in a 250 mL beaker containing 125 mL of NaPO_3 (40 g of Calgon per 1000 mL of distilled water) for approximately 16-hours.
3. After soaking, carefully transfer the sample to a dispersion cup and add distilled water until the cup becomes 2/3 full. Stir the contents of the cup with a malt mixer for 1 minute.
4. After dispersion, transfer the contents to a 1000-mL graduated cylinder, and add distilled water until the total volume becomes 1000-mL.
5. Place a stopper over the open end of the cylinder, and agitate the sample by inverting the cylinder back and forth for one minute.

6. Insert a 152H hydrometer in the sedimentation cylinder and begin taking readings at the following times: 30 seconds, 1, 2, 5, 15, 30, 60, 250, 430, and 1440 minutes.
7. Temperature readings of both the soil sample and the blank should be taken at the specified times given in step 6. The temperature of the contents makes corrections to the hydrometer readings.
8. After the hydrometer analysis, pour the contents of the sedimentation cylinder into a stack of sieves. Wash the sample through the stack with distilled water.
9. Transfer the portion of sample retained on each sieve to a beaker and oven-dry for at least 24 hours.
10. After drying, weigh the sample. This data combined with the hydrometer data can be used to calculate the percent of soil passing by weight.

APPENDIX C

Plots of Impounded Head versus Time

•
•
•
•
•

Figure C. 1.

Head versus Time
Test 1: Nilex 915

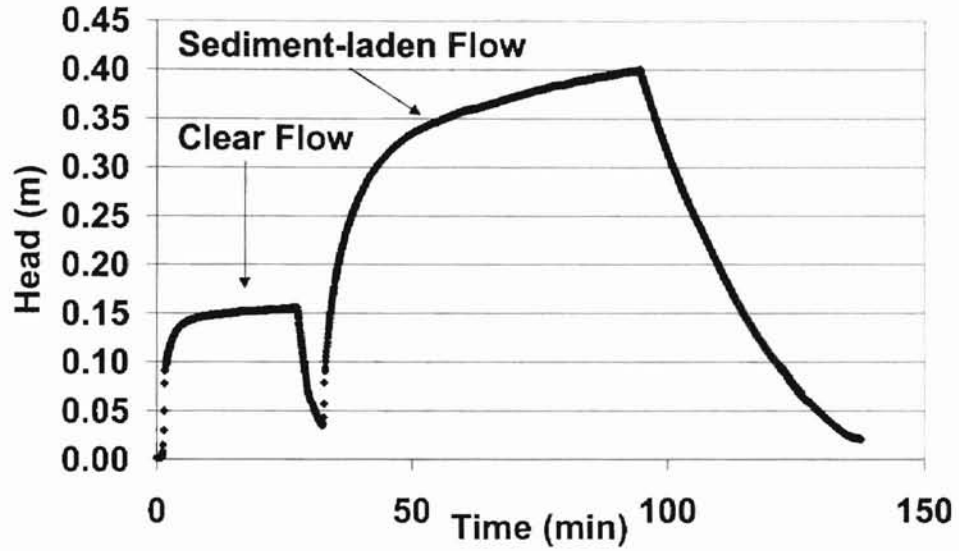


Figure C. 2.

Head versus Time
Test 2: Nilex 915

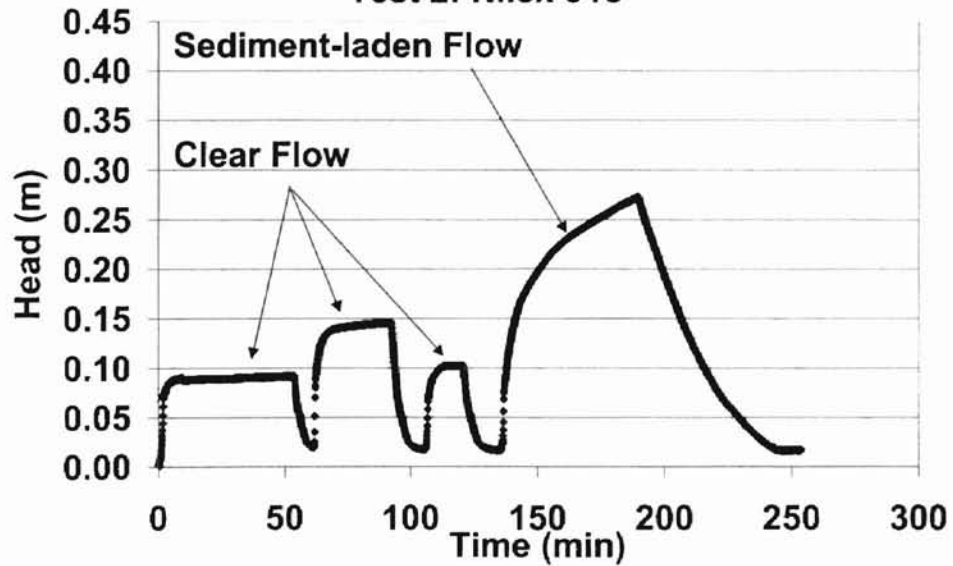


Figure C. 3.

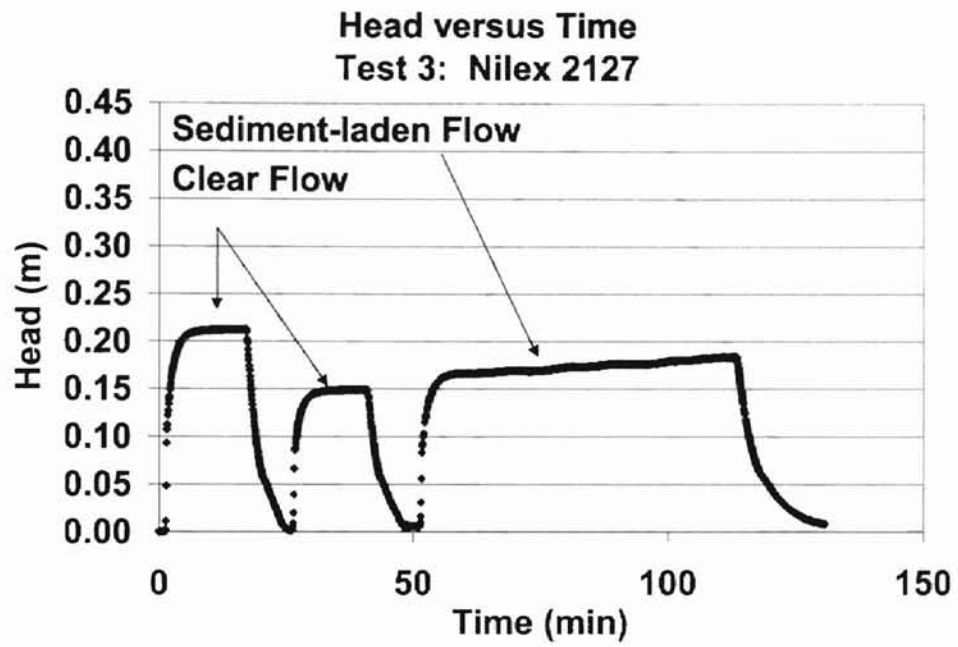


Figure C. 4.

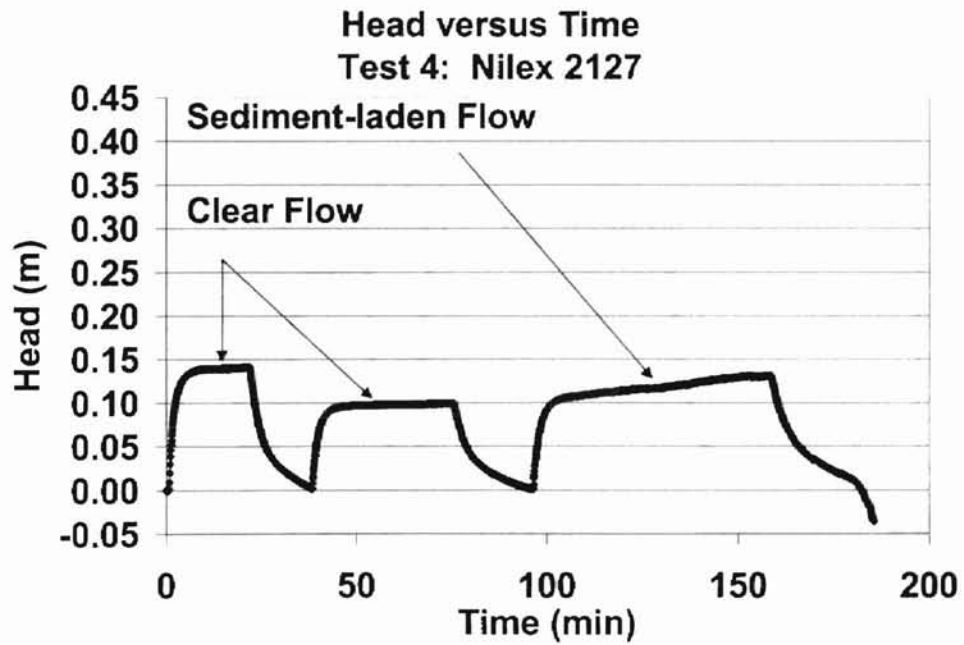


Figure C. 5.

Head versus Time
Test 5: Nilex 915

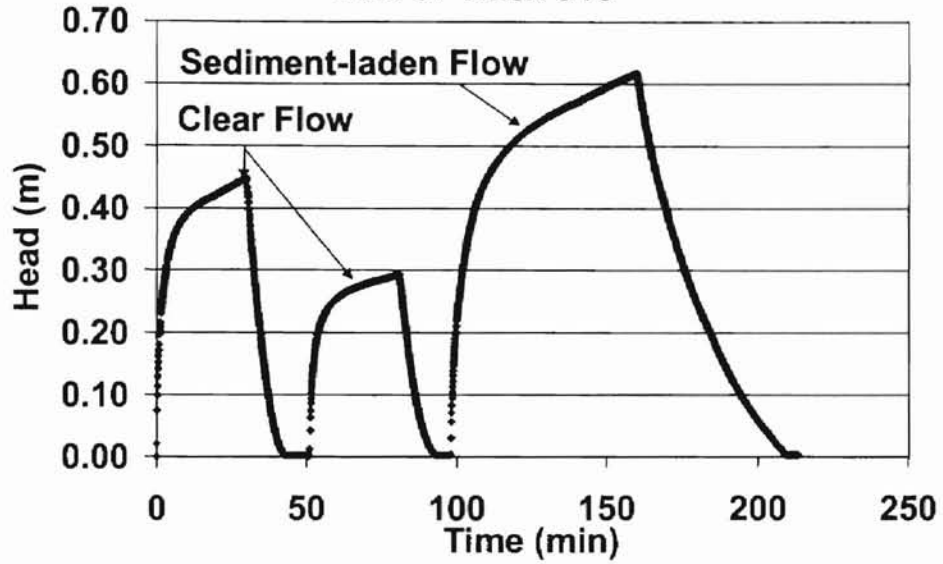


Figure C. 6.

Head versus Time
Test 6: Nilex 2127

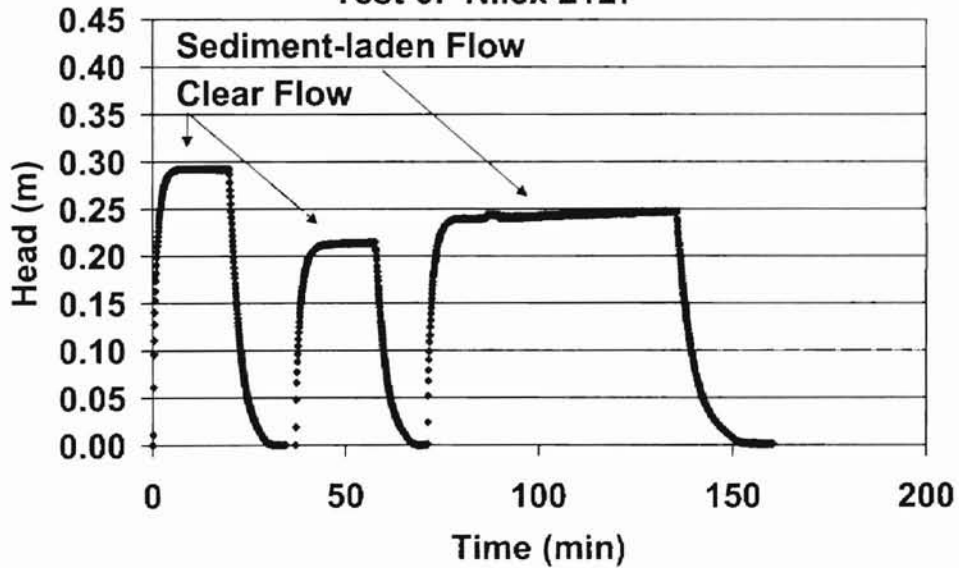


Figure C. 7.

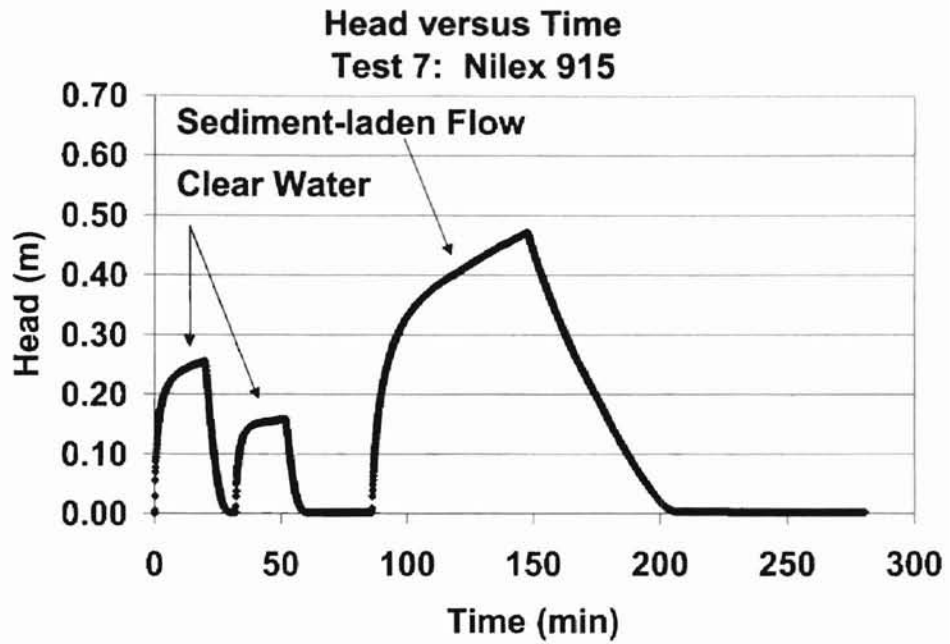


Figure C. 8.

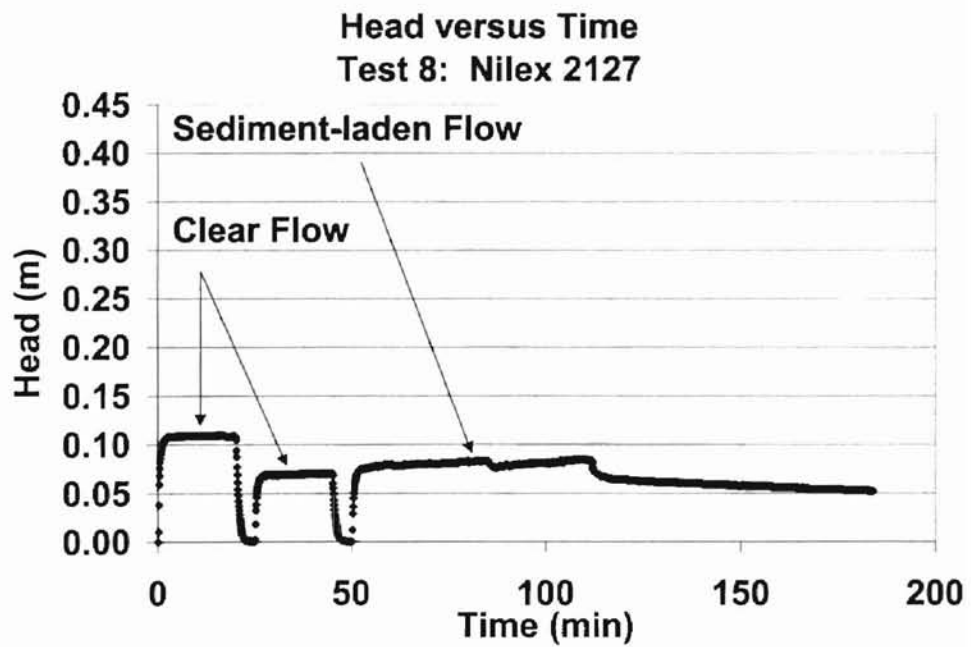


Figure C. 9.

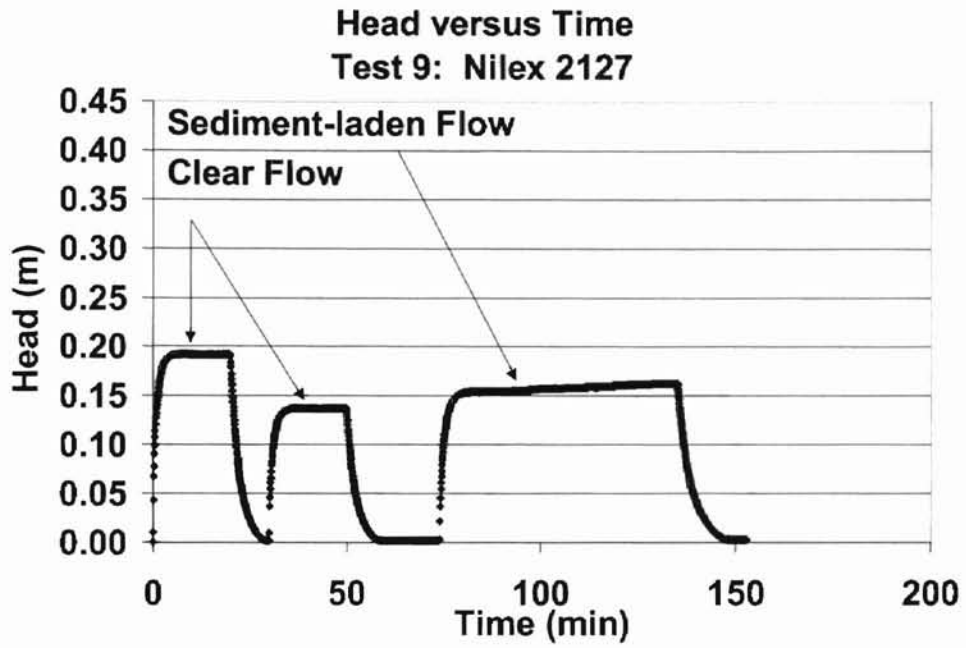


Figure C. 10.

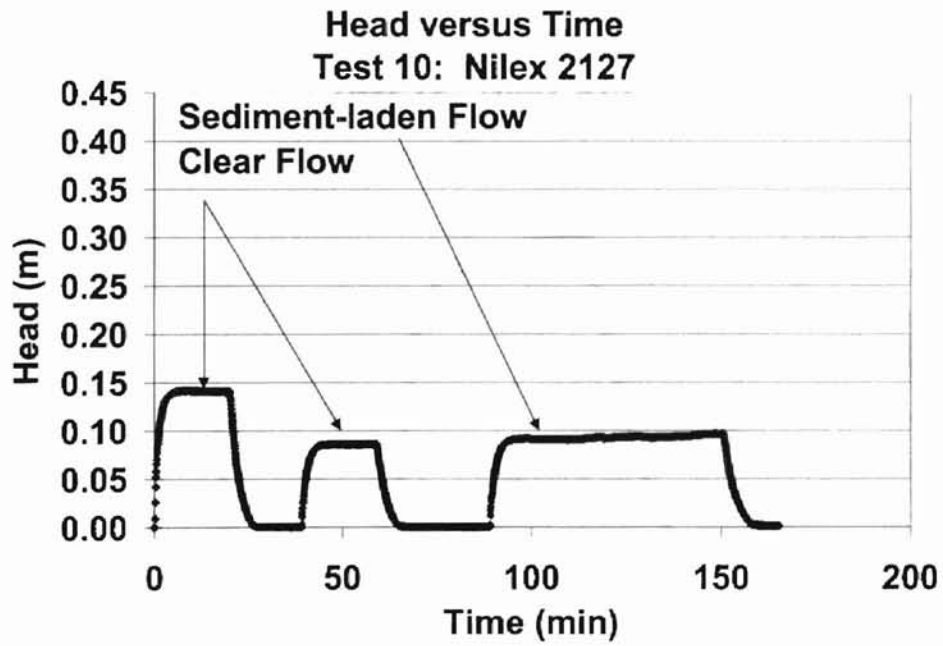


Figure C. 11.

Head versus Time
Test 11: Nilex 915

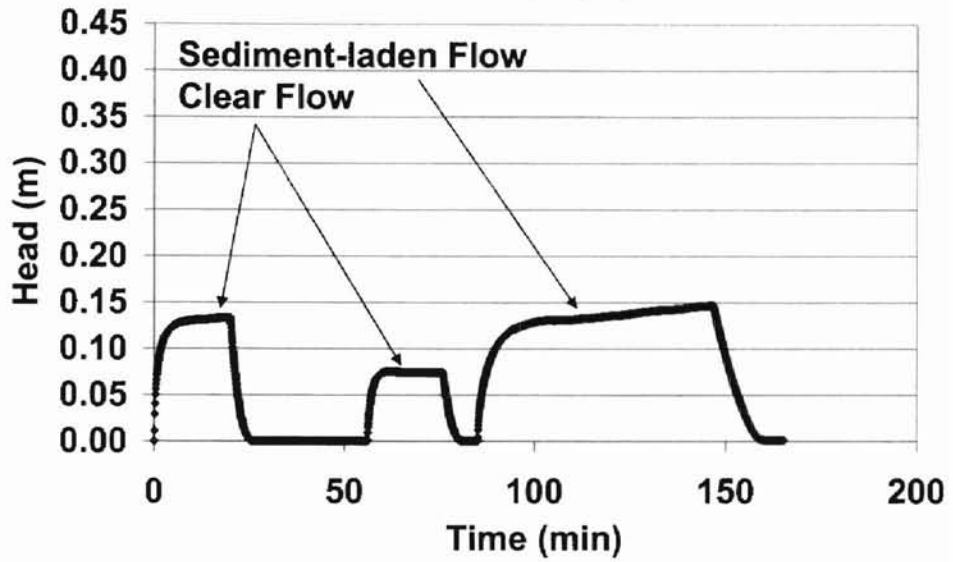


Figure C. 12.

Head versus Time
Test 12: Nilex 915

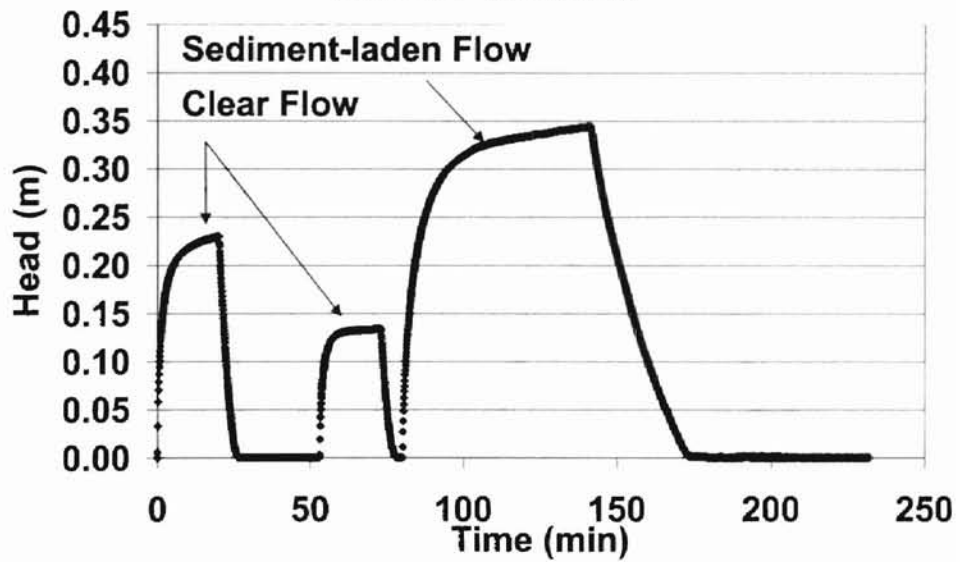


Figure C. 13.

Head versus Time
Test 13: Nilex 2127

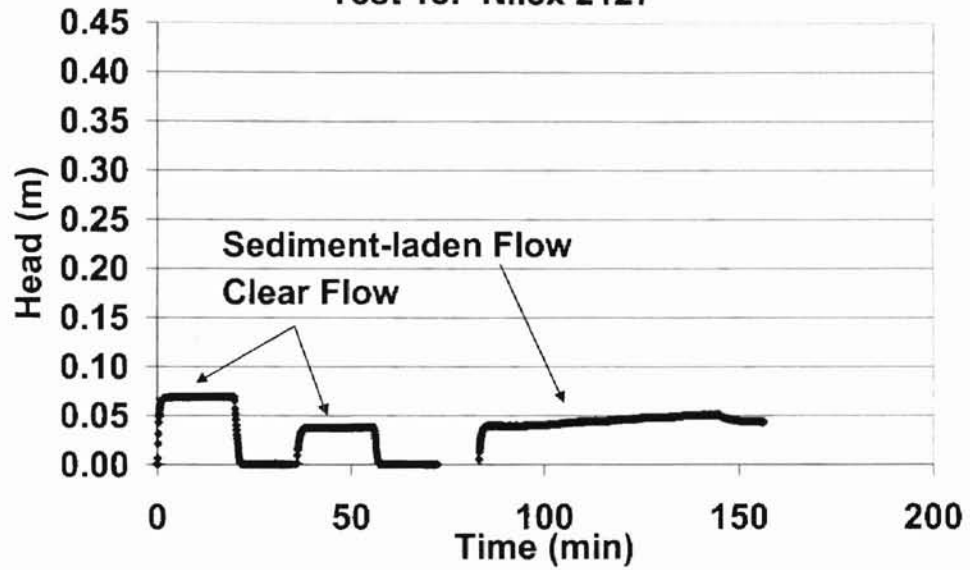


Figure C. 14.

Head versus Time
Test 14: Nilex 915

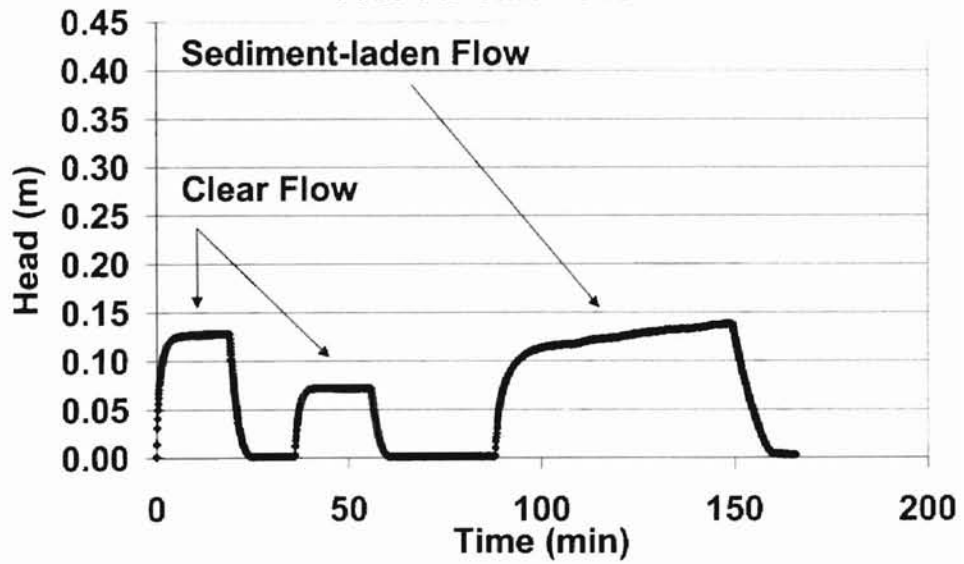


Figure C. 15.

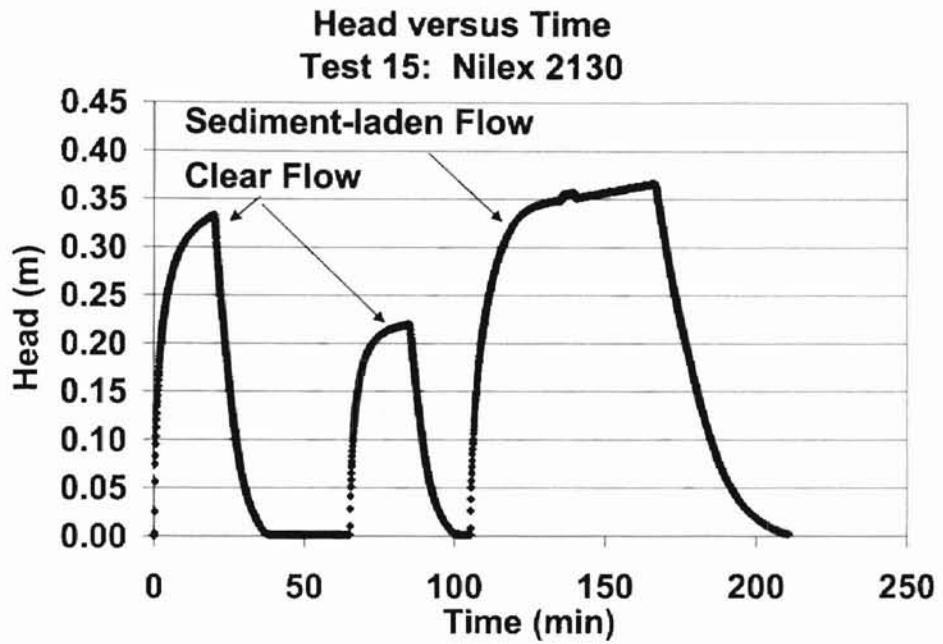


Figure C. 16.

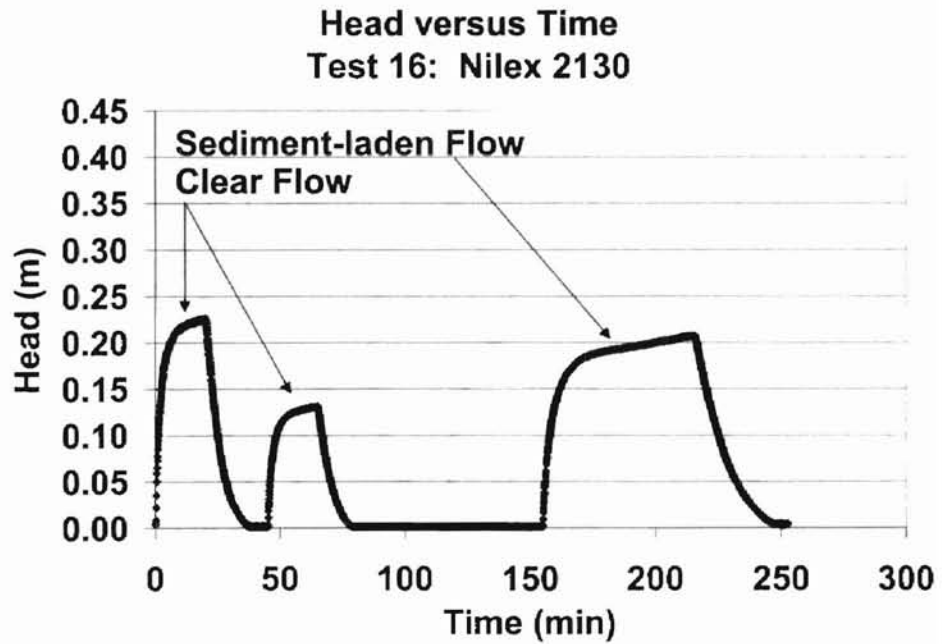


Figure C. 17.

Head versus Time
Test 17: Nilex 2730

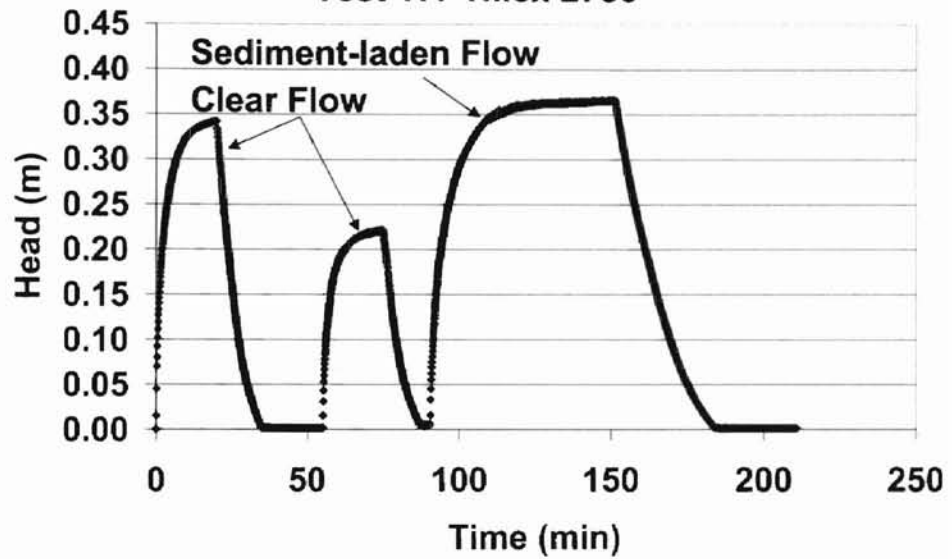


Figure C. 18.

Head versus Time
Test 18: Nilex 2130

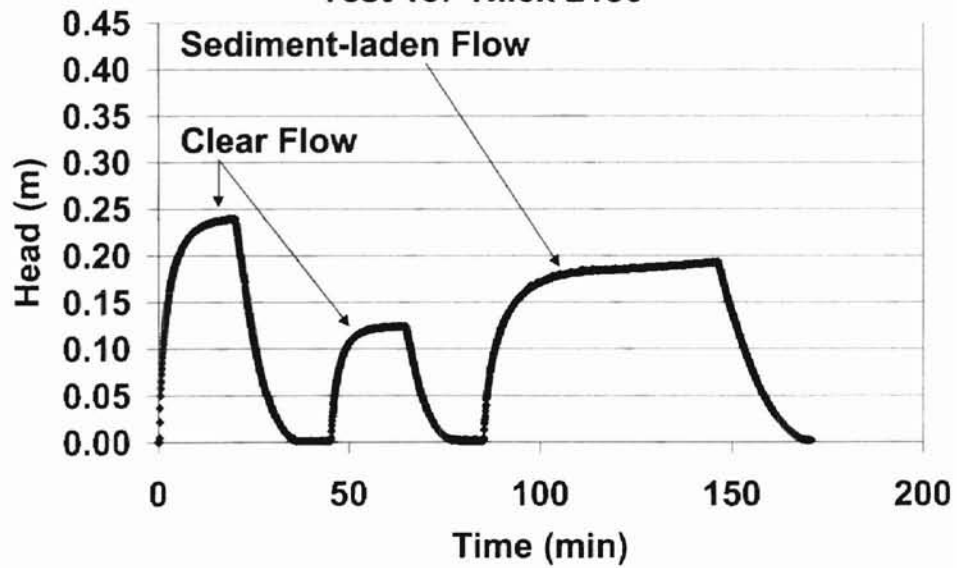


Figure C. 19.

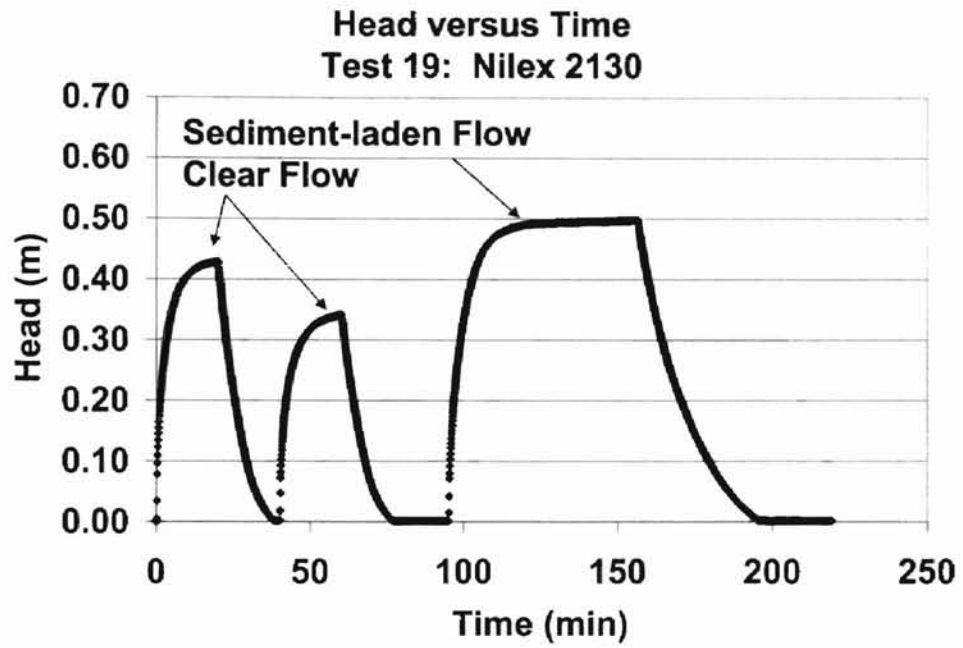


Figure C. 20.

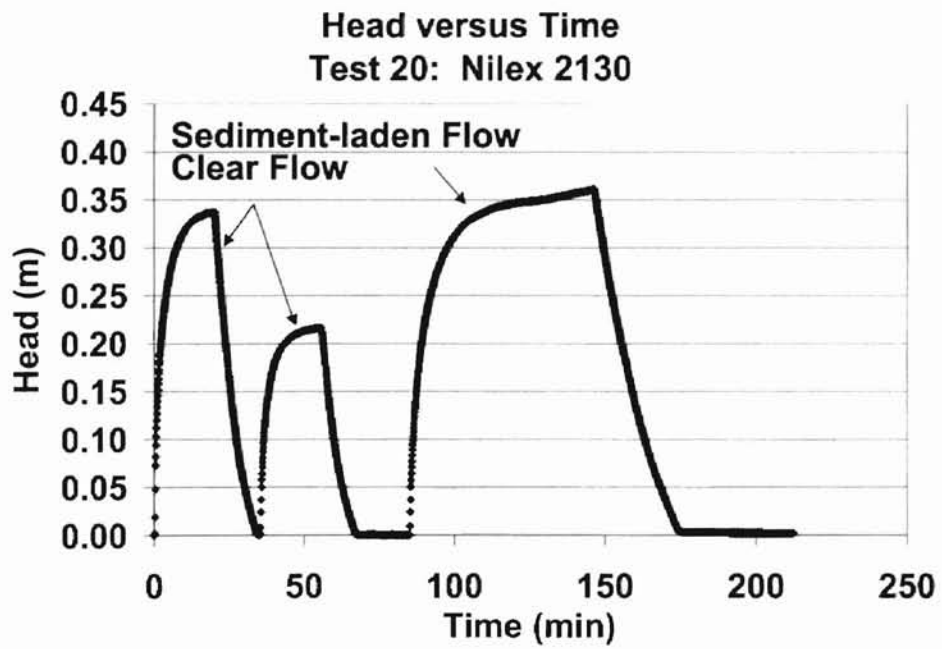
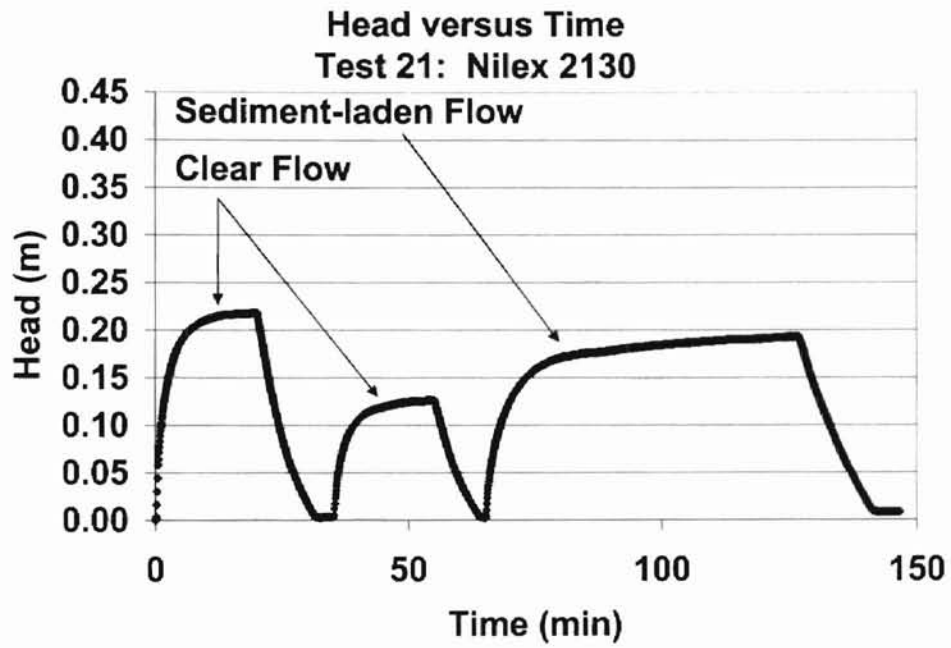


Figure C. 21.



APPENDIX D

Head-discharge Plots

Figure D. 1.

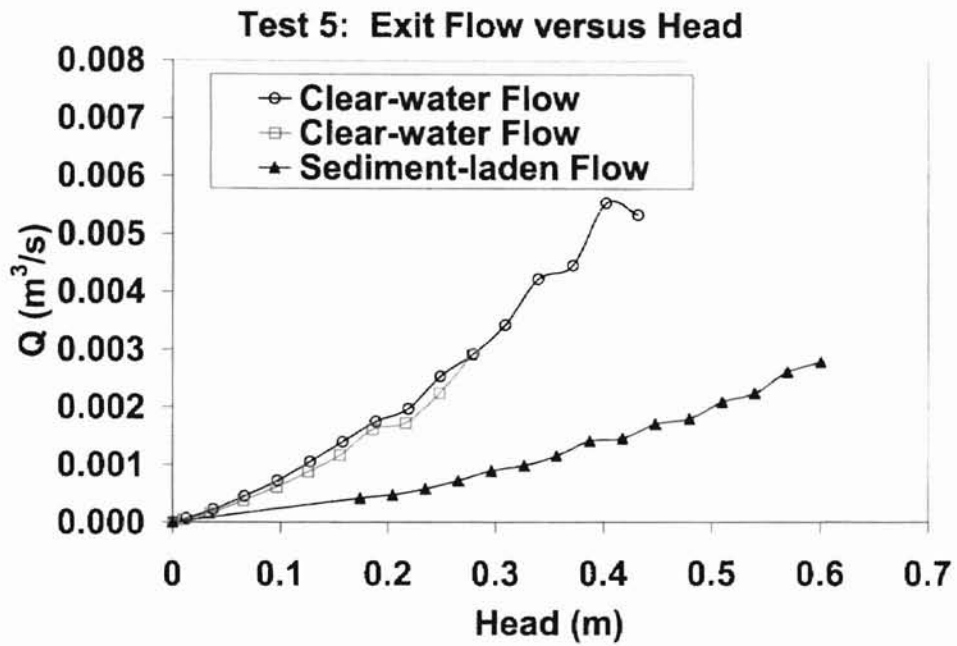


Figure D. 2.

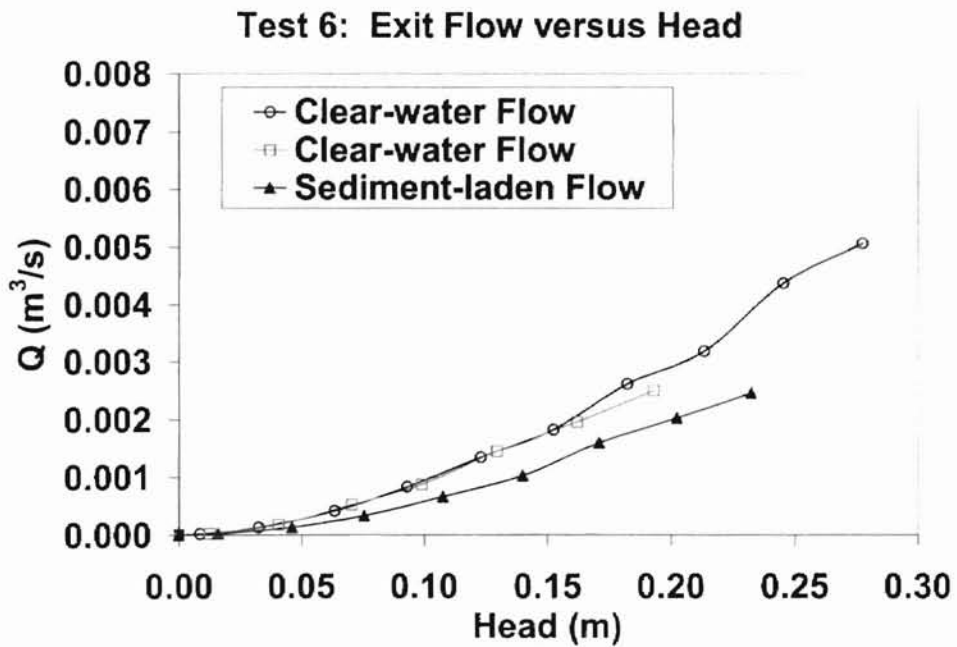


Figure D. 3.

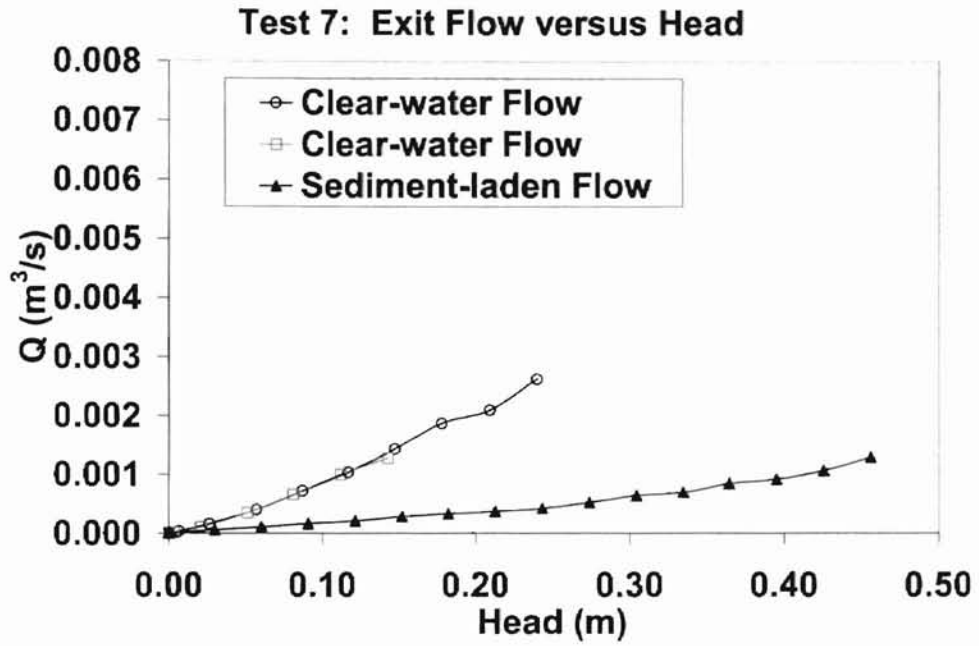


Figure D. 4.

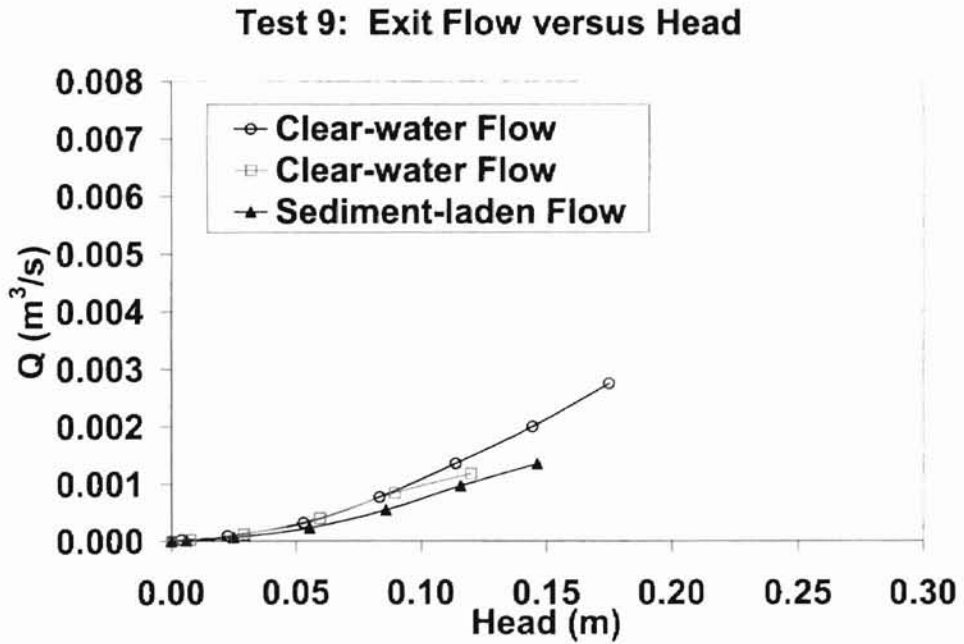


Figure D. 5.

Test 10: Exit Flow versus Head

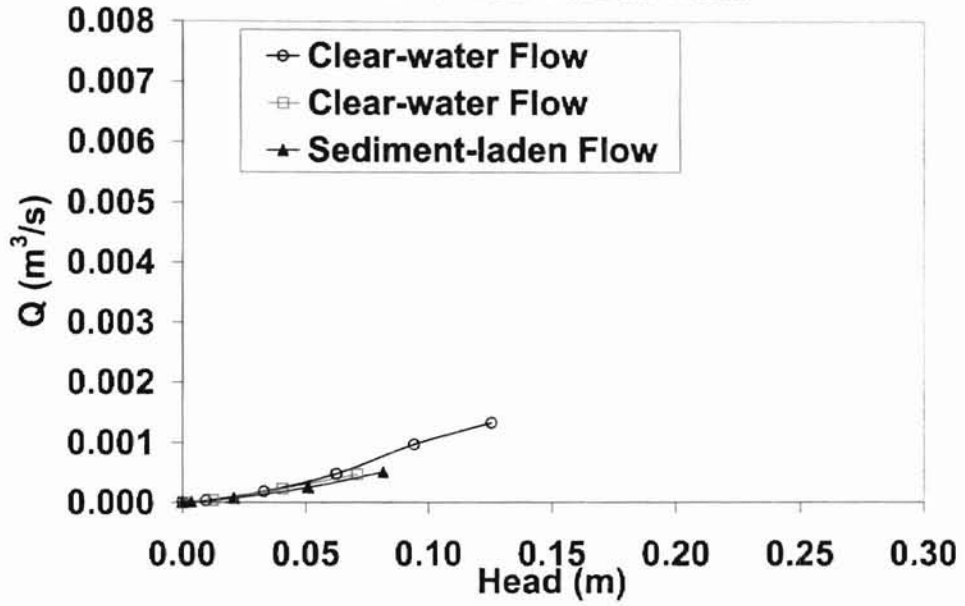


Figure D. 6.

Test 11: Exit Flow versus Head

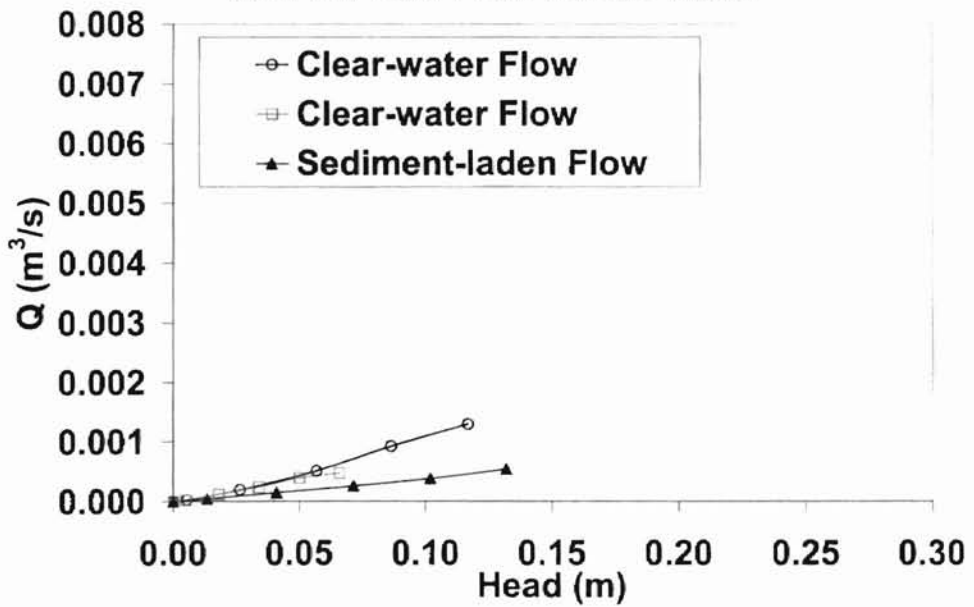


Figure D. 7.

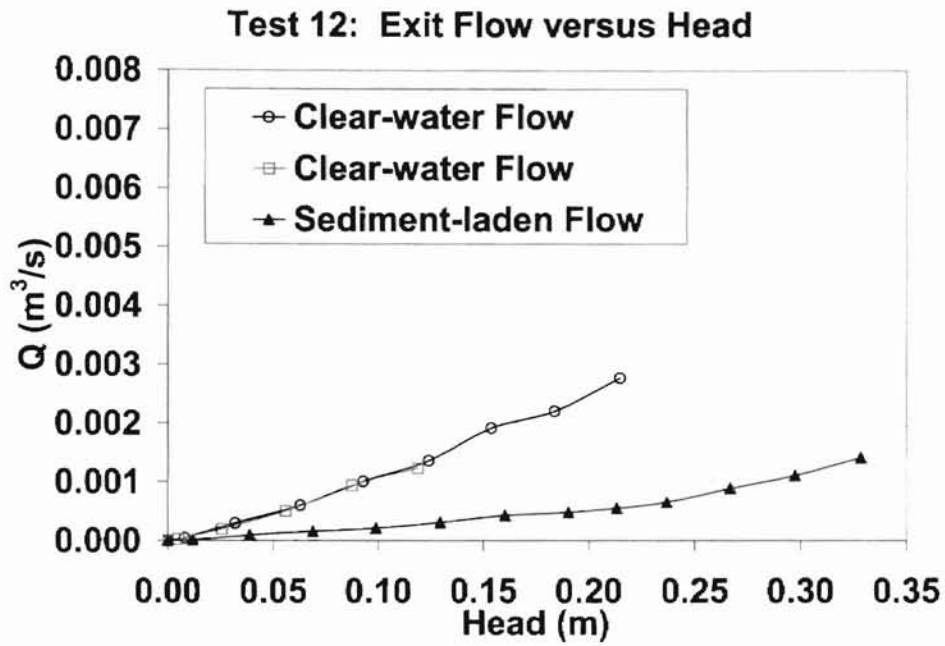


Figure D. 8.

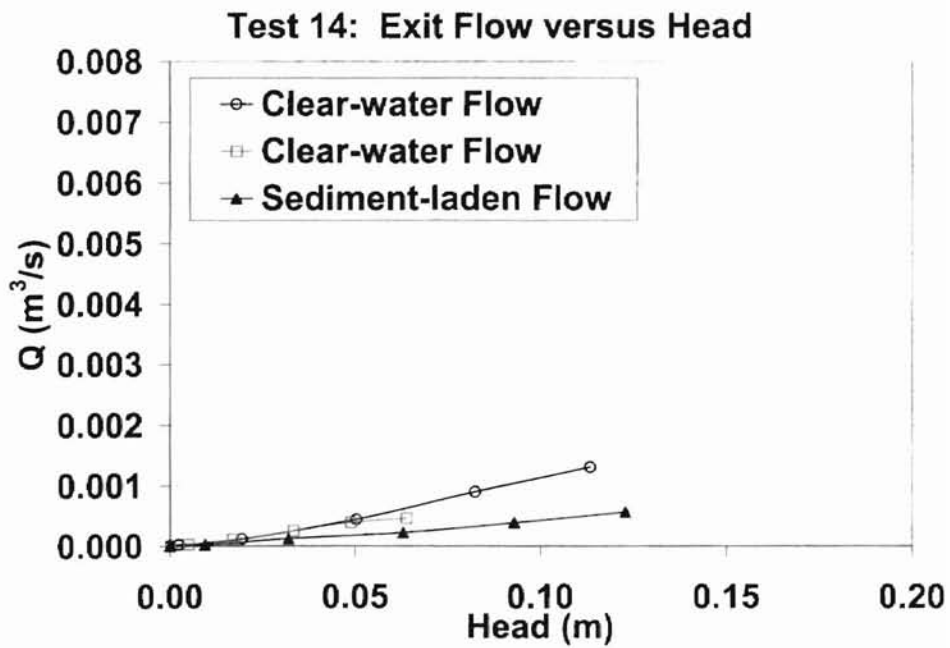


Figure D. 9.

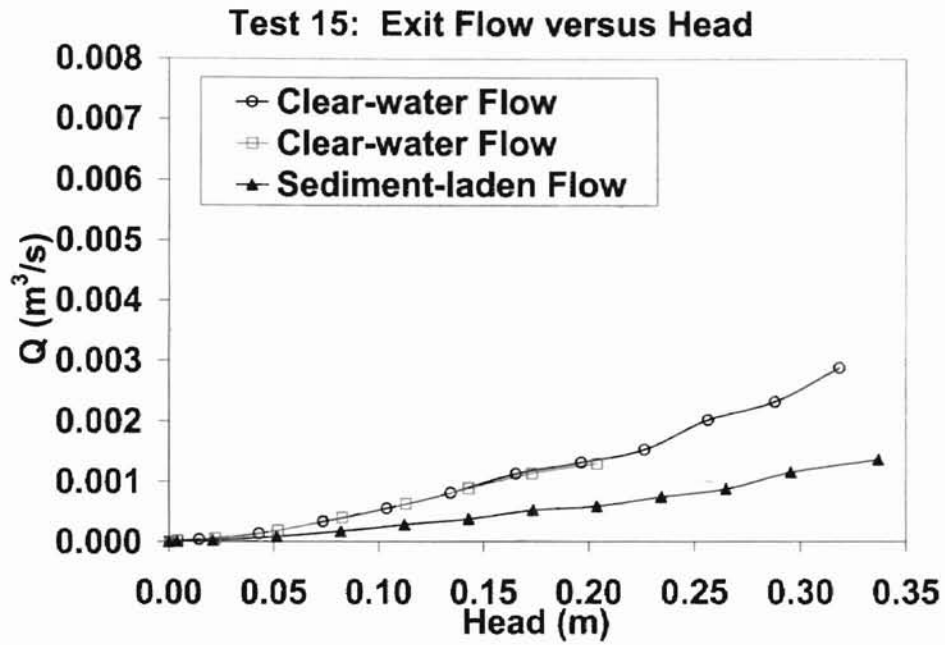


Figure D. 10.

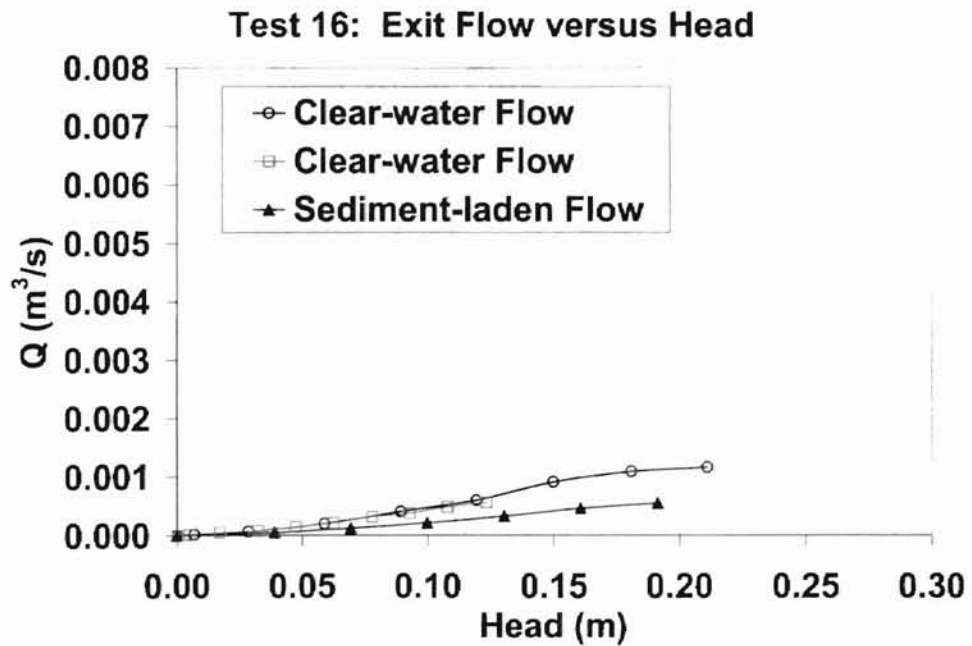


Figure D. 11.

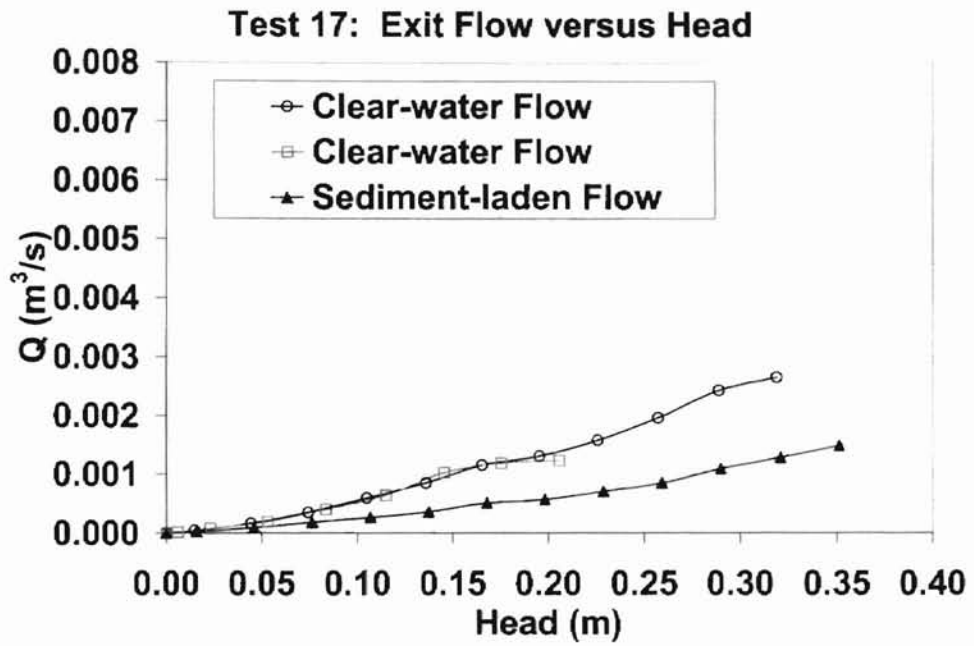


Figure D. 12.

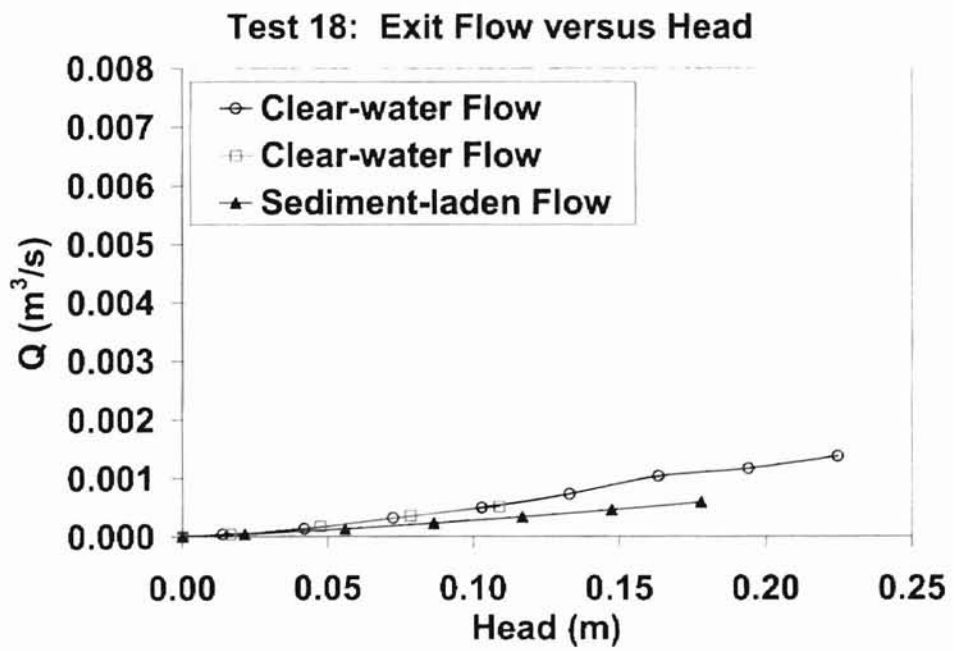


Figure D. 13.

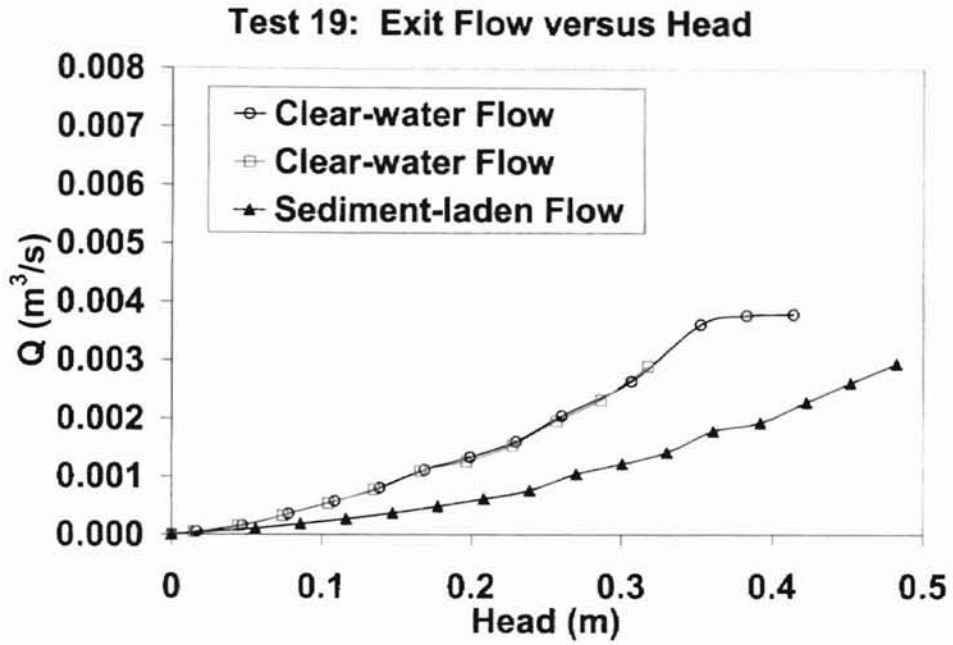


Figure D. 14.

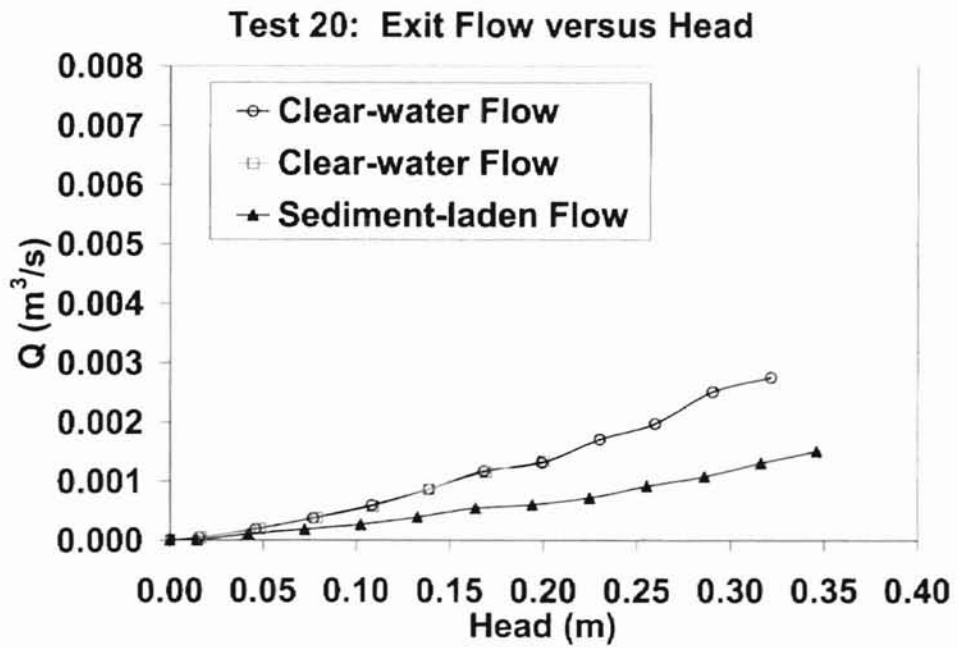
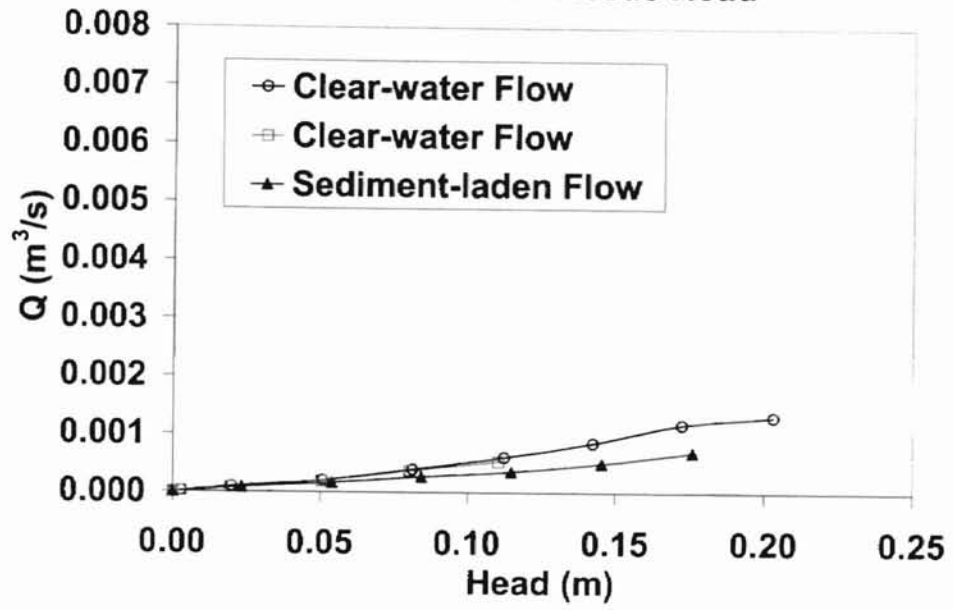


Figure D. 15.

Test 21: Exit Flow versus Head



APPENDIX E

Particle Size Distribution Plots

Figure E. 1.

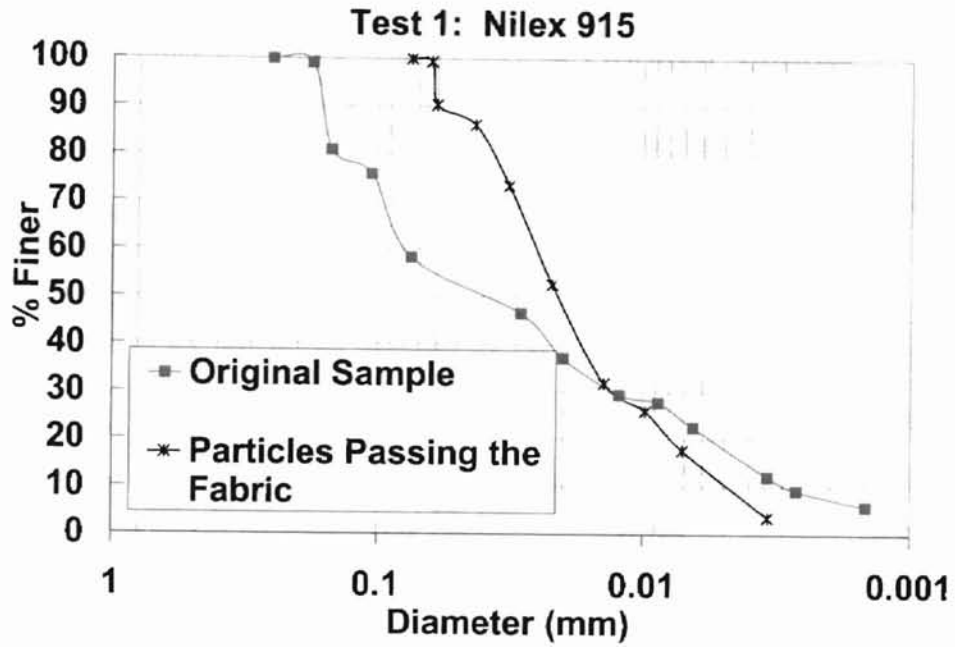


Figure E. 2.

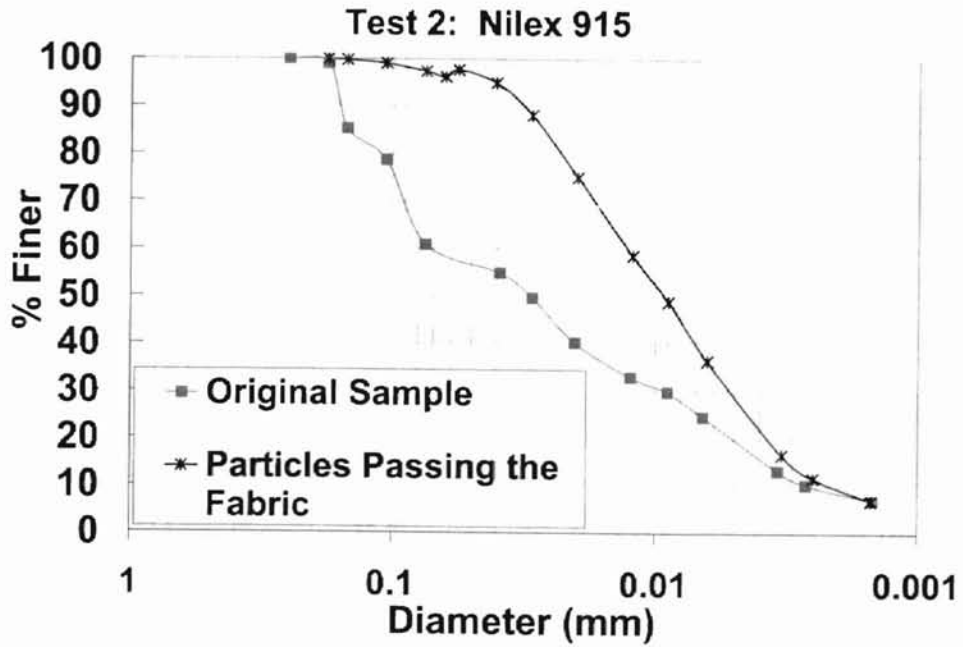


Figure E. 3.

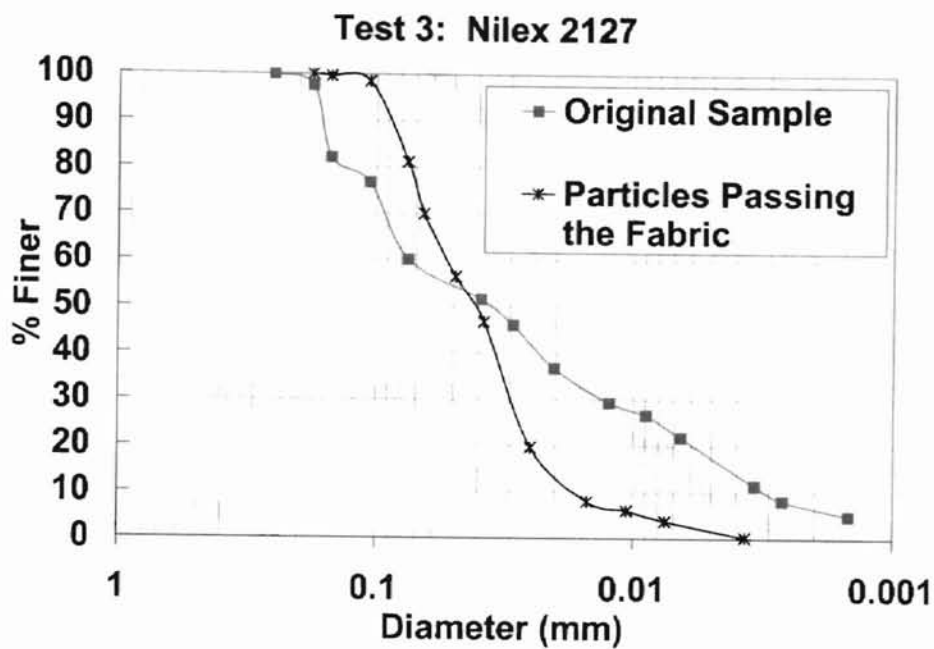


Figure E. 4.

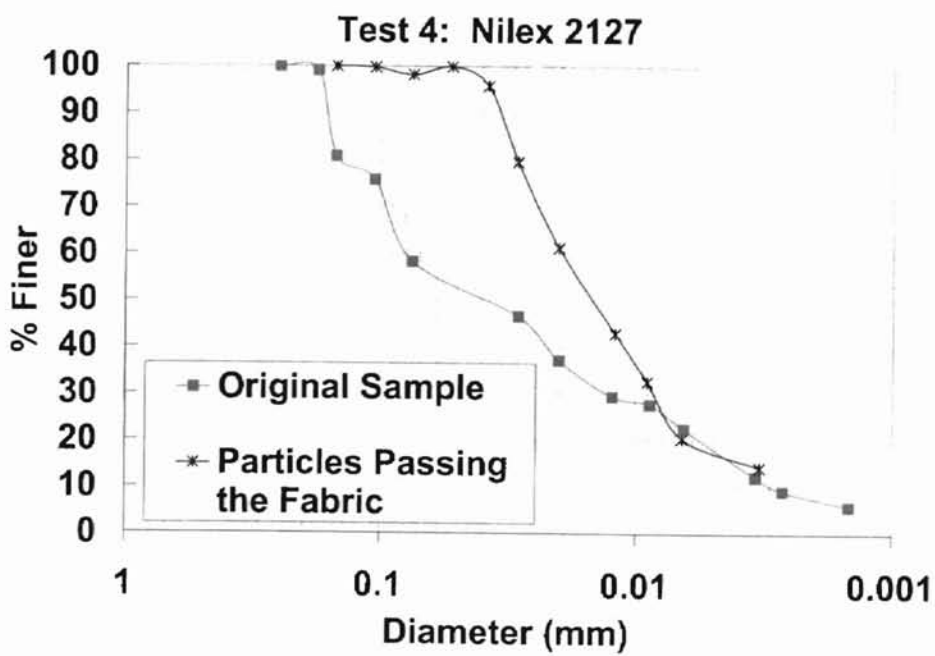


Figure E. 5.

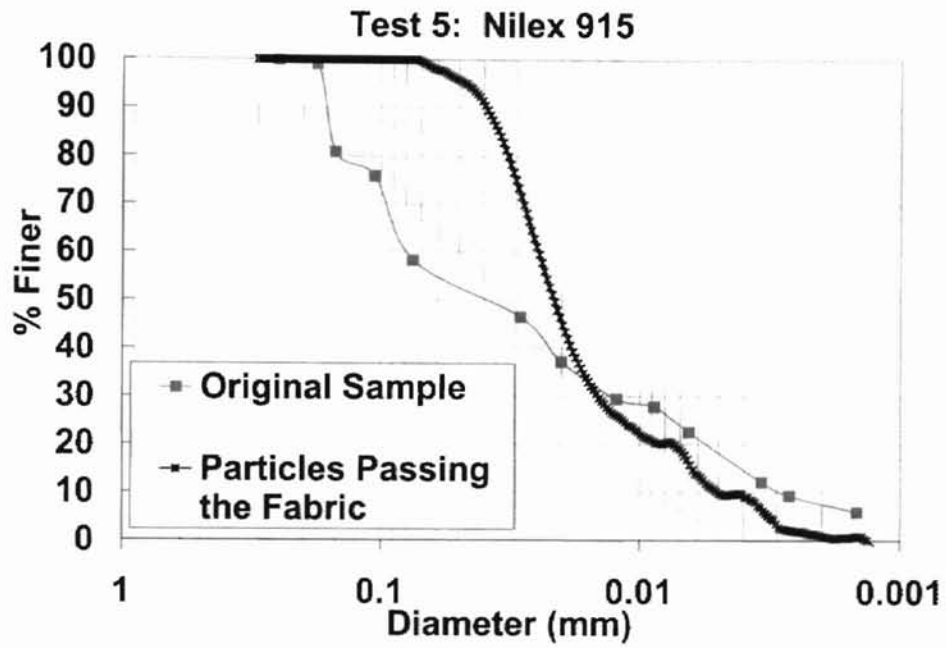


Figure E. 6.

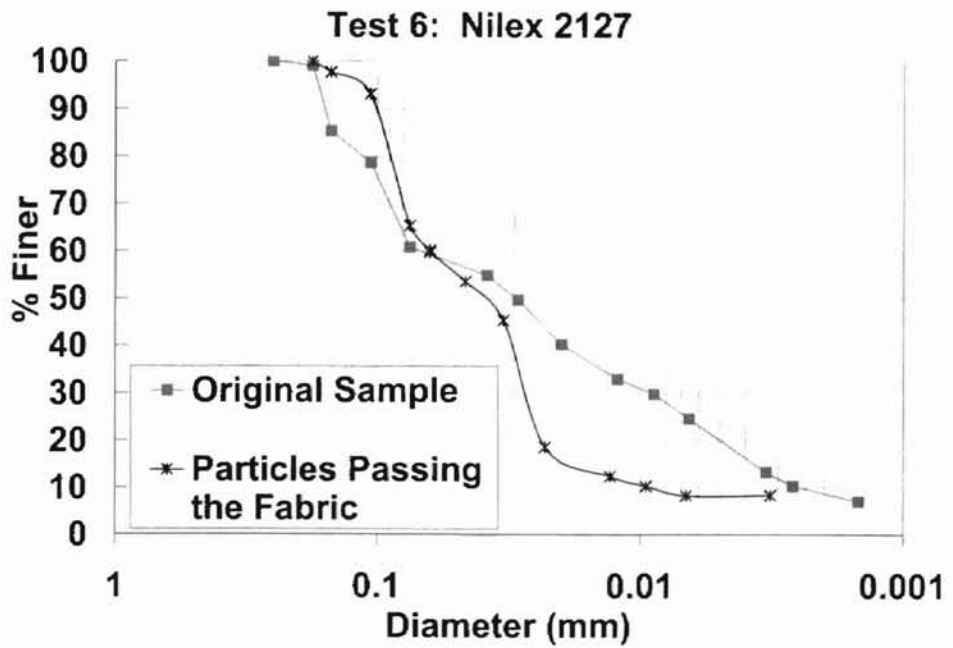


Figure E. 7.

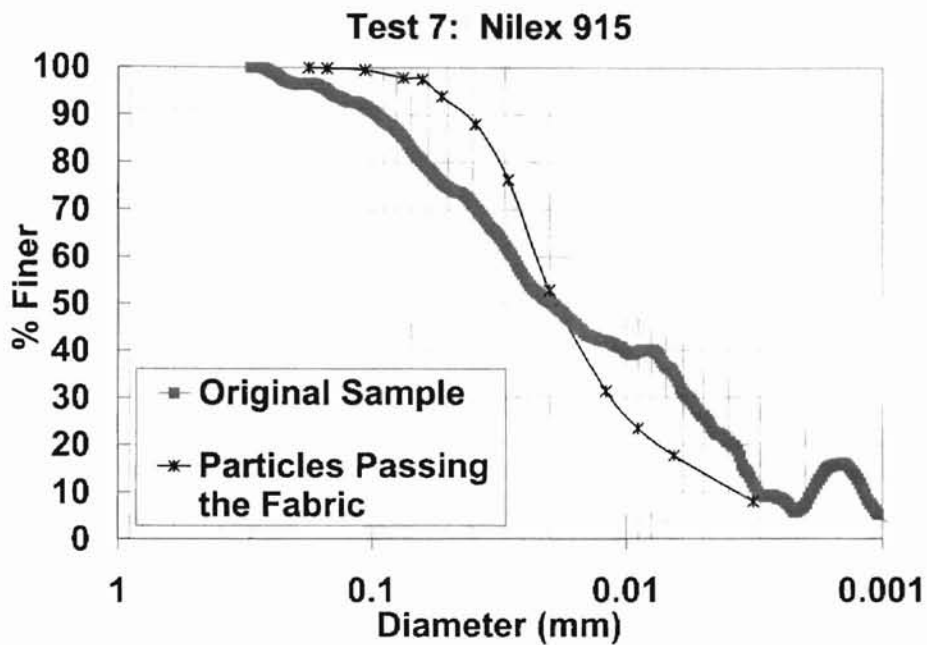


Figure E. 8.

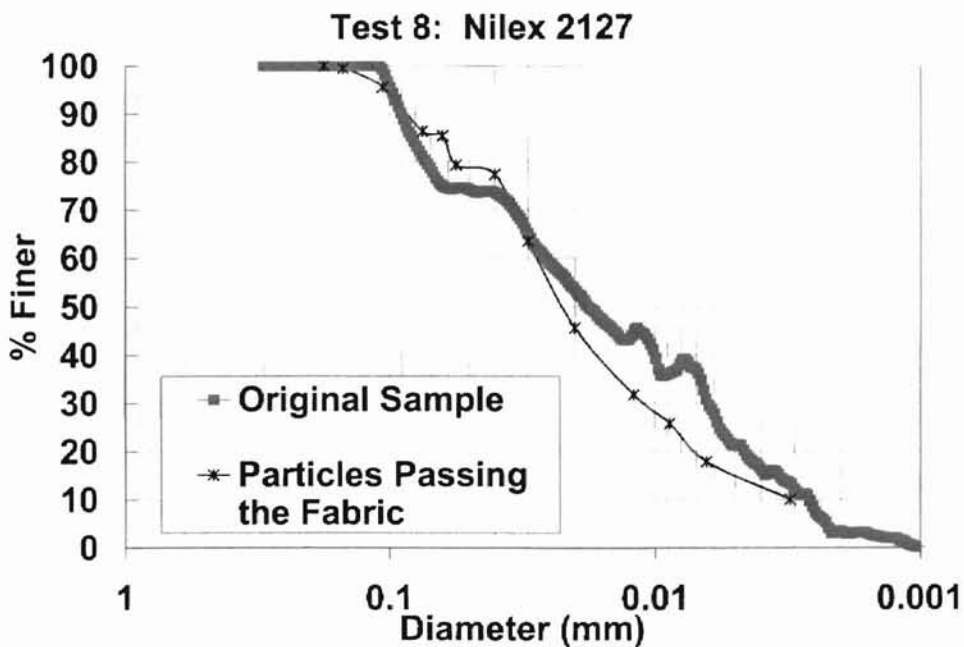


Figure E. 9.

Test 9: Nilex 2127

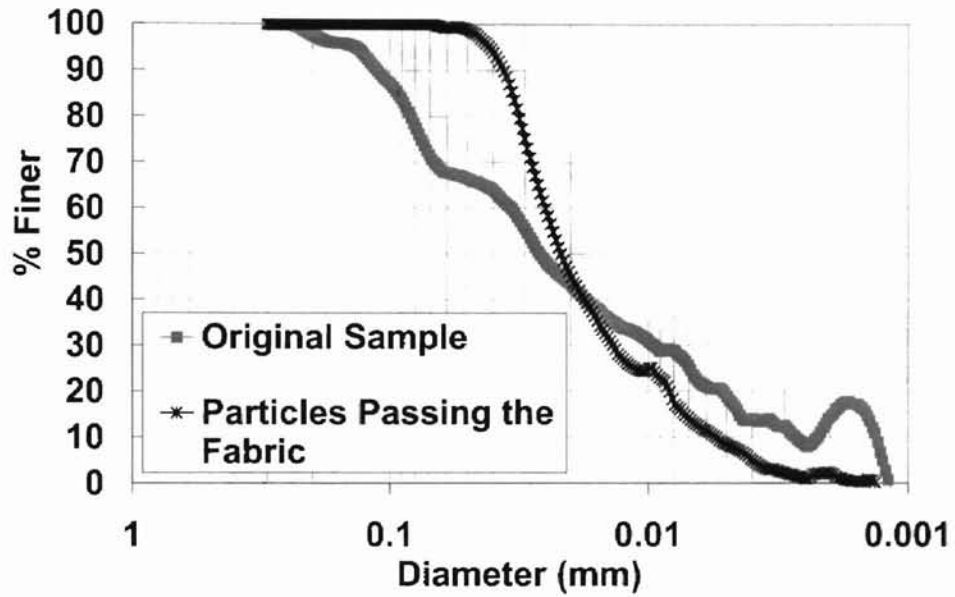


Figure E. 10.

Test 10: Nilex 2127

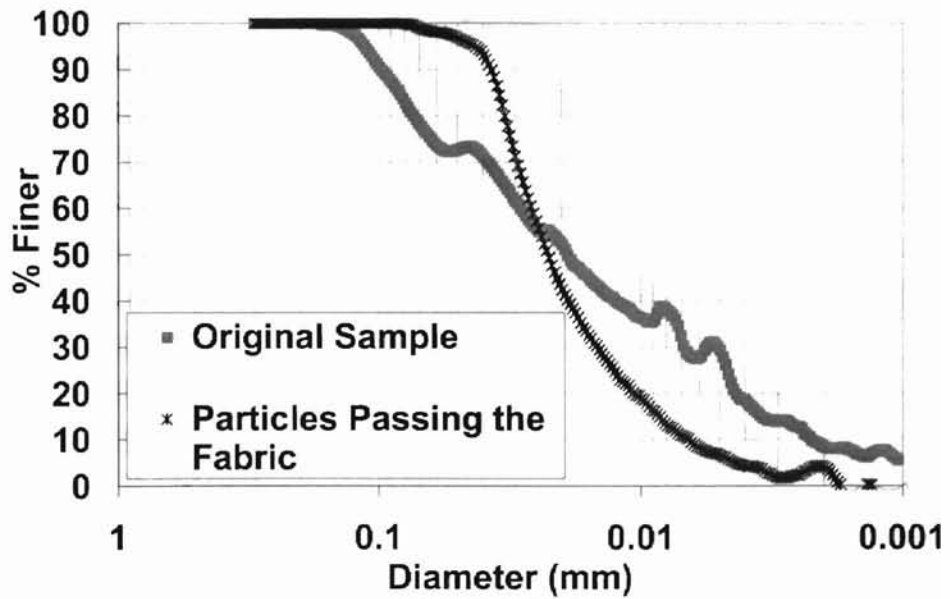


Figure E. 11.

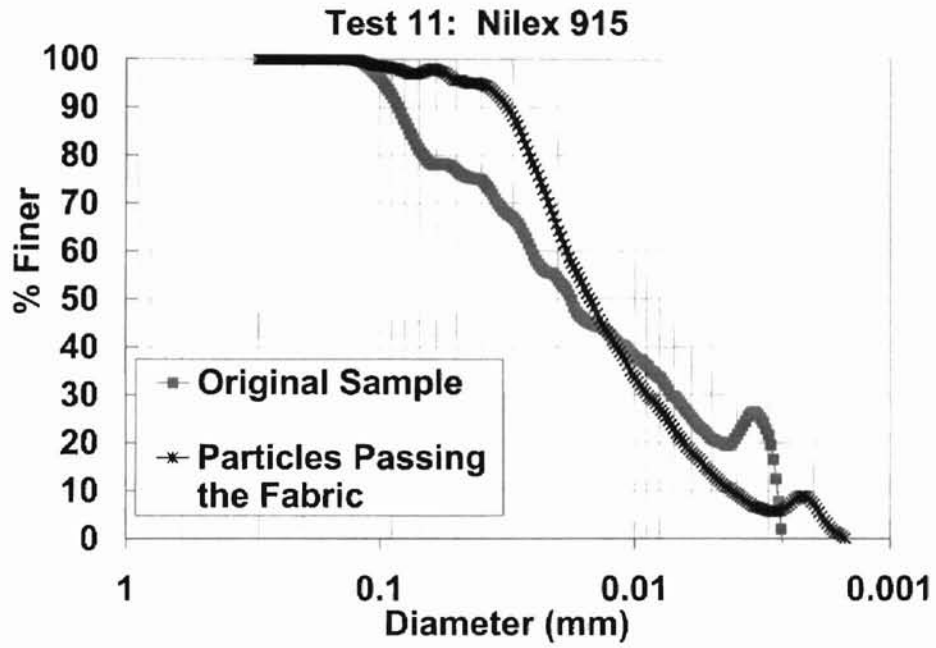


Figure E. 12.

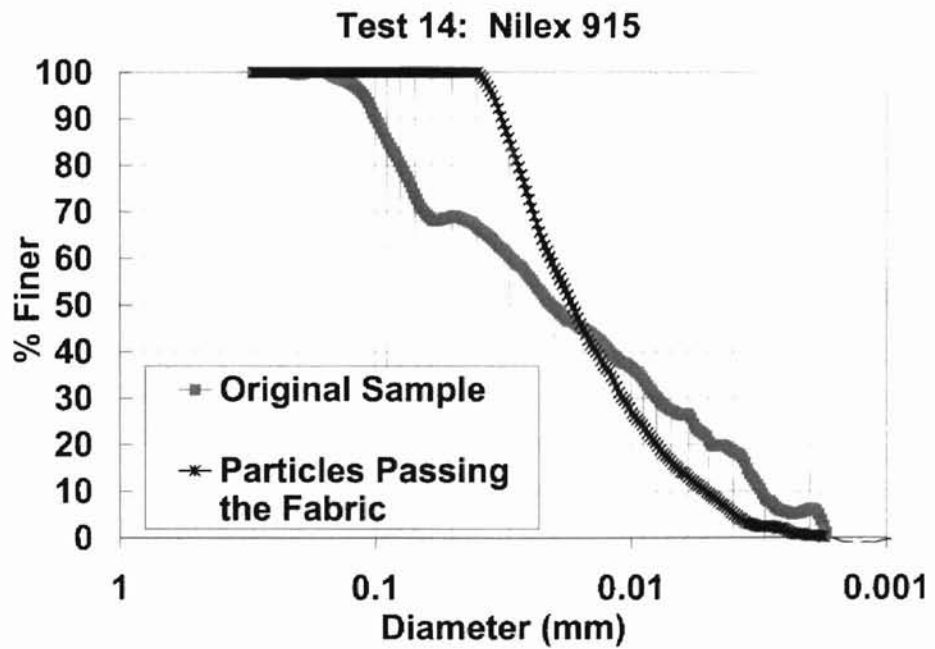


Figure E. 13.

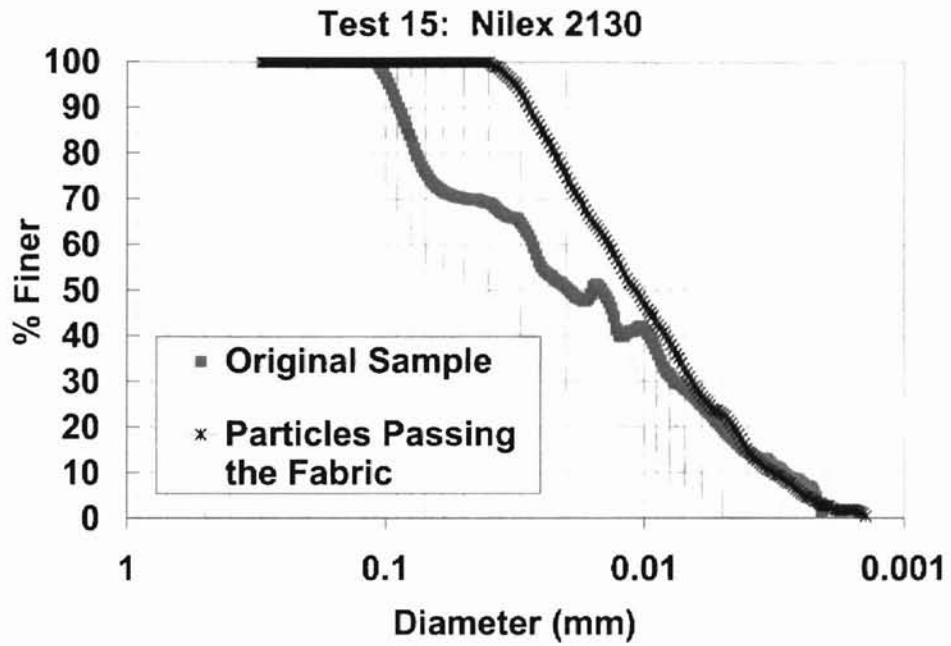


Figure E. 14.

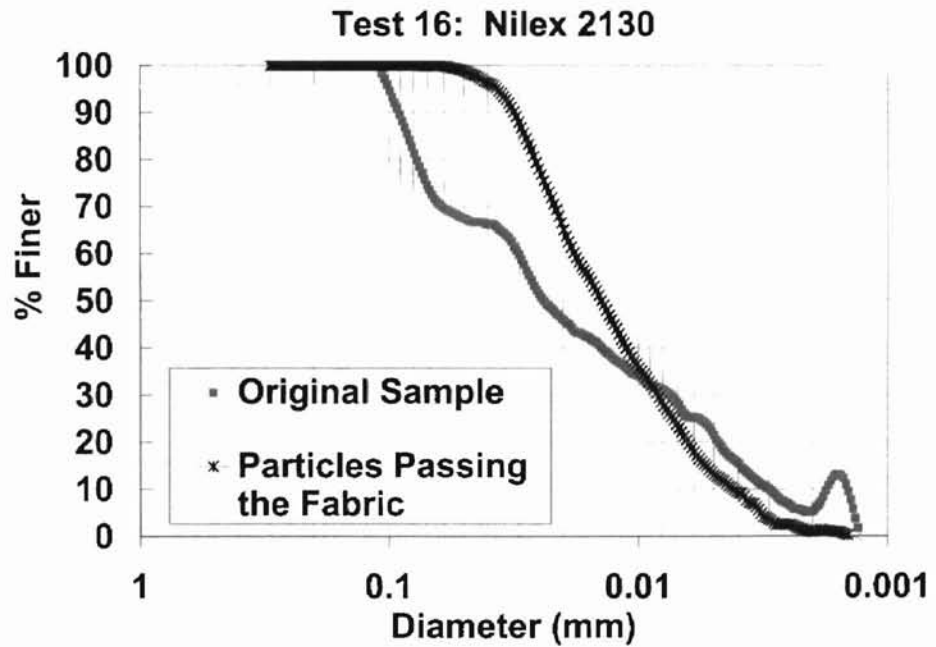


Figure E. 15.

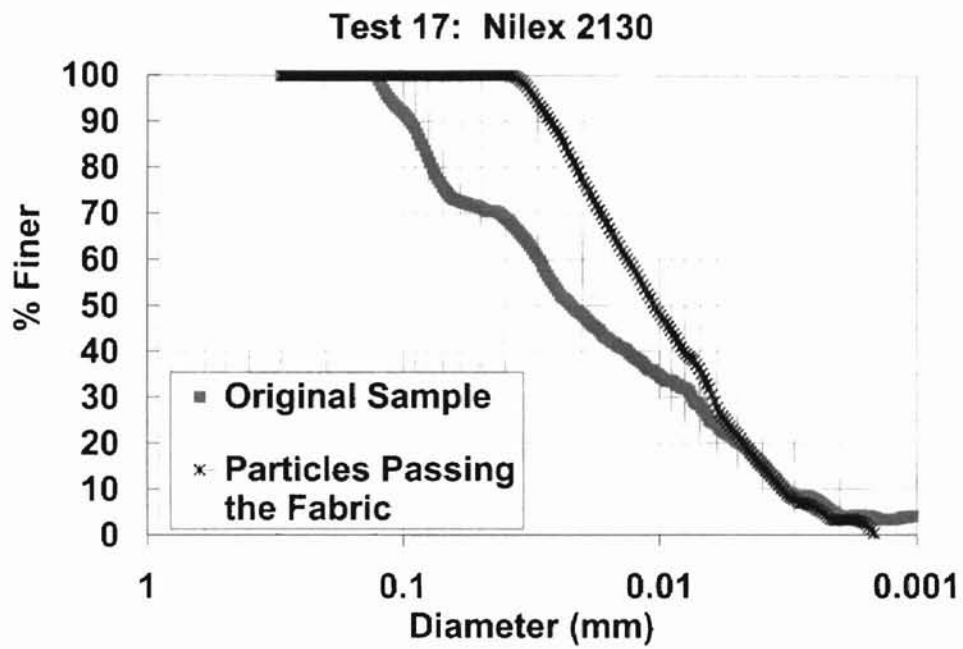


Figure E. 16.

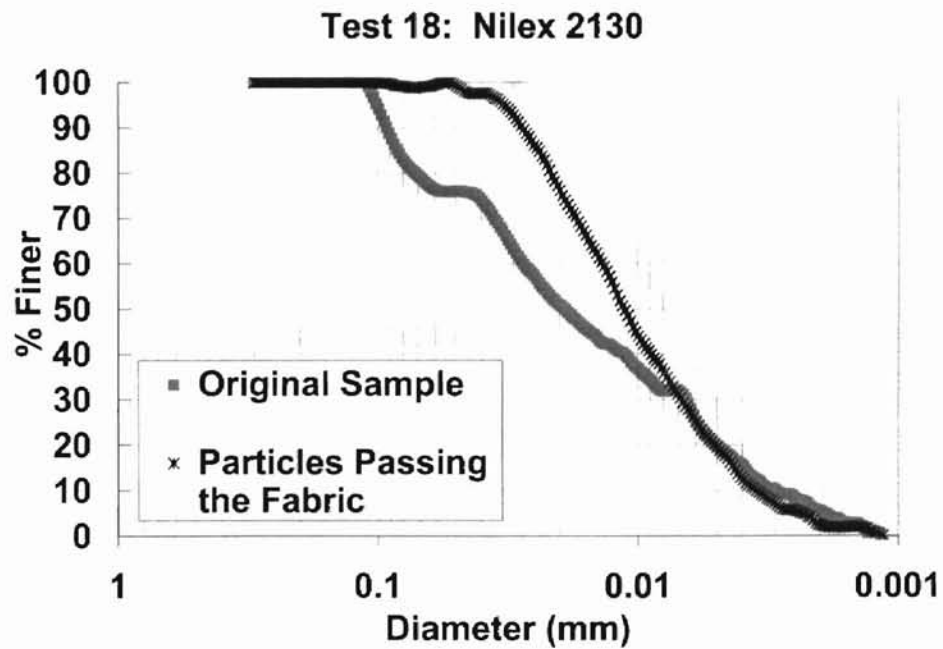


Figure E. 17.

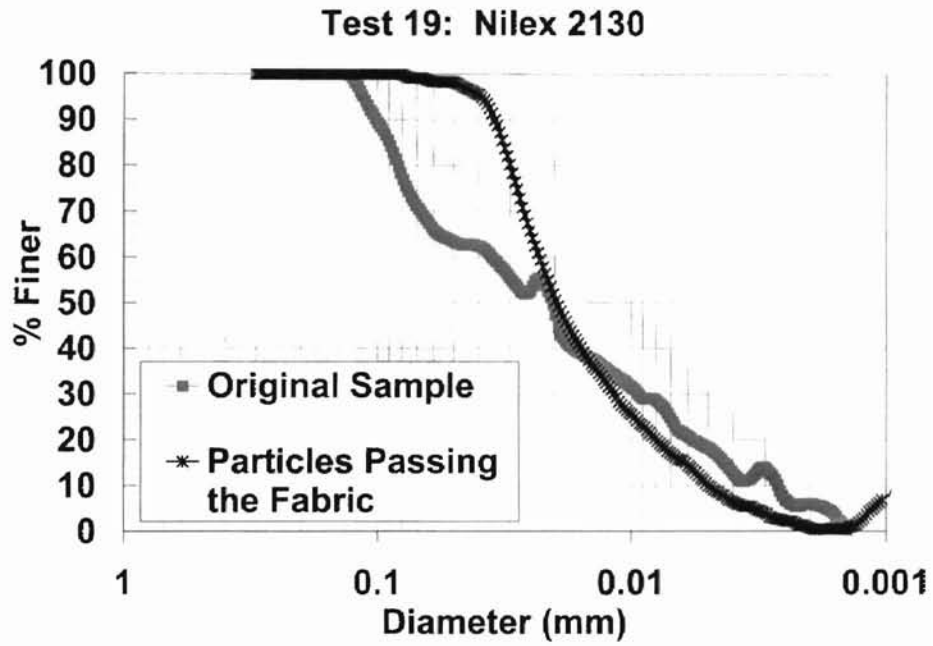


Figure E. 18.

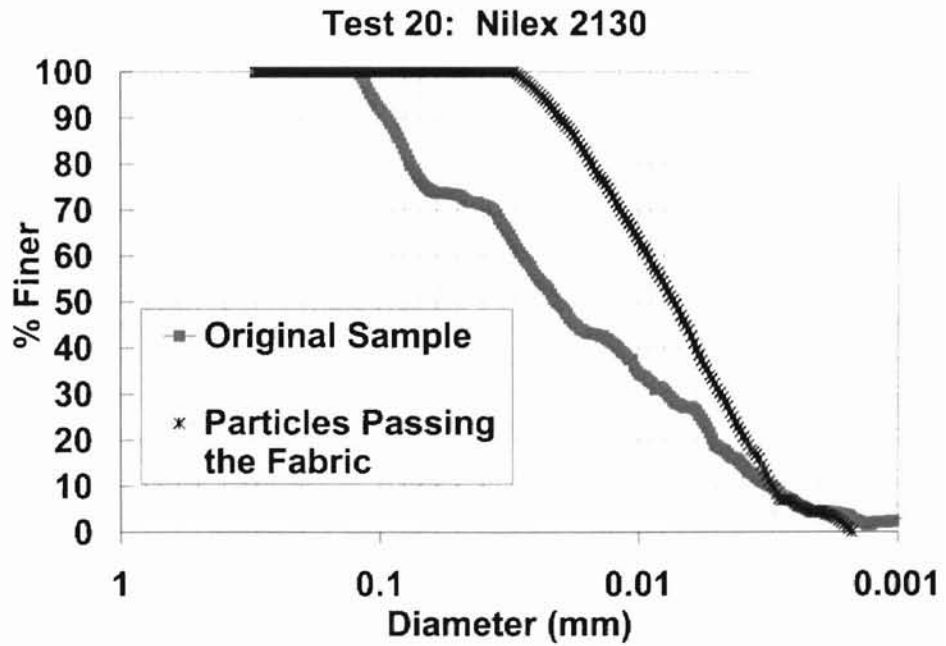
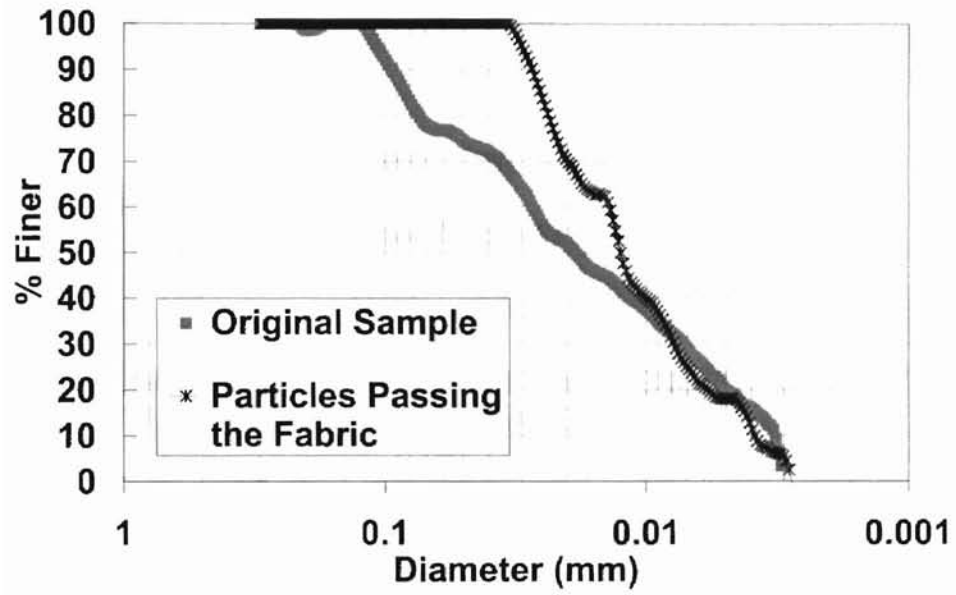


Figure E. 19.

Test 21: Nilex 2130



VITA

Sherry Lynn Britton

Candidate for the Degree of

Master of Science

Thesis: PERFORMANCE EVALUATION OF SILT FENCES FOR
CONTROLLING SEDIMENT RELEASE

Major Field: Biosystems Engineering

Biographical:

Personal Data: Born in Chickasha, Oklahoma on November 10, 1975, the daughter of Tommy Wayne (Buddy) and Janet Britton.

Education: Graduated from Binger-Oney High School, Binger, Oklahoma in May, 1994; received Bachelor of Science degree in Biosystems Engineering with the Environment and Natural Resources Option, Oklahoma State University, Stillwater, Oklahoma in July, 1999; completed the requirements for the Master of Science degree with a major in Biosystems Engineering at Oklahoma State University, December, 2000.

Experience: Design Engineer for the Oklahoma Natural Resources Conservation Service State Office, September, 2000 to present. Graduate Research Assistant for the Oklahoma State University Biosystems Engineering Department and the USDA-ARS Hydraulics Engineering Research Laboratory, June, 1999 to December, 2000. Research Assistant for the USDA-ARS Hydraulics Engineering Research Laboratory, May, 1998 to August, 1998.

Professional Memberships: Oklahoma State Board of Registration for Professional Engineers and Land Surveyors, certified Engineer Intern (EI No. 11288), American Society of Agricultural Engineers, Alpha Epsilon Agricultural Engineering Honor Society, and Soil and Water Conservation Society.